Center for Neutron Research

FY 2003 Programs and Accomplishments

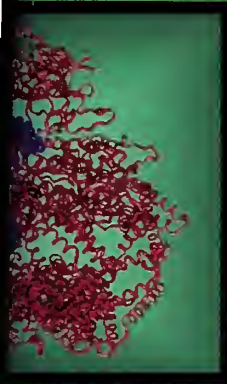

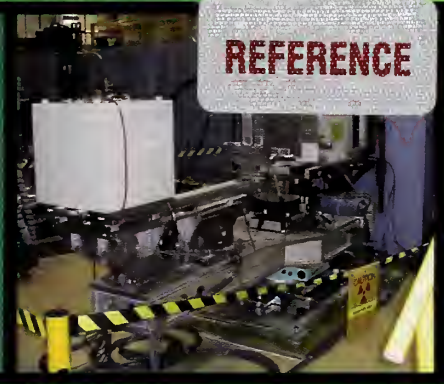

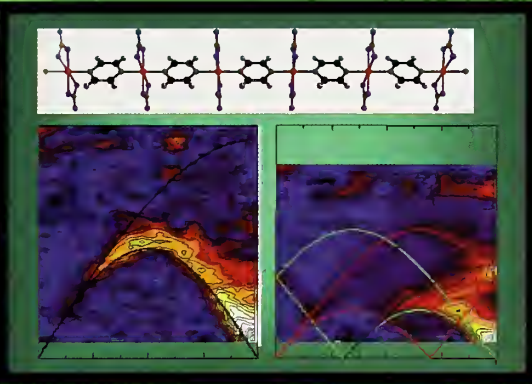

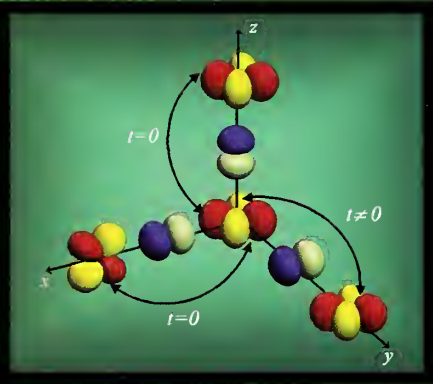

MSEL

NIST
National Institute of
Standards and Technology
ology Administration
epartment of
erce
7018
er 2003

On the Cover:

Diversity of projects at the NCNR is exemplified by images associated with highlight articles in this issue. From the front cover and continuing on to the back, right to left, the images refer to:

Hidden symmetries in perovskites, p.38.

Spin-1/2 chains, p.30.

New reflectometer for biology research, p.6.

Protein complex, p.22.

National Institute of Standards and Technology
Arden L. Bement, Jr.
Director

Technology Administration
Phillip J. Bond
Under Secretary of Commerce for Technology

U.S. Department of Commerce
Donald L. Evans
Secretary

Materials Science and Engineering Laboratory

FY 2003 Programs and Accomplishments

NIST Center for Neutron Research

J. Michael Rowe, Director

NISTIR 7018

October 2003

DISCLAIMER

Certain commercial entities, equipment, or materials may be identified in this document in order to describe an experimental procedure or concept adequately. Such identification is not intended to imply recommendation or endorsement by the National Institute of Standards and Technology, nor is it intended to imply that the entities, materials, or equipment are necessarily the best available for the purpose.

Contents

Robert S. Carter, Carl O. Muehlhause and Harry Landon honored at NIST Standards Alumni Association 2003 Portrait Ceremony

Robert S. Carter

Carl O. Muehlhause

Harry Landon

Portraits placed in the NIST Gallery of Distinguished Scientists, Engineers and Administrators

Photography by Barry Gardner

Harry Landon with Jack Rush and Fred Shorten

Photography by Barry Gardner

The honorees being congratulated by Mike Rowe at the presentation ceremony

Photography by Barry Gardner

NIST Director Arden Bement (second from left) joins Mike Rowe (left) and Jack Rush (center) in congratulating Harry Landon and Carl Muehlhause

NCNR Founders Honored at NIST

These distinguished alumni designed and oversaw the building of the NBSR and the starting of its science programs

December 7, 1967, criticality at the NBSR, left to right: NBS Director Allen Astin, Harry Landon, Carl Muehlhause, Robert Carter, and Associate Director Irl Schoonover

Left to right: Mike Rowe, Pat Gallagher, Carl Muehlhause, Tawfik Raby, Jack Rush, Bob Carter, Sheila Landon, John Cleary, Toni Carter, and Harry Landon tour the cold neutron guide hall of the NIST Center for Neutron Research

Photography by Barry Gardner

Muehlhause, Landon and Carter are presented with certificates by Mike Rowe

Photography by Barry Gardner

Sheila Landon and Mike Rowe share a moment at the reception

Foreword

This is the 15th report of the activities of the NIST Center for Neutron Research (NCNR) for which I have written an introduction, following the retirement of Dr. Robert S. Carter (who wrote all of the preceding introductions). It is particularly appropriate to note this milestone this year for two reasons. First, because Bob Carter, Carl Muehlhause, and Harry Landon, the designers of the NIST reactor, are being recognized this year by having their pictures hung in the NIST Portrait Gallery for their contributions to NBS/NIST. This is an honor well deserved, and we are hoping that they will all return in September for the ceremony. Second, this will be my last such introduction, as I intend to retire as Director before the next one is written. Therefore, I will not limit my remarks to this year's accomplishments only, but try to summarize my thoughts after 15 years as Director, and 31 years at NIST.

The source designed and guided through its formative years by Carter, Muehlhause, and Landon has been a tremendous success, providing remarkably cost-effective service to NIST and the nation. Its design has proved its worth over and over, as the focus of the program has shifted over the years from being primarily for local nuclear physics, irradiations for analytical chemistry, and neutron diffraction to in-house and collaborative thermal neutron scattering involving a broader community, to its present role as the major national center for thermal and cold neutron research, with a full suite of scattering instruments, an active analytical chemistry effort serving national as well as local needs, and a thriving program in neutron physics. With this continuing growth, expansion and transformation in our research and measurement activities, the need for predictable, dependable operation has increased greatly. It is a tribute to all of the people involved that the challenge has been met with only a moderate increase in cost and staff, in spite of increasing regulatory requirements, and an increase in power from 10 to 20 MW in 1985. For many years, as Chief of Reactor Operations and Engineering, Tawfik Raby set the highest standards for safe, reliable, and economical reactor operations, and his successor, Seymour Weiss, has continued in this tradition. Many of our most senior operators have retired or will in the next few years, but we have managed to hire outstanding young people to carry on. By the end of this year, we will apply for a license renewal for an additional 20 years of operation, and I am confident that it will be approved, and that the reactor will continue to serve NIST and the nation for the foreseeable future.

While the reactor has provided the constant source of neutrons required for success, the instrumentation around it has been continually improved and updated. When I first arrived at NIST in 1973, I worked with Jack Rush, Sam Trevino and Hank Prask to develop our first triple axis spectrometer (an instrument that has been modified and updated regularly, and for which the last "original" part should disappear in the next two years). (Incidentally, it was during the design of this instrument, which was done in part at Ames Laboratory, that I first met my wife Nancy Chesser, who was then a staff member at Ames.) This year alone, we have begun the installation of a next-generation doubly focusing thermal neutron triple axis spectrometer which will have unprecedented intensities and flexibility; installed a new cold neutron reflectometer/diffractometer as part of Cold Neutrons for Biology and Technology initiative; and commissioned a new facility for radiography that has been used to study operating fuel cells. We are also well into the detailed design of a new cold neutron double-focusing triple axis spectrometer, MACS, in partnership with The Johns Hopkins University. We are now on our third cold neutron source, which incorporates the experiences from the first D_2O ice source installed in 1985 and the first liquid hydrogen source. This source operates totally reliably, and achieved a 100 % availability (ready to run when the reactor is) this year. The pace of instrumentation development has accelerated continuously during my time here, to encompass ideas that we never considered even 15 years ago. For this I am

grateful to the many people who have worked so hard over the years — far too many to acknowledge here, but I would be remiss if I did not mention Ivan Schroder and his engineering colleagues, who have solved so many "impossible" engineering problems, and Bob Williams and more recently, George Baltic, and their technical team, who put into practice on the floor what we dreamt up in our offices. And Pat Gallagher has led the transition from the somewhat anarchic Cold Neutron Project to the Research Facility Operations Group, a fully functioning group that serves the user mission of the NCNR extraordinarily well.

Last, but far from least, the science group has grown from the 9 regular staff members that it had when I arrived to over 30 NIST employees and 36 long-term guest researchers. At the same time, the mission and focus of the group has evolved, with added responsibilities for instrument development, support for user operations, new research areas in soft matter, and many new interactions with the rest of NIST and with 200 outside organizations. Throughout my 31 years, Jack Rush, my good friend and colleague, has guided the fortunes of the research group with a sure and steady hand, ever alert to new opportunities, to good science, and to good people. As I have read through this year's science reports, and through earlier years, I have been struck by the continuing high quality of the research, even as the scientific emphasis has changed, the techniques have developed, and our mode of operation has been totally transformed. One of the greatest pleasures of this job has been the opportunity to walk through the facility to meet and learn from the intelligent and dedicated people who do the research. Young and not so young, they give me a high level of optimism for the future because of their infectious enjoyment of their activities (it seems wrong to call something so enjoyable work!). As always, the science highlights that form the bulk of this report are the final indicator of what we have done in the past year. I hope that you enjoy reading them as much as I did.

So, in closing, I thank everyone who has been part of my life here — I hope that what we have accomplished together over the years is a source of pride to you, as it is to me. I look forward to seeing the continual progress of the NCNR, for which the best is yet to come.

Mike Rowe

Groundbreaking for the cold neutron guide hall, Nov. 1987. L to R: MSEL Director Lyle Schwartz; DOC Dep. Secy. Clarence (Bud) Brown; Rep. Connie Morella, R-Md; NIST Dir., Ernest Ambler; and NCNR Dir., Mike Rowe.

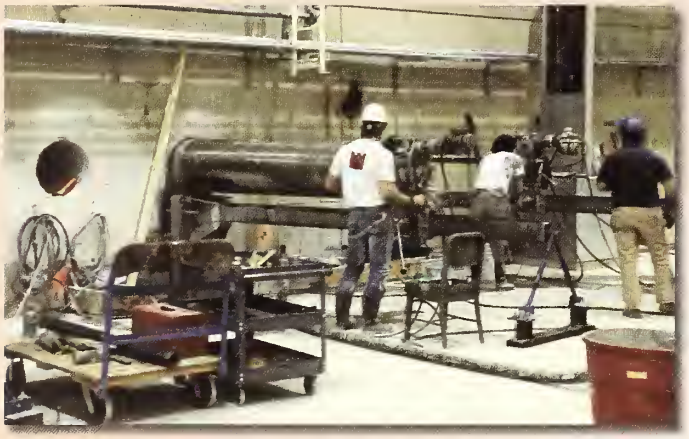

Drilling through 20' concrete wall to bring neutron guides from the source, 1989.

Mike and Nobel Laureate Clifford Shull share a lighter moment during Shull's visit to the NCNR, 1995.

NCNR Guide hall building recently completed (above), January 1989, and at present (right).

John McTague, then of Ford Motor Co., delivered a lecture in a series honoring NCNR founder Robert S. Carter (seated behind), May 1992.

NCNR facility tour by members and staff of the U.S. House Science Committee, May 2001. Clockwise from the poster on the right, the members are Rep. Vernon Ehlers (R-MI), Rep. Connie Morella (former R-MD), Rep. Gilbert Gutknecht (R-MN) just above and behind Rep. Morella, and Rep. Mark Udall (D-CO) just above and to the right of Rep. Morella. Former NIST Dir. Karen Brown is at bottom left of center. Mike is at far right.

The NIST Center for Neutron Research (NCNR)

Neutrons are powerful probes of the structure and dynamics of materials ranging from molecules inserted into membranes mimicking cell walls to protons migrating through fuel cells. The unique properties of neutrons (shown in box) can be exploited by a variety of measurement techniques to provide information not available by other means. They are particularly well suited to investigate all forms of magnetic materials such as those used in computer memory storage and retrieval. Atomic motion, especially that of hydrogen, can be measured and monitored, like that of water during the setting of cement. Residual stresses such as those inside stamped steel automobile parts can be mapped. Neutron-based research covers a broad spectrum of disciplines, including engineering, biology, materials science, polymers, chemistry, and physics.

The NCNR's neutron source provides the intense beams of neutrons required for these types of measurements. In addition to the thermal energy neutron beams from the heavy water or graphite moderators, the NCNR has a large area liquid hydrogen moderator, or cold source, that provides intense neutron beams for the only cold neutron facility presently operating in the United States.

There are currently 29 experiment stations: six provide high neutron flux positions for irradiation, and 23 are beam facilities most of which are used for neutron scattering research. The following pages show a schematic layout of the beam facilities. More complete descriptions of instruments can be found at www.ncnr.nist.gov.

The NCNR supports important NIST research needs, but is also operated as a major national user facility with merit-based access made available to the entire U.S. technological community. Each year, over 1700 research participants from all areas of the country, from industry, academia, and government use the facility for measurements. Beam time for research to be published in the open literature is without cost to the user, but full operating costs are recovered for proprietary research. Access is gained mainly through a peer-reviewed, web-based proposal system with beam time allocated by a Program Advisory Committee twice a year. For details see www.ncnr.nist.gov/beamtime.html. The National Science Foundation and NIST co-fund the Center for High Resolution Neutron Scattering (CHRNS) that operates six of the world's most advanced instruments. Time on CHRNS instruments is made available through the proposal system. Some access to beam time for collaborative measurements with the NIST science staff can also be arranged on other instruments.

Why Neutrons?

Neutrons at the NCNR reveal properties not available to other probes. They can behave like microscopic magnets, can diffract like waves, or set particles into motion as they recoil from them.

Wavelengths – range from 0.1 Å to 100 Å, allowing them to form observable ripple patterns from structures as small as atoms to as large as proteins.

Energies – of millielectronvolts, the same as that of motions of atoms in solids or liquids, waves in magnetic materials, or vibrations in molecules. Exchanges of energy between neutrons and matter as small as nanoelectronvolts and as large as tenths of electronvolts can be detected.

Selectivity – in scattering power varies from nucleus to nucleus almost randomly. Specific isotopes can stand out from other isotopes, even of the same kind of atom. Specific light atoms, difficult to observe with x-rays, are revealed by neutrons. Hydrogen, especially, can be distinguished from chemically equivalent deuterium.

Magnetism – makes the neutron sensitive to the magnetic spins of both nuclei and electrons, allowing the behavior of ordinary and exotic magnets to be detailed precisely.

Neutrality – of the uncharged neutrons allows them to penetrate deeply without destroying samples, and pass through walls controlling a sample's environment allowing measurements under extreme conditions. Properties ranging from the residual stresses in steel girders to the unfolding motions of proteins are amenable to measurement by neutrons.

Capture – characteristic radiation emanating from specific nuclei capturing incident neutrons can be used to identify and quantify minute amounts of material in pollutants or ancient pottery shards.

Photography by Lynn A. Shuman

Instruments in the cold neutron guide hall.

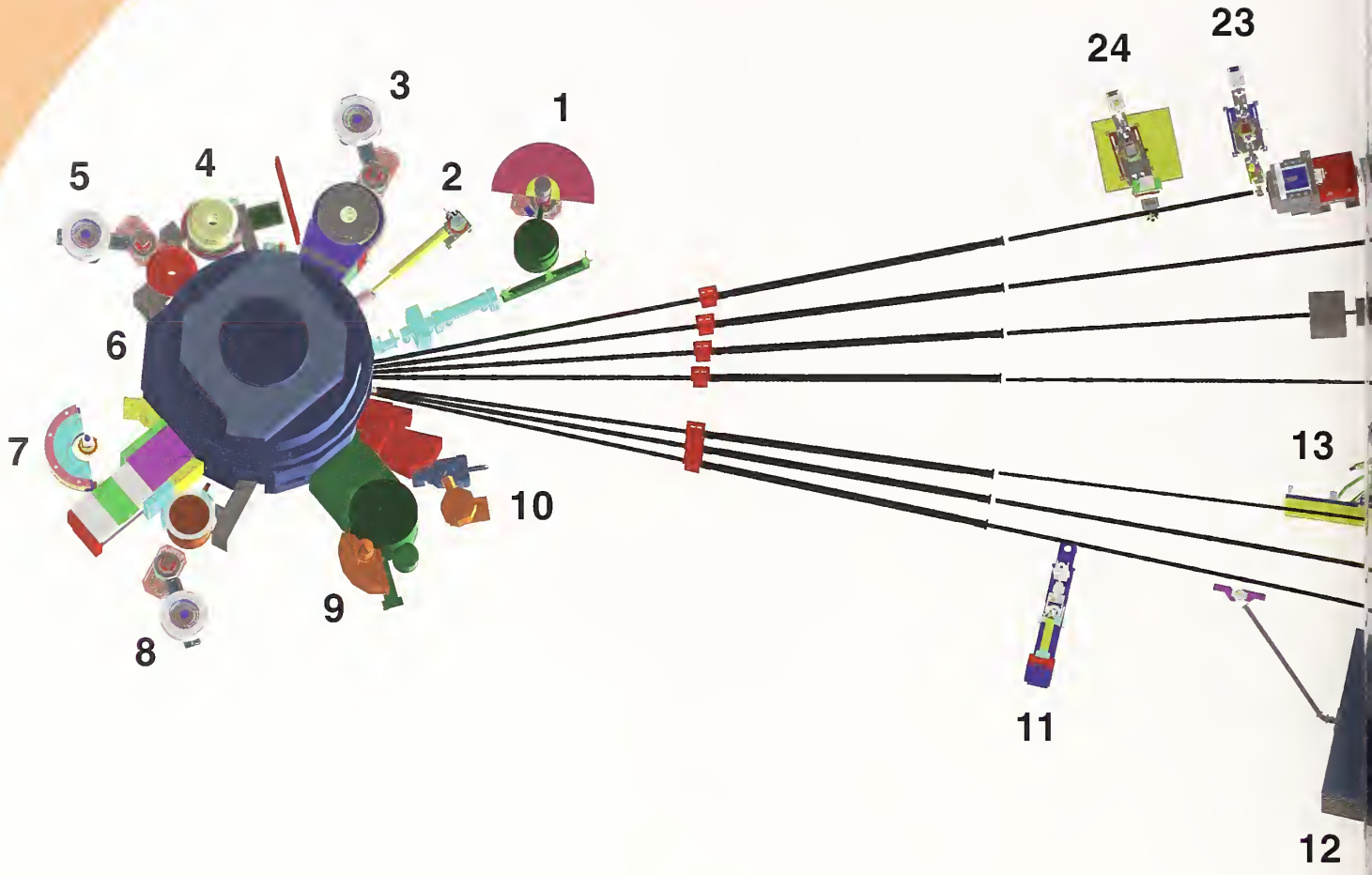

1 **A Cold Neutron Depth Profiling** instrument (not shown) for quantitative profiling of subsurface impurities currently at this site will be moved to another position. Shown is MACS, a cold neutron Triple Axis Crystal Spectrometer under construction with double focusing monochromator and multiple crystal analyzer/detectors that can be flexibly configured for several energies simultaneously or for high throughput at one energy.

2 **BT-6** (temporary location) **Neutron Imaging Facility** for imaging hydrogenous matter in large components such as water in fuel cells or lubricants in engines.

3 **BT-7 Triple Axis Crystal Spectrometer** with fixed incident energy for measurements of excitations and structure.

4 **BT-8 Residual Stress Diffractometer** optimized for depth profiling of residual stress in large components.

5 **BT-9 Triple Axis Crystal Spectrometer** for measurements of excitations and structure.

6 **Thermal Column** a very well-thermalized beam of neutrons used for radiography, tomography, dosimetry and other experiments.

7 **BT-1 Powder Diffractometer** with 32 detectors; incident wavelengths of 0.208 nm, 0.154 nm, and 0.159 nm, with highest resolution of $\delta d/d = 8 \times 10^{-4}$.

8 **BT-2 Triple Axis Crystal Spectrometer** with polarized beam capability for measurement of magnetic dynamics and structure.

9 **BT-4 Filter Analyzer Neutron Spectrometer** with cooled Be/Graphite filter analyzer for chemical spectroscopy.

10 **BT-5 Perfect Crystal Diffractometer SANS** small angle neutron scattering instrument for microstructure on the 10^4 nm length scale, sponsored by the National Science Foundation and NIST, part of the Center for High Resolution Neutron Scattering (CHRNS).

11 **NG-7 Horizontal Sample Reflectometer** allows reflectivity measurements of free surfaces, liquid vapor interfaces, as well as polymer coatings.

12 **Neutron Interferometry and Optics Station** with perfect silicon interferometer; vibration isolation system provides exceptional phase stability and fringe visibility.

13 **Spin Polarized Triple Axis Spectrometer (SPINS)** using cold neutrons with position sensitive detector capability for high-resolution studies — part of CHRNS.

NIST Center for Neutron Research Layout

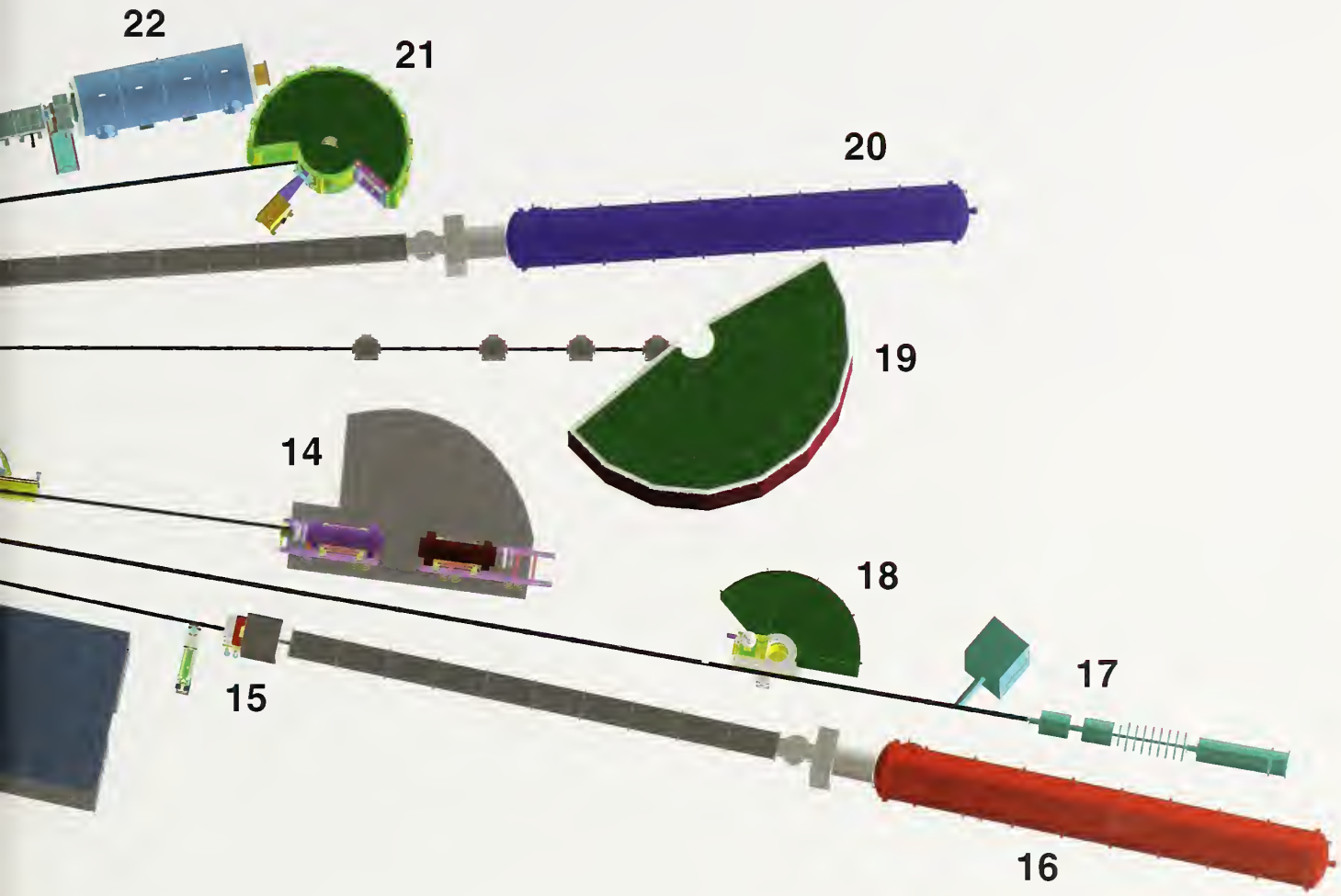

14 Spin Echo Spectrometer offering neV energy resolution, based upon Jülich design, sponsored by NIST, Jülich and ExxonMobil — part of CHRNS.

15 Prompt Gamma Activation Analysis cold neutron fluxes allow detection limit for H of 1 μg to 10 μg. Focused beams are available for profiling.

16 NG-7 30 m SANS for microstructure measurements sponsored by NIST, ExxonMobil, and the University of Minnesota.

17 Neutron Physics Station offering three cold neutron beams having wavelengths of 0.5 nm, 0.9 nm, and "white" that are available for fundamental neutron physics experiments.

18 Fermi Chopper hybrid time-of-flight (TOF) Spectrometer for inelastic scattering with selected incident wavelengths between 0.23 nm and 0.61 nm.

19 Disk Chopper TOF Spectrometer a versatile time-of-flight spectrometer, with beam pulsing and monochromatization effected by 7 disk choppers. Used for studies of dynamics in condensed matter, including macromolecular systems — part of CHRNS.

20 NG-3 30 m SANS for microstructure measurements sponsored by the National Science Foundation and NIST — part of CHRNS.

21 Backscattering Spectrometer high intensity inelastic scattering instrument with energy resolution < 1 μeV, for studies of motion in molecular and biological systems — part of CHRNS.

22 NG-1 10 m SANS (under construction.) It replaces the current 8 m SANS and will be made available for CHRNS use along with use by the NIST Polymers Division.

23 Vertical Sample Reflectometer instrument with polarization analysis capability for measuring reflectivities down to 10^{-8} to determine subsurface structure.

24 Advanced Neutron Diffractometer / Reflectometer (AND/R), a vertical sample reflectometer with polarization analysis and off-specular reflection capabilities for measuring reflectivities down to 10^{-8}. It is part of the Cold Neutrons for Biology and Technology program committed to studies of biological membrane systems.

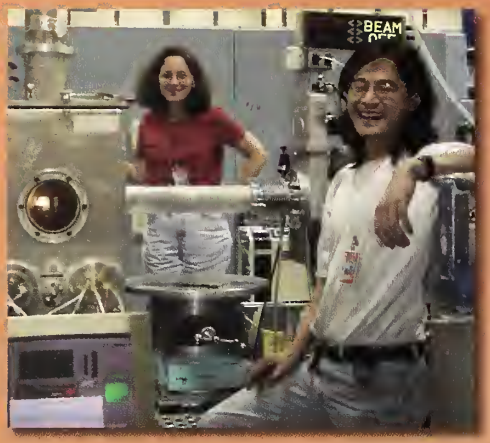

The flame produces *in situ* soot for a SANS study by WPI's Barb Wyslouzil and U Del.'s Hai Wang

NCNR's John Copley points out salient features of DCS to summer school students

Theory, Modeling and Neutron Scattering Workshop attendees, August 2003

Photography by Lynn A. Shuman

NCNR's Inma Peral (back to camera) and Yiming Qiu (second from right) with students watching and analyzing data at DCS

NCNR's Inma Peral prepares a cryostat at DCS

NCNR Images 2003

Photography by Lynn A. Shuman

NCNR's Richard Azuah extols the virtues of Backscattering to summer school fans

U. Bristol's Terry Cosgrove and collaborators take a pointer from NCNR's Lionel Porcar

Photography by Lynn A. Shuman

U Del.'s Eric Kaler discusses a SANS pattern with his group

SURF student Andrew Rockwell at the NG-1 reflectometer controls with NCNR's Chuck Majkrzak

Oberlin's Steven FitzGerald supervises his undergraduate collaborators loading a sample

Photography by Lynn A. Shuman

Look up and smile! NCNR's Seung-Hun Lee and Peter Gehring (rear) with summer school students at the SPINS analyzer

The Advanced Neutron Diffractometer/Reflectometer (AND/R)

The recently installed (July 2003) Advanced Neutron Diffractometer/ Reflectometer (AND/R) adds new capabilities for bio-membrane research and diffuse scattering measurement to the NCNR. It aims to provide a focal point for structural biology research, combining an increased in-house staff to serve and interact with an expanded user program. Furthermore, it will benefit the NCNR reflectometry program by increasing available beam time overall. Of the AND/R beamtime, 75 % will be available to the CNBT partners and 25 % to general users through the NCNR proposal system. With the AND/R located just upstream of NG-1 reflectometer, this pair of instruments will share common facilities, equipment, and expertise.

The AND/R is the centerpiece of the Cold Neutrons for Biology and Technology (CNBT) program, which is committed to the development of advanced neutron scattering instruments for studies of membrane systems. CNBT was funded by the National Institutes of Health (NIH), National Center for Research Resources on 30 September 2001 with additional support from NIST, the University of California at Irvine and the University of Pennsylvania. The CNBT partnership consists of investigators from six universities: UC Irvine (principal investigator Stephen H. White), Johns Hopkins University, Penn, Rice, Duke, Carnegie Mellon and investigators from NIST. Additional collaborators are from UC San Diego, Los Alamos National Laboratory, and the NIH. The facilities consist of the AND/R, a 30 m small-angle neutron spectrometer (SANS) dedicated 10 % to CNBT, a fully equipped biology laboratory, and two state-of-the-art computer facilities (one at U C Irvine, and one at NCNR) for molecular dynamics computations. This combination provides a new capability for the United States.

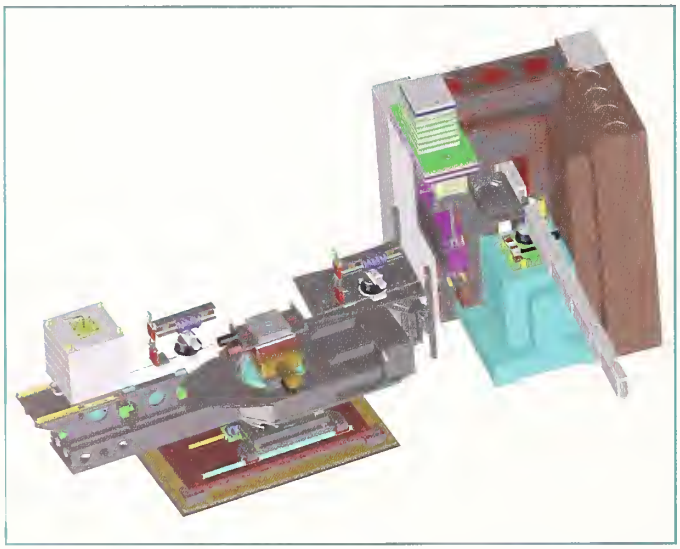

The Advanced Neutron Diffractometer Reflectometer, shown in polarized beam mode with the "pencil" detector enclosed within the box at left. (For clarity, some shielding is not shown.)

The AND/R is modeled after the highly successful polarized beam reflectometer on the NG-1 neutron guide. Like the NG-1 reflectometer, the AND/R will have a horizontal scattering plane, which provides unrestricted access to higher scattering angles. Other features common to both instruments are the polarized beam capability to enable the use of magnetic reference layers for phase inversion of data, and a vertically focusing monochromator to increase the flux on the sample.

Additional features make the instrument well suited for both reflectometry and diffraction investigations of biological systems. First, the AND/R can operate using either a larger 5 cm "pencil" detector (increasing the flux at higher momentum transfer, Q) or a 2-dimensional position sensitive detector (PSD). By simultaneously measuring non-specular scattering from large areas in reciprocal space, the PSD will make it much more efficient to obtain information on in-plane structures. Also, the sample tables will accommodate larger sample environments (up to 26 cm (10.2")) from tabletop to beam center and up to 454 kg (1000 lb) or an Eulerian cradle (for diffraction experiments from a single crystal). Variable sample to monochromator distance (from 206 cm (81") to 236 cm (93")) and sample to detector distances (from 61 cm (24") to 173 cm (68")) will allow the user to select the Q range covered by the PSD. Optical benches, both inside and outside the shutter, will make customization and upgrades of the neutron optical components simpler to implement. An increased number of motorized axes as well as additional supporting software provided by a dedicated programmer in the CNBT program will make this user-friendlier instrument.

A number of general areas of investigation of biological membrane and biomimetic thin film structures are currently envisioned for the AND/R instrument. These include specular reflectometry measurements to reveal the compositional depth profile along the surface normal (with spatial resolution approaching a fraction of a nanometer) as well as non-specular scattering studies of in-plane density variations and structures. The specular reflectometry can be performed on single bilayer membrane or multilayered systems to determine the location of certain macromolecular entities of biological interest, such as cholesterol, various toxins, or transmembrane proteins. Non-specular measurements of in-plane objects typically will require multilayered samples to obtain sufficient signal.

The NCNR cold source and guide combined with optimized neutron optics and the capabilities described above are expected to make measurements using AND/R especially well suited to addressing key scientific issues on biological membranes.

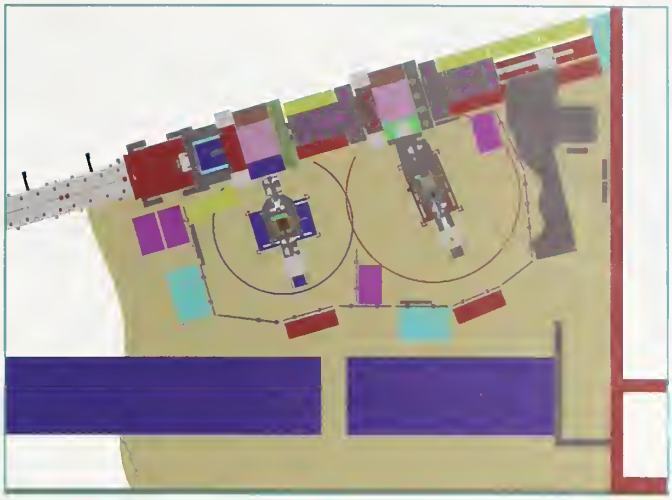

AND/R (right) and NG-1 Reflectometer floor plan. The large circles indicate the travel of the detector arm in its fully extended position. Blue, purple and red rectangles are the control desks, electronic racks and beamstops respectively. The instruments will be separated by both a fixed rail and a tensile barrier (not shown).

NCNR staff and CNBT visitors gather at the completed AND/R instrument. Left to right: Michael Paulaitis, JHU; Kevin O'Donovon, NCNR; Don Pierce, NCNR; Huey Huang, Rice; Steven White, UCI; Anne Plant, NIST Biotech; Mathias Lösche, JHU; Jack Rush, NCNR; Tom Macintosh, Duke; Joe Dura, NCNR; Susan Krueger, NCNR; Chuck Majkrzak, NCNR.

J. A. Dura, D. J. Pierce, C. F. Majkrzak
NIST Center for Neutron Research
National Institute of Standards and Technology
Gaithersburg, MD 20899

A New Neutron Imaging Facility at BT-6 for the Non-Destructive Analysis of Working Fuel Cells

A dramatic step toward analyzing the performance and the operational characteristics of a working fuel cell has taken place at the NCNR. A new Neutron Imaging Facility (NIF) shown in Fig. 1 has been constructed in a cooperative effort between the Department of Commerce and the Department of Energy. This facility uses neutrons to peer inside the fuel cell to view water forming and moving throughout the cell. In a fuel cell, water is formed as a by-product of the reaction between hydrogen and oxygen. If the water does not drain quickly and efficiently, then fuel cells will not work properly. Water formation is also a signature of activity in a fuel cell, so the lack of water formation demonstrates a defective area of the fuel cell.

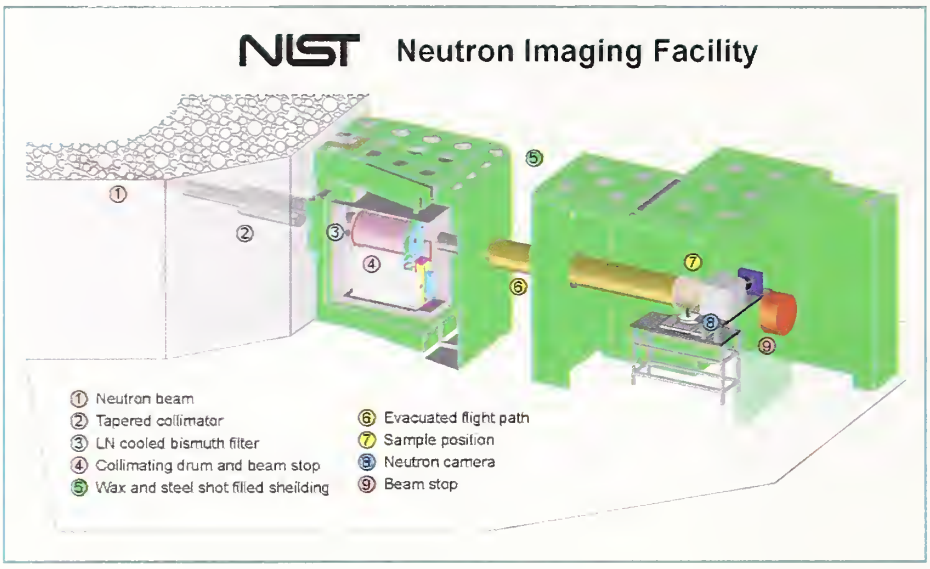

Fig. 1. The new thermal neutron imaging facility at the NCNR.

Since fuel cells are not transparent to visible light, other forms of penetrating radiation (example: x-rays, neutrons) must be used to analyze their operation. X-ray imaging is not suitable because hydrogen is nearly invisible to the high energy x-rays required to penetrate the metallic encasement of the fuel cell. Neutrons, which are neutral particles, can easily penetrate metals and still be extremely sensitive to water in quantities less than a microgram. The reason for this is best illustrated by a comparison of the relative scattering cross-sections shown in Fig. 2. The large x-ray cross-section of Al compares to a small neutron cross-section. Conversely the x-ray cross-section for hydrogen is small compared to the neutron cross-section. This makes neutrons ideal for sensing microgram quantities of water. An example of neutron imaging fuel cells is shown in Fig. 3. In the image the gas distribution system of a fuel cell shows up as the serpentine tracks. The purpose of these channels is to distribute gas evenly to the membrane and to act as a drain for water coming out. In these images the neutrons easily penetrate the fuel cell when dry. As the fuel cell runs, water builds up and appears as a darker shadow region of the images on the left. Computer analysis allows the scattering from the dry cell to be removed, revealing only the water formation in both the flow channels and the gas diffusion media, as shown in the colorized images on the right. Large amounts of water appear as red and dry regions appear as black.

Although this new facility has been constructed for the specific purpose of imaging fuel cells, it has potentially many other applications in industrial and applied research. Among these are imaging of automotive parts to study metal-casting techniques, oil lubrication in an automotive engine, and non-destructive analysis of archeological artifacts.

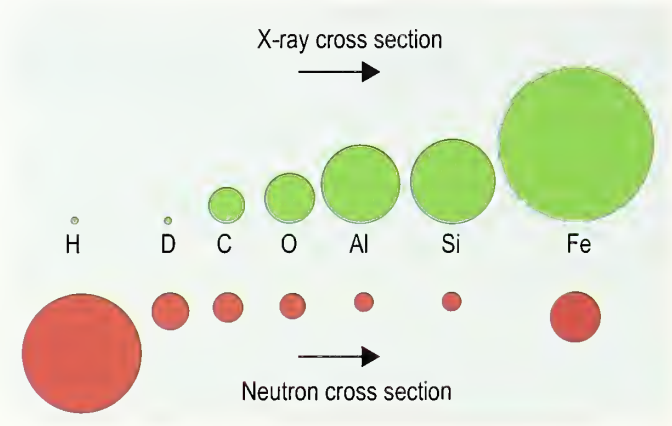

Fig. 2. Neutron and x-ray scattering cross-sections compared. Note that neutrons penetrate through Al much better than x rays do, yet are strongly scattered by hydrogen.

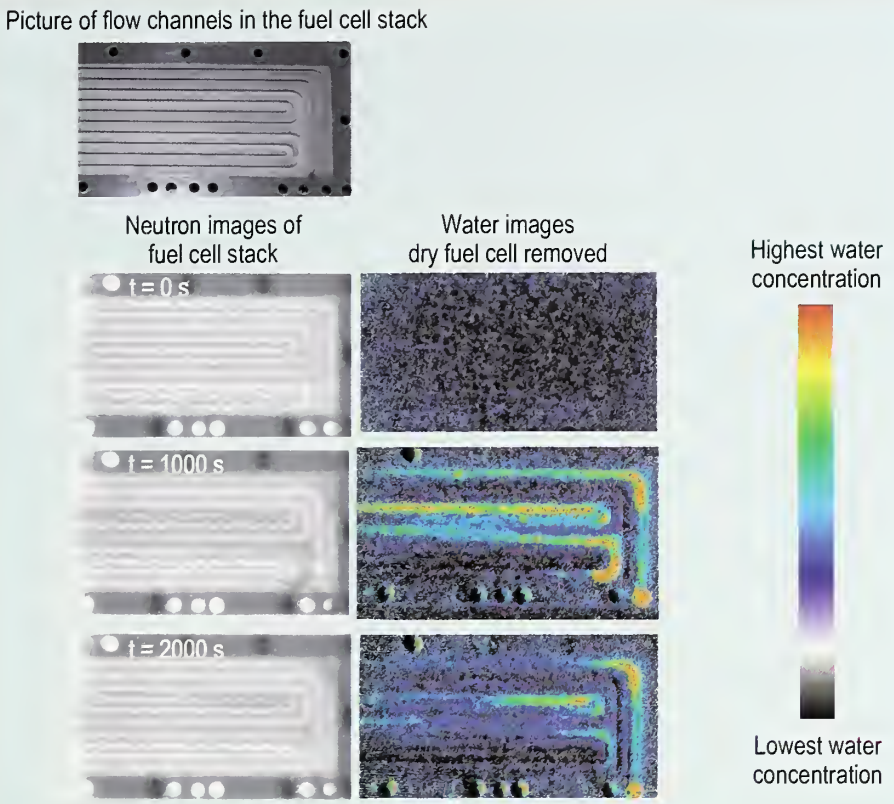

Fig. 3. A fuel cell: gas distribution channels shown disassembled on top. When assembled, images of the operating cell were taken every second for 2000 seconds. The water build-up in both the gas diffusion media and the flow channels is most clearly visible in the colorized images in which the underlying dry fuel cell has been computationally removed.

The very different sensitivities to various elements of x-ray and neutron scattering illustrated in Fig. 2 means that the two techniques could be considered complimentary methods of non-destructive analysis. Because of this broad range of applications, this facility was optimized for beam size, spatial resolution and neutron flux. Currently the beam exiting the collimator traverses ≈ 4 m and bathes the sample over an 18 cm diameter circle with a uniform neutron fluence rate of 10^8 cm^{-2} sec^{-1}, making it possible to image large objects (see Fig. 4.)

Future detector development of this method should be able to extend time resolution to the 30 ms level and spatial resolution to the 10 μm level. In addition, the methods of coded-source imaging could allow 3-dimensional imaging of the membrane and gas diffusion media. These developments would be able to provide a critical tool for fuel cell developers to analyze how small design changes affect a real fuel cell.

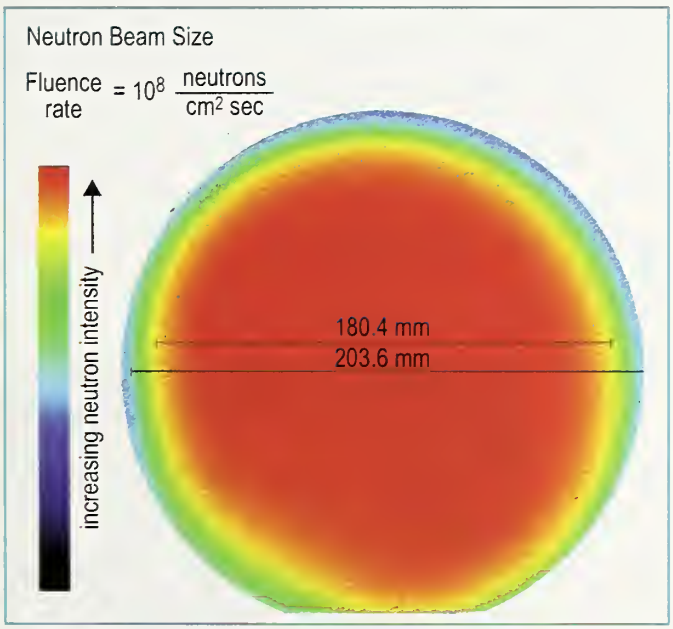

Fig. 4. Beam size at the sample position. The large diameter beam having a uniform fluence rate is important for imaging industrial scale objects.

D. Jacobson, M. Arif, and P. Huffman
Physics Laboratory Ionizing Radiation Division
National Institute of Standards and Technology
Gaithersburg, MD 20899

R. Satija
Duke University
Durham, NC 27708

Measurement of Deuterium Scattering Length

A recent high precision measurement of the scattering length, b, of deuterium gas has been performed using neutron interferometry at the NIST Neutron Interferometer and Optics Facility [1, 2]. Accurate measurement of the scattering length is important to the fundamental nature of how a neutron scatters from an atom. This scattering length depends on the nature of the nuclear potential, and, therefore, the prediction of this value is an important test for models of the nuclear potential. Currently only few nucleon systems can be accurately modeled, and measurements of scattering lengths of light nuclei are considered to be the most interesting. To date the most accurate methods to measure the scattering length have been neutron optical methods, and prior to this work the most accurate determination of the scattering length of deuterium has been that of gravity reflectometry. These neutron optical methods measure the bound coherent scattering length, b, by accurately determining the index of refraction, n, given by,

$$n = n_r + in_i \approx 1 - \sum_m \left[(N_m \lambda^2/2\pi)\sqrt{b_m^2 - (\sigma_m/2\lambda)^2} + iN_m \sigma_m (\lambda/4\pi) \right]. \quad (1)$$

In Eq. (1), m is the elemental species (important when correcting for contaminants); b is the local mean forward coherent scattering length averaged over the two spin dependent free scattering channels

$$b = \left(\frac{m_n + m_d}{m_d} \right) \left[(1/3)\,{}^2a_{nd} + (2/3)\,{}^4a_{nd} \right] \quad (2)$$

where ${}^{2S+1}a_{nd}$ (for S = total spin = [1/2 or 3/2]) are the free doublet and quartet scattering lengths; m_n is the neutron mass and m_d is the deuteron atomic mass; λ is the neutron deBroglie wavelength; σ is the total cross section made up of the scattering and absorption cross sections; n_r is the real part of the index of refraction; and N is the atom density of the material. For all elements the real part of n is nearly unity: the magnitude of $(n_r - 1)$ for typical neutron-nucleus potentials is approximately 1×10^{-5}. The imaginary part of Eq. (1) accounts for the attenuation of the wave amplitude due to scattering and absorption. Although such inelastic processes do not contribute to the interference of the amplitudes that travel on the two different paths through the interferometer since they make the path distinguishable in principle, they appear in the expression for the forward scattering amplitude as a result of the optical theorem. The interferometer efficiently filters out such inelastic processes that occur in the sample and in the Si interferometer blades.

Neutron interferometry is mainly sensitive to the real part of the refractive index by measuring the phase shift of a sample placed on one of two indistinguishable paths in the silicon neutron interferometer [3]. This phase shift can be written as

$$\Delta\phi = (n_r - 1)kD_{eff} = -\sum_m \lambda N_m b_m D_{eff} \quad (3)$$

where D_{eff} stands for the effective thickness of the medium along the direction of wave propagation. This phase shift can be very large; thus the neutron interferometric method is very sensitive to the index of refraction. Here we present the results of a measurement of the phase shift of a 1 cm thick sample of D_2 gas. The experimental setup for this measurement is shown in Fig. 1. The phase shift data converted to scattering length by inverting Eq. (3) are shown plotted in Fig. 2. Finally, averaging all values in Fig. 2 and combining the statistical and systematic uncertainties, we obtain the value for the scattering length b_{nd} = (6.665 ± 0.004) fm, which is plotted relative to previous measurements of the scattering length in Fig. 3. The new world average is then b_{nd} = (6.669 ± 0.003) fm,

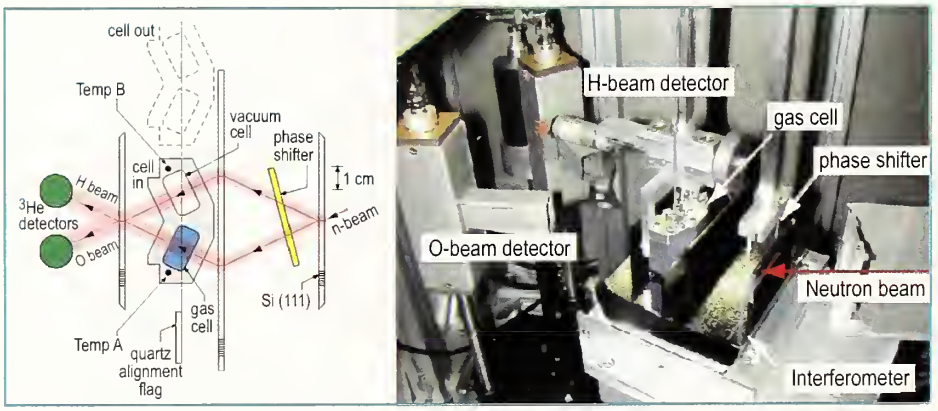

Fig. 1. A picture of the setup is shown on the right and a schematic plan view is shown on the left.

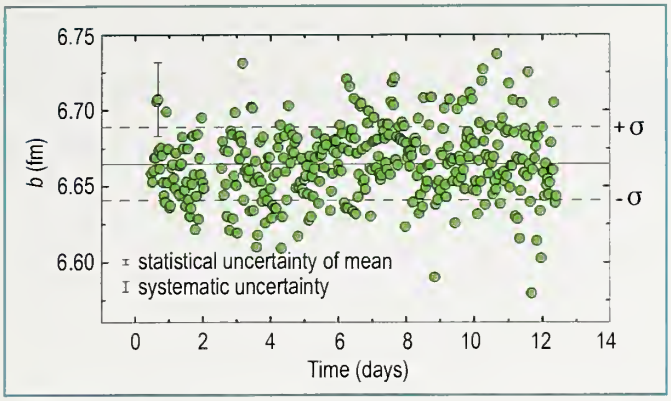

Fig. 2. All of the phase shift measurements made are shown here. The estimated statistical uncertainty per point agrees well with the statistical scatter of the data. The sizes of the final statistical and systematic uncertainties are also shown here for comparison purposes.

which is slightly lower than the previous world average of b_{nd} = (6.673 ± 0.0045) fm.

This measurement has improved on the uncertainty reported by previous interferometric measurements by more than a factor of 10, and by nearly a factor of two over the previous results from gravity reflectometry. Such precision measurements of the scattering length are important for various theories dealing with 3 nucleon forces (3NF). Looking back at Eq. (2), the quartet scattering length, which is a long-range nuclear interaction, can be calculated accurately from nucleon-nucleon potentials and is insensitive to 3NF effects that are currently used to calculate the shorter range doublet scattering length. Because the effective range function in the quartet spin channel is a smooth function of energy, the quartet scattering can be accurately extracted from an energy dependent phase shift analysis, so that experimental measurement of the bound coherent scattering length and theoretical calculation of the quartet scattering length allow

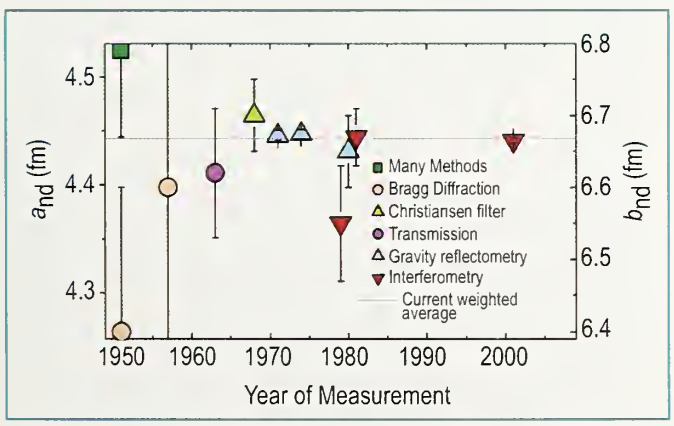

Fig. 3. Shown here are all the values and names of methods used to measure *b* for deuterium over the years. The average is a weighted average including all of these measurements.

the doublet scattering length to be extracted and compared to calculation using 3NF models. Only one of the scattering length calculations reported previous to this result falls within the (± 1)σ confidence band of this measurement shown in Fig. 4.

Future experiments will be able to lower the combined systematic and statistical uncertainty by as much as a factor of 5. This would allow one to measure higher order effects due to molecular binding in H_2 and D_2. Other elements such as ^3He and $^3H_2$ could also be measured with lower uncertainties than those currently in the open literature.

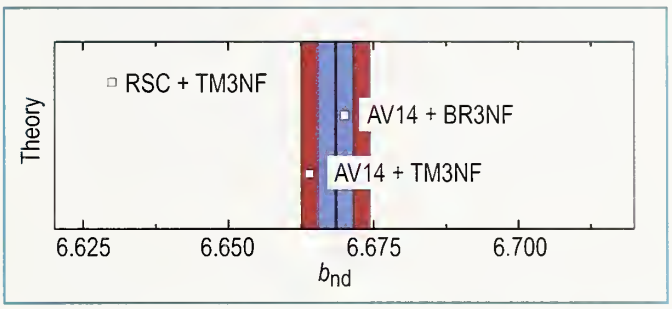

Fig. 4. The 1σ (blue) and 2σ (red) confidence intervals are shown here. Only two theories fall within 2σ of this result.

References

[1] T. C. Black, P. R. Huffman, D. L. Jacobson, W. M. Snow, K. Schoen, M. Arif, H. Kaiser, S. K. Lamoreaux, and S. A. Werner Phys. Rev. Lett. **90**, 192502 (2003).

[2] K. Schoen, D. L. Jacobson, M. Arif, P. R. Huffman, T. C. Black, W. M. Snow, S. K. Lamoreaux, H. Kaiser, and S. A. Werner Phys. Rev. C **67**, 044005 (2003).

[3] H. Rauch, S. Werner, *Neutron Interferometry: Lessons in Experimental Quantum Mechanics*, Oxford University Press, 2000.

P. R. Huffman, D. L. Jacobson and M. Arif
Physics Laboratory Ionizing Radiation Division
National Institute of Standards and Technology, Gaithersburg, MD 20899-8461

S. A. Werner
Physics Laboratory Ionizing Radiation Division
National Institute of Standards and Technology, Gaithersburg, MD 20899-8461
and
University of Missouri-Columbia, Columbia, MO 65211

K. Schoen and H. Kaiser
University of Missouri-Columbia, Columbia, MO 65211

T. C. Black
University of North Carolina at Wilmington, Wilmington, NC 28403-3297

W. M. Snow
Indiana University/IUCF, Bloomington, IN 47408
and

S. K. Lamoreaux
Los Alamos National Laboratory
Los Alamos, NM 87545

Demonstration of the Metrological Basis of Instrumental Neutron Activation Analysis

Instrumental neutron activation analysis (INAA) held a unique position in analytical chemistry and trace element research during the 1960s and 1970s and has continued to prosper with applications in environmental sciences, biology, medicine, archaeology, criminology, geo- and cosmo-chemistry, and industry. Its position, nevertheless, has been challenged by increasingly sensitive and versatile elemental analysis techniques, such as atomic absorption spectrometry, inductively coupled plasma emission spectrometry and mass spectrometry, which today are used widely in applications that had been a domain for INAA. However, INAA techniques still occupy a solid niche in analytical chemistry because of the nuclear principle of analysis with its unique advantages, such as the insensitivity to the chemical form, as well as the ability to completely describe the analytical process with mathematical equations of well-determined parameters having known uncertainties. These principles form the metrological basis of INAA; this experimental work explores and demonstrates the seamless integration of the experimental requirements with the nuclear physics principles for highest quality in the results.

In its most common form, the comparator technique, the INAA procedure compares, by means of gamma-ray spectrometry, the neutron-induced activities in an unknown sample with the activities induced in a standard with known composition. This relationship is shown in the equation:

$$C_x = \left(C_z \cdot \frac{A_{0x}}{A_{0z}} \cdot R_\theta \cdot R_\phi \cdot R_\sigma \cdot R_\varepsilon \cdot R_\theta - B \right) \cdot \frac{m_z}{w m_x}$$

where C_x is the analyte amount content in the unknown sample, with C_z the analyte amount content in the primary assay standard, m_x and m_z are the masses of sample and primary assay standard with a dry mass correction factor w if applicable. The decay corrected counting rates for the indicator gamma-ray of unknown A_{0x} and of standard A_{0z} are derived from the measurement. The ratios of isotopic abundances R_θ for unknown and standard, of neutron fluences R_ϕ (including fluence drop off, self shielding, and scattering), of effective cross sections R_σ if neutron spectrum shape differs from unknown to standard, and of counting efficiencies R_ε (differences due to geometry, γ-ray self shielding, and counting effects), are controllable experimental parameters. The highest accuracy is usually attained when the measurement conditions are so designed that the ratio factors R are near unity. INAA can be carried out essentially blank free, but possible contributions from interferences, background, or contamination are considered with the term B. The decay corrected gamma-ray counting rate (A_0) for a measured nuclide is calculated according to $A_0 = N \lambda \exp(\lambda t_1) / [1 - \exp(-\lambda \Delta)]$ where N is the number of counts measured in the indicator gamma-ray peak, with normalization to the end of irradiation ($t = 0$) calculated using λ, the decay constant for the indicator nuclide, t_1, the decay time to start of count, and Δ, the elapsed time of count.

To illustrate the performance of INAA, we selected the determination of chromium in SRM 1152a Stainless Steel by direct non-destructive comparison with the pure metal in the form of crystalline chromium. The experimental plan was guided by setting a goal of minimizing the uncertainty in the analytical procedure as much as was reasonably achievable; in the case of SRM 1152a, this uncertainty should be comparable or smaller than the uncertainty of the certified value. A review of the uncertainty parameters in the determination of amount content by INAA guided the selection of sample and standards preparation, irradiation, and counting processes to achieve the stated goal.

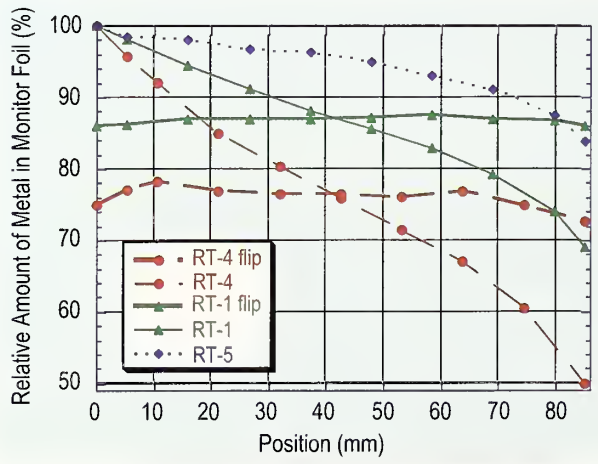

Fig. 1. Plot of the flux gradients found along the axis of the irradiation rabbits in three NBSR irradiation channels depicted by INAA of zinc (RT-4) and nickel (RT-1, RT-5) flux monitor foils, metal amount content based on a foil in position "0 mm" (100 %). When the rabbit is flipped at the irradiation mid point, a nearly linear average flux distribution is found in the center of the rabbit.

Table 1. INAA results achieved in inter-laboratory comparisons conducted under the auspices of CCQM.

	Matrix	Element	Mass Fraction			
CCQM number			Unit	Value	Expanded Uncertainty	Relative Uncertainty
P-25	Low Alloy Steel	Cr	%	0.4863	0.0031	0.64 %
		Mn	%	0.4478	0.0037	0.83 %
		Mo	%	0.9442	0.0154	1.63 %
P-34	Aluminum	Cr	%	0.4097	0.0025	0.61 %
		Mn	%	0.3892	0.0038	0.98 %
		Fe	%	0.3594	0.0067	1.86 %
		Cu	%	0.2063	0.0049	2.38 %
P-11	Oyster Tissue	As	µg/g	9.645	0.112	1.16 %
K-31	Oyster Tissue	As	µg/g	8.397	0.160	1.91 %
K-24	Rice Flour	Cd	nmol/g	14.30	0.33	2.31 %
P-29	Rice Flour	Zn	nmol/g	355.9	8.5	2.39 %

The neutron fluence distribution over the sample set was determined as one key component in minimizing uncertainties. For this work, flux gradients in all three pneumatic irradiation channels of the NBSR were re-determined with metal foil flux monitors. The 0.1 mm thick, 6 mm diameter foils of Zn or Ni were positioned in the irradiation rabbit along the axis. The thin foils provided an exact axial location for the estimation of the gradients; radial gradients have been found negligible [1]. Figure 1 illustrates the range of fluence drop-off over the length of the irradiation capsule. An INAA determination of the metal amount in Zn or Ni foils, based on the proximal "0 position" foil as the standard, gives directly relative flux values. The steeper gradients towards the ends of the rabbit may be explained by some channeling of neutrons towards the rabbit at the proximal end, and the void of the flight tube at the distal end. The observed linear drop-off in RT-1 and RT-4 between 20 mm and 65 mm provides a nearly homogeneous neutron field for samples placed in this space when the capsule is inverted at mid-point of the irradiation. This is shown with the data from the flipped irradiations. Small deviations from a unity level remain in the center space and are best assayed with flux monitors or sample matrix elements (*e.g.*, iron in steels) in each irradiation set.

Other measures to minimize uncertainty included careful control of neutron self-shielding and gamma-ray self-absorption in samples and standards, correction for remaining small counting geometry differences, and full accounting of dead time and pile-up losses in the gamma-ray spectrometer via the virtual pulse technology [2]. Sufficiently large ($> 10^6$) numbers of counts were acquired for the indicator gamma rays for samples and standards. Applying the discussed measures, an arithmetic mean value of 17.768 % Cr was obtained from eight determinations. This compared very well with the certified value of (17.76 ± 0.04) % Cr. The expanded uncertainty of 0.035 % Cr (0.2 % relative) met the goal of the experimental work.

The Nuclear Methods Group is using this INAA comparator method in highly precise and accurate measurements in the comparisons organized by the Consultative Committee for Amount of Substance (Comité Consultatif pour la Quantité de Matière, CCQM); Table 1 summarizes the recent contributions. This work has provided results in excellent agreement with reported values and has shown that the principle is applicable to the determination of all concentration levels: major elements are determined with similar accuracy as trace elements. The largest components of uncertainty are related to the sample material. In case of the metal analyses, the values of uncertainty in the fluence ratio R_ϕ were larger than in the determinations of SRM 1152a, since the test materials were in form of rather irregular metal chips. In the determinations of the biological materials, the uncertainty in the moisture correction w was the most significant factor that contributed to the reported uncertainty. In all instances, the reported INAA uncertainties were comparable to or smaller than the other techniques' uncertainties.

The measurements are subject to some restrictions that are dependent on the form and composition of the samples provided. High-density materials with high macroscopic neutron absorption cross sections require corrections for the fluence ratio based on measurements of uniform dimensions (thickness) of the samples and knowledge of the complete sample composition. These corrections call for careful experimental design and may limit the applicability of INAA in the analysis of these materials. The applications in light matrix (biological) samples are governed by "unity" ratios with associated small uncertainties. In addition, the non-destructive nature of the INAA procedures offers a true alternative to techniques that require dissolution, a sometimes troublesome process. Direct comparison with primary elemental standards provides desirable traceability of the amount of substance of an element.

References

[1] D. A. Becker, J. Radioanal. Nucl. Chem. **244**, 361 (2000).

[2] G. P. Westphal, J. Radioanal. Chem. **70**, 387 (1982).

R. Zeisler, R. M. Lindstrom, E. A. Mackey, and R. R. Greenberg
Analytical Chemistry Division
National Institute of Standards and Technology
Gaithersburg, MD 20899-8395

Structural and Vibrational Characterization of Tetracene as a Function of Pressure

The multi-billion dollar electronic and optical device industry is always searching for inexpensive and adaptable materials for use in a wide variety of applications such as display screens for communications, entertainment and computers. Semiconducting organic molecules are currently under intense investigation in this regard as it is possible to precisely tune their properties through synthetic modification and to easily control self-assembly. However, for the full promise of organic semiconductors to be realized, a thorough understanding of the physical properties that control electronic charge transport and photonic behavior is required.

Tetracene, an aromatic molecule consisting of 4 fused benzene rings, adopts a layered, herringbone structure in the solid state (Fig. 1). When a layer of tetracene is incorporated as the functional component of a field effect transistor, the edge-on-face molecular orientation within the *ab*-plane of the crystal evidently provides sufficient π-electron cloud overlap between adjacent molecules to enable conduction of charge carriers. Conduction measurements have been performed on tetracene as a function of pressure between ambient and 620 MPa at room temperature [1]. The results indicate a linear increase in conductance between ambient pressure up to ≈ 300 MPa and a sharp quenching of conduction as the pressure is increased above 300 MPa. In order to ascertain the physical underpinnings of this observation (which yield insight into the conduction mechanism), neutron powder diffraction and inelastic neutron scattering measurement techniques have been employed to characterize the pressure-dependent structural and vibrational behavior of tetracene up to approximately 360 MPa at 298 K.

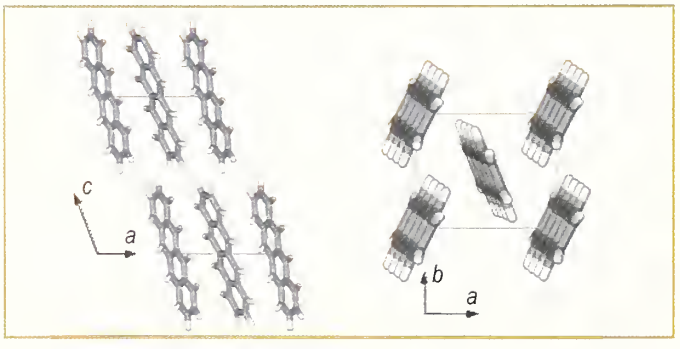

Fig. 1. The crystal structure of tetracene.

The diffraction data were collected at NCNR's High Resolution Neutron Powder Diffractometer at BT-1 using the Cu(311) monochromator and neutron wavelength of 1.54 Å. The six unit-cell parameters were extracted by fitting the powder diffraction patterns using the graphical user interface EXPGUI to the General Structure Analysis System (GSAS) program assuming the known solid tetracene structure [2, 3].

These unit cell parameters are shown as a function of pressure in Fig. 2. As the pressure is increased, each side of the unit cell contracts, resulting in a material with a higher electron density. It is likely that the increase in electron density accounts for the observed increase in conduction in tetracene at pressures up to 300 MPa. However, apparent from the unit cell angle parameters alpha and gamma is a modification of the crystalline structure between 210 MPa and 280 MPa. The change in trend of the unit cell angle parameter is likely due to a strain-induced phase transition that is believed to result in the relative rotation of adjacent tetracene molecules within the herringbone layer [4]. It is thought that this structural modification is of sufficient magnitude to disrupt the continuous π-electron cloud overlap in the low-pressure phase of tetracene to the extent that it is no longer able to conduct charge carriers.

In order to ascertain the role of molecular vibrations on the conduction behavior of tetracene as a function of pressure, inelastic neutron scattering (INS) spectra were collected using the NCNR Filter Analyzer Spectrometer at BT-4. The INS spectra at ambient, 218 MPa, and 359 MPa pressures are shown in Fig. 3. In addition to the experimental data, a theoretical spectrum was constructed from the results of an *ab initio* density functional theory (for an individual molecule) employing the B3LYP functional and 6-31-G* basis set. The spectral peaks in the experimental data at 27, 41, and 47 meV are affected relatively strongly by the application of pressure (indicated by their shifts to higher energy), whereas the peaks at 34 and 59 meV are moderately shifted and the peaks at 37, 56 and 68 meV display almost no shift with increasing pressure.

Trajectories defining the atomic displacement of the tetracene molecule for each calculated vibrational mode observed in the experimental data are schematically depicted in Fig. 4. The vibrational modes of tetracene can

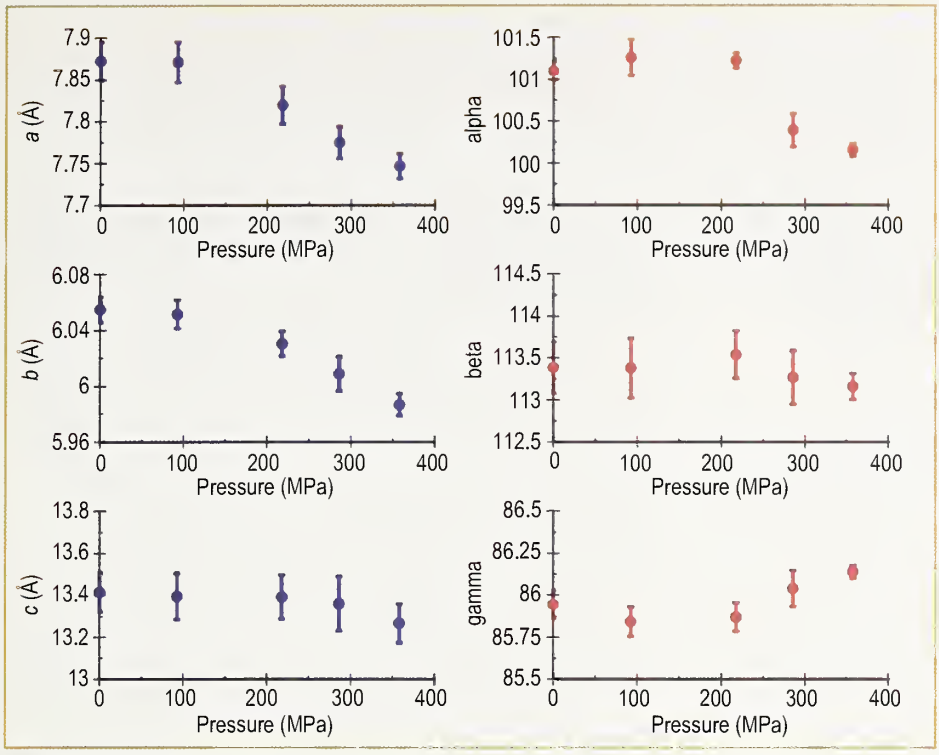

Fig. 2. The unit cell parameters of tetracene as a function of pressure at 298 K determined by fitting the neutron powder diffraction data with EXPGUI and GSAS.

be divided into two types of motions, occurring either within or perpendicular to the *ab* crystal plane. Comparison of the vibrational trajectories with the peak shifts observed in the INS data indicates that vibrational modes occurring within the *ab* crystal plane are affected by the application of pressure and those perpendicular remain unaffected. Because the vibrational modes do not indicate a discrete change in behavior upon transition to the high pressure structural phase, it appears that the phase transition does not affect the dynamic behavior of the molecules within the resolution and pressure range of these experiments.

In summary, we have utilized neutron scattering to investigate the physical properties of tetracene as a function of pressure. The conduction mechanism appears to be more strongly dependent on the structural arrangement of molecules within the crystal lattice, most likely associated with changes in π-electron cloud overlap, than on the vibrational behavior of the molecules. Further studies on a series of molecules will indicate whether this observation is generic to all organic semiconductors or unique to tetracene.

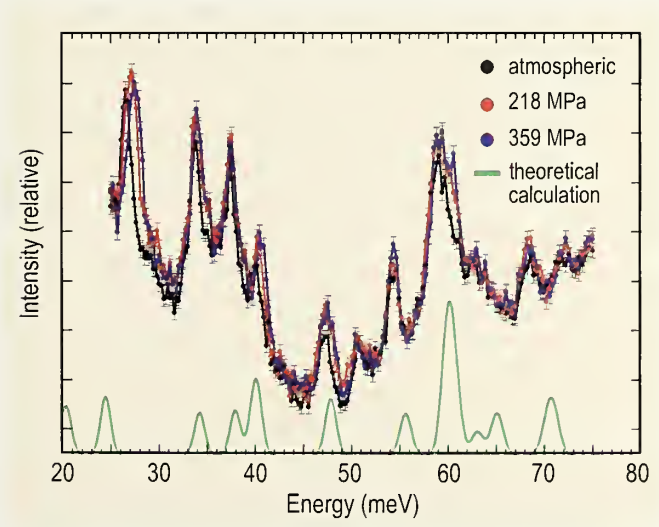

Fig. 3. Inelastic neutron scattering spectra of tetracene at 298 K at pressure and the theoretically calculated spectrum of a tetracene molecule.

References

[1] Z. Rang, A. Haraldsson, D. M. Kim, P. P. Ruden, M. I. Nathan, R. J. Chesterfield, and C. D. Frisbie, Appl. Phys. Lett. **79**, 2731 (2001).

[2] B. H. Toby, J. Appl. Cryst. **34**, 210 (2001).

[3] A. C. Larson and R. B. von Dreele, Los Alamos National Laboratory Report LAUR 86-748 (2000).

[4] R. Jankowiak, H. Bässler, and A. Kutoglu, J. Phys. Chem. **89**, 5705 (1985).

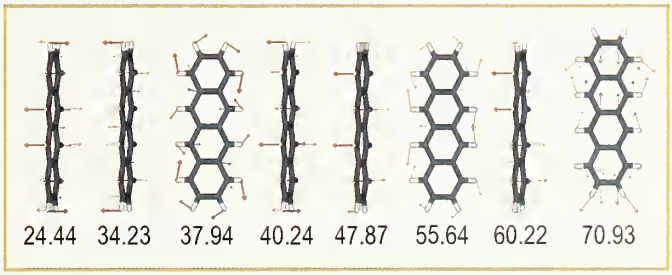

Fig. 4. Schematic representation of the atomic trajectories of the theoretically calculated vibrational modes of tetracene between 20 meV and 75 meV.

A. M. Pivovar and J. B. Leao
NIST Center for Neutron Research
National Institute of Standards and Technology
Gaithersburg, MD 20899-8562

R. J. Chesterfield and C. D. Frisbie
University of Minnesota
Minneapolis, MN 55455-0132

Fast Dynamics in Stabilization of Proteins

Proteins can be effective agents for catalysis and biochemical signaling, but to provide an appreciable shelf life, as needed in fields like regenerative medicine or biopharmaceuticals, one must stabilize these inherently labile species under dry, in-vitro conditions. Nevertheless, it is anticipated that proteinaceous pharmaceuticals will account for half of all the new drugs in the next 10 to 20 years [1]. It is also understood that tissue scaffolds for regenerative medicine need to contain stabilized signaling protein or DNA. Protein preservation is becoming a critical technology. However, according to Robert Langer, Chair of the FDA's Science Committee, improving protein stabilization technology is now one of the greatest challenges in the fields of biomaterials and pharmaceuticals.

Preservation can be achieved by embedding a protein in a glassy matrix, typically a polyalcohol or sugar. Ideally the stabilized protein is reconstituted under physiological conditions when its function is required. Unfortunately though, there is a loss of activity that increases as a function of storage time. Understanding the reasons for this loss of protein activity is a complex problem. From a thermodynamic perspective it is important that the preservation matrix have the ability to "replace" water in terms of the hydrogen bonding with the hydrophilic shell of the protein. However, water replacement alone is not sufficient; not all hydrogen bonding glass-forming compounds are effective preservation materials. In the present we illustrate the importance of dynamics in the glassy matrix for stabilizing proteins.

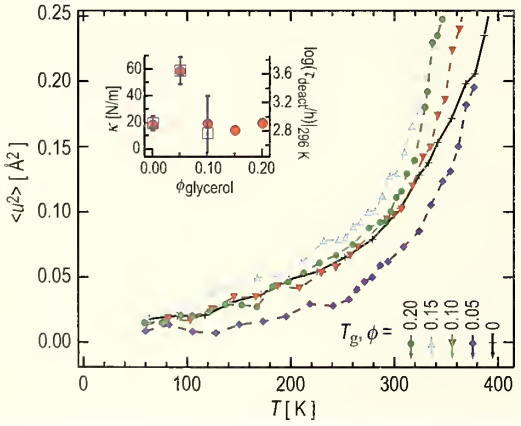

Fig. 1. Debye-Waller factors from trehalose glasses with $\phi_{glycerol}$ = (+) 0, (♦) 0.05, (▼) 0.10, (▲) 0.15, and (●) 0.20. Inset: "spring constants" of low temperature glasses (left axis), and HRP stability lifetimes (right axis).

Previous studies showed that the stability of horseradish peroxidase (HRP) and yeast alcohol dehydrogenase (YADH) could be significantly improved embedding these proteins in glassy trehalose diluted with small amounts of glycerol [2]. Here we use the High Flux Backscattering Spectrometer (HFBS) and the Fermi-Chopper time-of-flight Spectrometer (FCS) to illustrate that effective preservation is achieved through a suppression of picosecond to nanosecond relaxations and/or *collective* atomic vibrations. These local motions in the glass couple to the protein and suppress the necessary precursor motions that ultimately lead to larger scale motions that occur on the typical physiological time and length scales.

Fig. 1 shows the hydrogen-weighted average mean square atomic displacement $\langle u^2 \rangle$ for a series of lyophilized trehalose glasses diluted with increasing amounts of glycerol. The Q-dependence of the incoherent elastic scattering from the HFBS spectrometer is analyzed in terms of the Debye-Waller factor to extract $\langle u^2 \rangle$ from a simple harmonic oscillator approximation, whereby $I_{elastic} \propto \exp(-Q^2\langle u^2 \rangle/3)$. As the temperature T increases there is a decrease in $I_{elastic}$ and $\langle u^2 \rangle$ is simply proportional to the slope of $\ln(I_{elastic})$ vs Q^2 at any given T. The 0.85 μeV energy resolution of the HFBS means that only motions faster than 200 MHz give rise to an increase of $\langle u^2 \rangle$; slower motions are seen as static.

The signatures of an effective preservation glass are immediately evident in the T dependence of $\langle u^2 \rangle$ in Fig. 1. Namely, the best protein preservation glass ($\phi_{glycerol}$ = 0.05) yields the smallest values of $\langle u^2 \rangle$. Below 250 K the nearly linear T dependence of $\langle u^2 \rangle$ and the harmonic oscillator approximate can be used to calculate an effective spring constant (κ) for the glass. The inset shows a pronounce peak in κ (left axis) at $\phi_{glycerol}$ = 0.05. The inset to Fig. 1 also displays the time constant for degradation of HRP (τ_{deact}) in room-temperature trehalose glasses as a function of $\phi_{glycerol}$. At $\phi_{glycerol}$ = 0.05, where the suppression of $\langle u^2 \rangle$ is the greatest, the HRP stability is the greatest, more than five times better than the undiluted trehalose. While we do not show the data, the same effect is observed for YADH.

Parameters τ_{deact} (room T) and κ (below 250 K) are determined from different T regimes. To better correlate dynamics and preservation, Fig. 2 parts (a)-(c) shows the $1/T$ dependencies of $1/\langle u^2\rangle$, τ_{deact} for HRP, and τ_{deact} for YADH over the same T regime. The motivation for Fig. 2(a) comes from the empirical observation that log(viscosity) is proportional to $1/\langle u^2\rangle$ [3]. The data trends of panels (a)-(c) are summarized in panel (d) in terms of the apparent activation energies, E_a, defined by the slopes of the lines. All three data sets show a maximum of E_a at $\phi_{glycerol} = 0.05$, indicating that suppressing the 200 GHz and faster dynamics of the glass leads to enhanced protein stability.

We can gain further insight into the dynamics that facilitate protein degradation by looking at the relative ratio of the relaxations reflected in the quasielastic scattering (QES) to the collective atomic vibrations boson peak intensities (BP). Fig. 3 shows a typical $S(Q,E)$ spectrum for trehalose at 100 K obtained from a FCS measurement.

The minimum in the spectrum at –1.7 meV can be used, in a model-independent way, to delineate the relative strength of oscillatory and relaxational dynamics; integrating the green and blue areas provides a relative comparison of the BP and QES intensities respectively. In the inset to

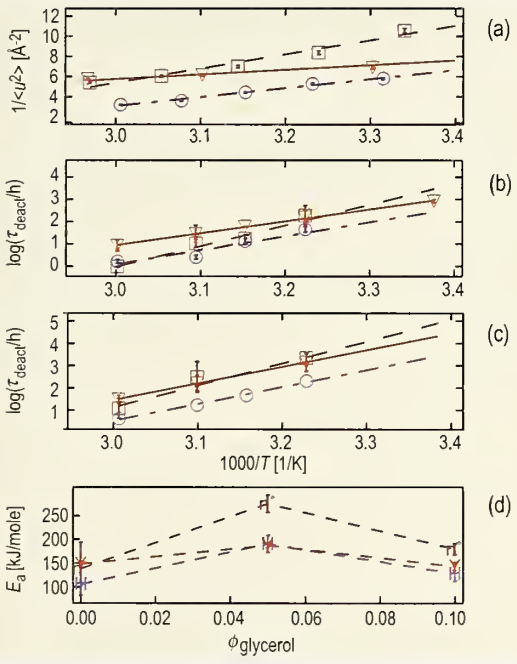

Fig. 2. Enzyme preservation and dynamics in plasticized trehalose glasses with $\phi_{glycerol}$ (▼) 0, (■) 0.05, and (●) 0.10. Panel (a) shows $1/\langle u^2\rangle$, which is proportional to local dynamics (see text). Panel (b) shows HRP activity lifetimes, and panel (c) shows YADH activity lifetimes. Panel (d) shows apparent activation energies as a function of glycerol content measured by HRP lifetimes (H), YADH stability (Y), and $1/\langle u^2\rangle$ (n°). Error bars represent standard uncertainties of +/- 1 standard deviation.

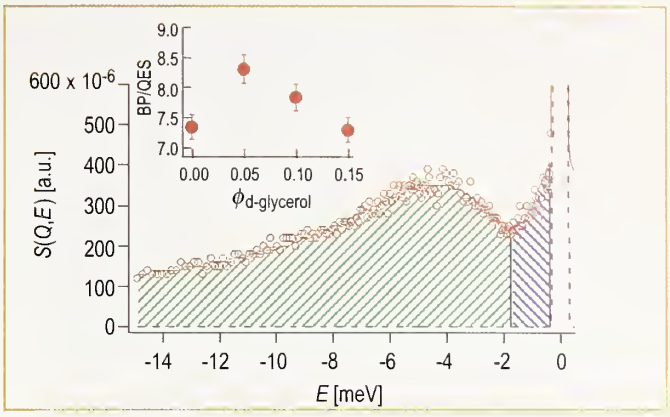

Fig. 3. Inelastic scattering response for trehalose at 100 K (○). See text for explanation of crosshatched areas. Inset, estimate of boson peak to quasielastic scattering integrated intensities.

Fig. 3 there is a maximum in the relative ratio of picosecond vibrations to relaxations at $\phi_{glycerol} = 0.05$, coincident with the peaks in κ and protein stability. The suppression of relaxations relative to the vibrations in the best preservation matrix is consistent with the fact that diffusive type motions ultimately lead to protein deactivation. These diffusive motions could be simple like the diffusion of a reactive gas through the matrix into the protein or complex like the irreversible unfolding of the protein.

We have shown for the first time that fast ($\omega > 200$ MHz) dynamics of the host glass are crucial in stabilizing proteins. This is consistent with recent light scattering data that indicates that the protein dynamics couple to the glassy host, even in very viscous media [4]. When formulating a glassy matrix for preservation, it is important to tune the high frequency coupling such that the glass suppresses the protein dynamics. Previous folklore implied that high T_g glasses make better preservation materials. This was based on the notion that deeper in the glassy state the protein would be more effectively suspended in a vitreous state of animation. However, a higher T_g does not necessitate suppressed dynamics at the relevant pico- to nanosecond time scales, as illustrated here. Adding small amounts of glycerol to trehalose decreases the T_g, but yields a superior preservation matrix.

References

[1] C. M. Henery, C&E News **78** (43), 85 (2000).

[2] M. T. Cicerone, A. Tellington, L. Trost, and A. Sokolov, BioProcess Intl. **1** (1), 23 (2003).

[3] U. Buchenau and R. Zorn, Europhys. Lett. **18** (6), 523 (1992).

[4] G. Caliskan, D. Mechtani, S. Azzam, A. Kisliuk, M. T. Cicerone and A. P. Sokolov, submitted.

M. T. Cicerone and C. L. Soles
Polymers Division
National Institute of Standards and Technology
Gaithersburg, MD 20899-8541

Bio-Membrane Flexibility Studied in the Presence of Cholesterol and Salt

Living cell membranes are made of phospholipids assembled in two-dimensional bilayers in such a way that the hydrophobic chains are being shielded from the surrounding water as illustrated in Fig. 1. Due to their extreme softness the phospholipid bilayers exhibit thermal undulations in an aqueous environment that give rise to repulsive forces between the cells or between cells and substrates. These forces govern important phenomena in the life process such as cell coagulation and the ability of the cells to sense and react to their surroundings. Here, we report results on the thermal undulations of phospholipid bilayers obtained through the Neutron Spin Echo (NSE) method, the only technique covering the time scale of these motions, 1 ns to 10 ns [1, 2].

The thermal undulations of phospholipid bilayers are strongly dependent on the mechanical properties of the bilayer such as the bending elasticity. Following earlier studies by other methods [3, 4] we have studied the dynamics of a model system, multilamellar vesicles (MLV, see Fig. 1) in water, as a function of temperature, the presence of cholesterol, and the presence of salt. Temperature is expected to influence several properties. Increase in temperature decreases the solvent viscosity and increases the thermal undulation amplitudes. The hydrophobic core of the phospholipid membranes exhibits a sharp phase transition from the crystalline to the liquid phase at a certain temperature T_c that depends on the length of the hydrophobic chains. Above T_c the interior of the phospholipid membrane is much more disordered and is expected to be less rigid. Cholesterol, an important constituent of the living cell, nestles in between the fatty tails, changing the mechanical properties of the bilayers and hence their motions. Finally, the presence of sodium chloride as an electrolyte has a screening effect on electrostatic interactions and may affect the thermal undulations of electrostatically charged bilayers.

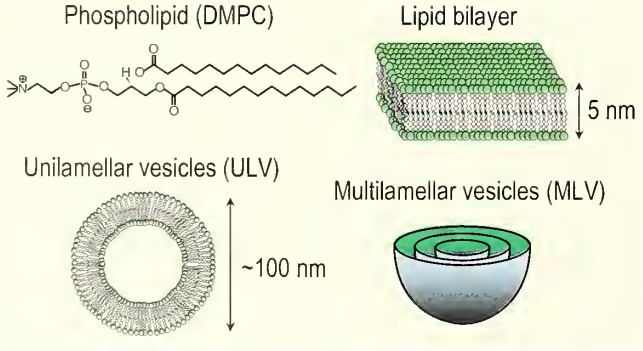

Fig. 1. Illustrations of a typical phospholipid (DMPC), a phospholipid bilayer, a unilamellar vesicle and a multilamellar vesicle.

Three MLV samples are prepared for this study. Sample I ("vesicles"), which serves as a reference, is a MLV made mainly of 1,2-Dimyristoyl-sn-Glycero-3-Phosphocholine (DMPC) in deuterated water (D_2O) to provide scattering contrast. The DMPC vesicles were stabilized through enhanced electrostatic repulsion between the bilayers by addition of a small amount (0.05 mol to 1 mol DMPC) of 1,2-Dimyristoyl-sn-Glycero-3-[Phospho-rac-(1-glycerol)]-sodium salt (DMPG), a phospholipid that is structurally similar to DMPC. In sample II ("vesicles & chol") cholesterol was added in the ratio of 0.3 mol cholesterol to 1 mol of lipids. In sample III ("vesicles & salt") 0.05 mol L^{-1} of NaCl was added. MLV were prepared by extrusion through a filter with a 200 nm pore size that predetermines their average diameter, as confirmed by dynamic light scattering.

The NSE technique provides a measurement of the real component of the intermediate scattering function in the time domain $I(Q,t)$. Thermal diffusive motions lead to an exponential time decay of $I(Q,t)$. Therefore we have fitted our data for each sample at each temperature with $I(Q,t)/I(Q,0) = \exp(-D_{eff}Q^2t)$, where the effective diffusion coefficient D_{eff} is a sum of two parts: D_{def}, representing the diffusive motions associated with the fluctuations within each vesicle, the thermal undulations; and D_{tr}, the translational diffusion coefficient of the vesicles in the solution [5]. The latter can be neglected because the vesicles prepared here are quite large, $R \approx 100$ nm, and according to the Stokes-Einstein hydrodynamic equation the corresponding translational diffusion D_{tr} is less than 2.6×10^{-12} m^2 s^{-1}. Samples "vesicles" and "vesicles & chol." were studied at temperatures of 20 °C, 35 °C and 45 °C to cover regions below and above T_c of DMPC which is 24 °C. Sample "vesicles & salt" was measured at 35 °C to study the effect of added electrolyte. Selected results are shown on Fig. 2 and summarized in Table 1.

Table 1. Effective diffusion coefficient of DMPC vesicles at different compositions and temperatures.

Sample	t/°C	$D_{eff} \times 10^{12}$ /m^2 s^{-1}	$\eta_{D_2O} \times 10^3$ /N s m^{-2}	$D_{eff}\eta/T$
vesicles	20	3.9 ± 0.7	1.25	0.30
vesicles	35	19.4 ± 4.6	0.871	1.00
vesicles	45	22.6 ± 3.9	0.714	0.92
vesicles & chol.	20	3.4 ± 1.1	1.25	0.26
vesicles & chol.	35	9.7 ± 2.6	0.871	0.50
vesicles & chol.	45	10.4 ± 1.2	0.714	0.43
vesicles & salt	35	11.7 ± 1.1	0.871	0.60

To take into account the effect of the solvent viscosity and temperature we have calculated the ratio $D_{eff}\eta/T$ and normalized it to that at 35 °C. All deviations of the normalized parameter $D_{eff}\eta/T$ from 1 can be attributed solely to the mechanical properties of the phospholipid bilayer and are not related to changes in the viscosity of the surrounding water.

The analysis of the normalized parameter $D_{eff}\eta/T$ as a function of temperature leads to the following conclusions (see Fig. 3):

- Scaling the diffusion coefficient D_{eff} that measures the thermal undulations of DMPC bilayers like $D_{eff}\eta/T$ mitigates the effects of temperature and the viscosity of the surrounding fluid. Above the bilayer interior crystal/liquid phase transition the scaled effective diffusion coefficient for DMPC vesicles remains constant with temperature.
- The bilayer liquid to crystalline phase transition increases the rigidity of DMPC bilayers by a factor of 3 for vesicles and by a factor of 1.5 for vesicles in presence of cholesterol.
- Cholesterol increases the rigidity of the DMPC bilayers in a bilayer-liquid state by a factor of 2 but has no effect on the DMPC bilayers in a bilayer-crystalline state.
- Addition of 0.05 mol L^{-1} of NaCl reduces the fluctuations of the DMPC bilayers by a factor of 2. This effect can be attributed either to the reduced electrostatic repulsion between the DMPC bilayers or to the effect of the osmotic pressure that can deflate the MLV.

These results are in good agreement with those obtained from other methods [3, 4]. They are a direct confirmation that cholesterol stiffens cell membranes thus reducing the cell — cell repulsions that originate from undulation forces. The significant difference in the thermal undulations below and above the bilayer liquid to crystalline phase transition temperature shows the importance of temperature for the proper functioning of the cell membranes. Finally, it has been shown that the NSE method provides a direct means of observing thermal undulation of biological membranes.

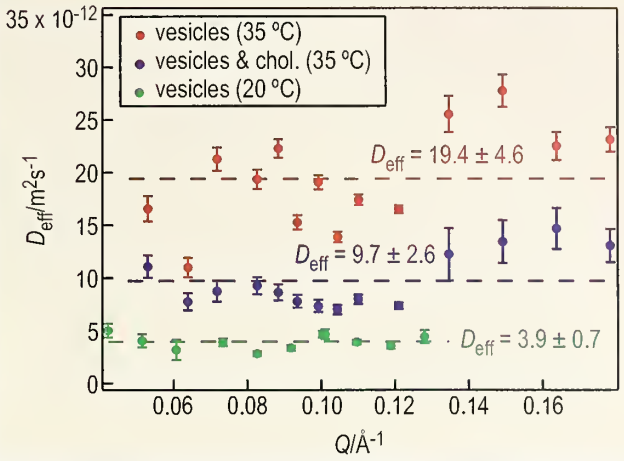

Fig. 2. Effective diffusion coefficient of DMPC vesicles as a function of the scattering vector Q. D_{eff} reflects mainly the thermal undulations of the phospholipid bilayer.

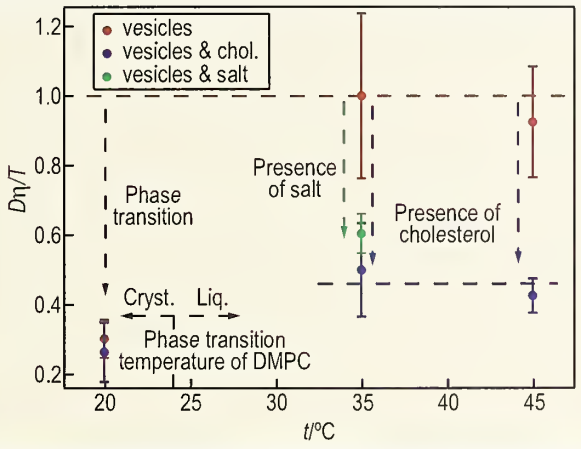

Fig. 3. Effective diffusion coefficient of DMPC vesicles, scaled by the solvent viscosity and temperature, and normalized to that at 35 °C.

References

[1] W. Pfeiffer, S. Köning, J. F. Legrand, T. Bayerl, D. Richter, and E. Sackmann, Europhys. Lett. **23**, 457 (1993).

[2] T. Takeda, Y. Kawabata, H. Seto, S. Komura, S. K. Shosh, M. Nagao, and D. Okuhara, J. Phys. Chem. Solids **60**, 1375 (1999).

[3] H. P. Duwe, and E. Sackmann, Physica A **163**, 410 (1990).

[4] C. Hofsäß, E. Lindahl, and O. Edholm, Biophys. J. **84**, 2192 (2003).

[5] S. T. Milner, and S. A. Safran, Phys. Rev. A **36**, 4371 (1987).

D. P. Bossev and N. S. Rosov
NIST Center for Neutron Research
National Institute of Standards and Technology
Gaithersburg, MD 20899-8562

Dynamics of Glucose Solutions

In a process called cryoprotection, simple sugar molecules are produced in response to desiccation or freezing by a number of species of plants and animals specifically adapted to survive extreme cold or drought [1]. The mechanism of this protective activity has been much debated, with many theories invoking a direct or indirect interaction with elements of cells such as proteins and membrane bilayers. However, the fact that a number of these sugars, such as the disaccharides sucrose and trehalose, have unusually high glass transition temperatures suggests that dynamical properties may also play a contributing role in cryoprotection. For this reason, information about the dynamics of sugars could be of considerable interest for understanding cryoprotection.

The technique of quasielastic neutron scattering (QENS) can probe motions such as molecular diffusion and rotation on the nanosecond to picosecond timescales, depending on the spectrometer. The wave vector and energy dependences of the QENS signal provide information about the geometry of the motions as well as rates of diffusion. Glucose is an appropriate subject for these studies since it is the canonical sugar prototype as well as a basic monomeric component of sucrose and trehalose. The present work [2, 3] focuses on the effects of the solute and solvent molecules through the choice of different energy windows and resolutions using the NCNR backscattering (HFBS) and disk-chopper spectrometer (DCS) instruments.

Selective H:D isotope substitution is a valuable tool for sorting out the dynamics of a complex organic system with QENS. Since the total bound-atom scattering cross section for H (81.7 b) is much larger than that of D (7.6 b) and most other atoms, the measured intensity is dominated by the scattering from the H atoms. Moreover the scattering from H is 98 % incoherent so that the complicating effects of interference in the scattering between different atoms can generally be neglected.

Our analysis for both the glucose and water molecule dynamics follows a model [4] that is based on the assumption that the vibrational, translational and rotational degrees of freedom are dynamically independent. In practice, this assumption results in a scattering function that is the sum of two Lorentzians, one representing translational and the other rotational motion. The latter gives rise to a peak too broad to be accurately fit in the energy windows measured in this experiment. In the incoherent approximation the rapid jump diffusion model for the translational Lorentzian has a full width at half maximum (FWHM) given by: $2\Gamma_t = 2\hbar DQ^2/(1 + D\tau_0 Q^2)$, where D is the diffusion constant and τ_0 is the period between jumps. The two Lorentzians were convolved with an instrumental resolution function to fit the measured spectra.

Since the dynamics of water molecules have been found to be generally much faster than those of sugar molecules, the motion of the two can be separated effectively through the judicious choice of energy window and energy resolution of the instrument. To explore the dynamics of the glucose molecules, the sugar, in which the exchangeable hydrogen atoms had been pre-deuterated, was dissolved in D_2O and studied on HFBS with an energy window of ±36 μeV. Even though the coherent scattering cross section of water is comparable to the incoherent cross section of glucose, the faster dynamics of the water results in a broad contribution to the observed signal that does not contribute to the translational motion lineshape.

Three aqueous glucose solutions were studied at 280 K with glucose to water ratios of 1:11, 1:20, and 1:55. Two Lorentzians were used to fit the spectra (Fig. 1), although the rotation component was generally too broad to be accurately fit in the given energy window. The effect of concentration on the glucose translational motion

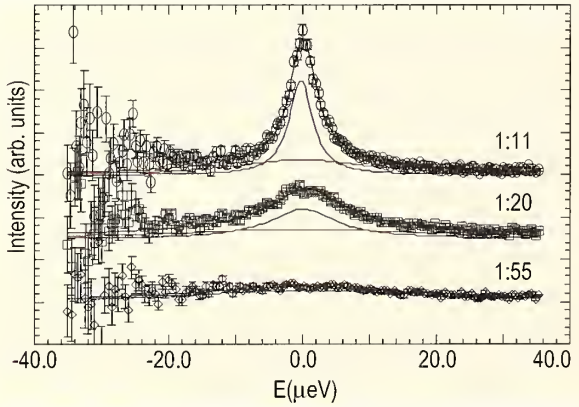

Fig. 1. HFBS QENS spectra and fits (black line) of glucose/D_2O solutions at 280 K varying sugar to water ratios at Q = 0.99 Å^{-1}. The energy resolution at elastic scattering is 1.01 μeV. The narrow Lorentzian corresponding to glucose translational motion (blue line) and the broad glucose rotational Lorentzian (red line) are also shown.

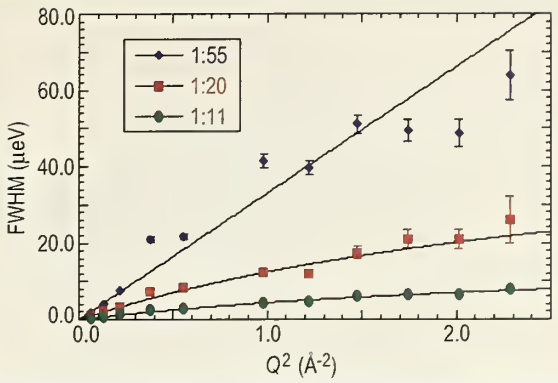

Fig. 2. HFBS data probing glucose motion. The FWHM of the narrower Lorentzian versus Q^2 for the three hydrogenated glucose solutions: 1:11 (closed circle), 1:20 (closed square), and 1:55 (closed diamond) at 280 K.

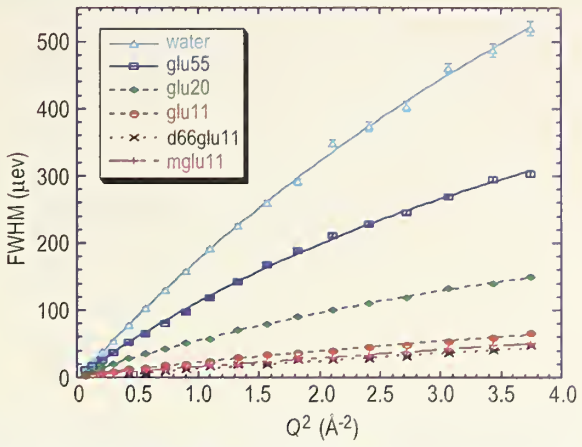

Fig. 3. FWHM of the narrower Lorentzian corresponding to water translational motion fitted to the QENS spectra for the various glucose solutions at 280 K derived from DCS data at 110 μeV energy resolution at elastic scattering. See the text for sample descriptions.

is evident. The narrow Lorentzian reduces in width with increasing glucose concentration as the diffusive motion slows. The FWHM for the two highest concentrations was found to follow the random jump diffusion model (Fig. 2) while the lowest concentration manifested the characteristics of continuous diffusion: $\Gamma_r = hDQ^2$. As the concentration of the glucose increases, the diffusion rates decrease by almost a factor of 6 from 25.1 ± 0.2 x 10^{-7} cm^2/s for the 1:55 ratio solution to 4.5 ± 0.1 x10^{-7} cm^2/s for the 1:11 solution.

The larger energy window and energy resolution (δE = 110 μeV) available on DCS permitted the examination of the water dynamics in aqueous glucose solution to the exclusion of the glucose dynamics. The slower dynamics of the glucose as observed on HFBS results in the signal primarily contributing to an elastic peak on DCS. To further minimize the incoherent contribution from the glucose, the unexchangeable hydrogen atoms on the molecule were replaced by deuterium atoms. Again three different aqueous glucose solutions were studied with the same ratios as on HFBS. In addition to the fully deuterated glucose, glucose deuterated only at the C6 carbon atom (d66glu) and deuterated glucose with a methoxy group at the C2 carbon atom (mglu) were studied at the various concentrations. The full width at half maximum of the narrow Lorentzian from the fit, corresponding to the translational motion of the water molecules, had a Q^2 dependence typical of the random jump diffusion model (Fig. 3).

The diffusion rate dropped by a factor of 7 from 1.08 ± 0.02 x10^{-5} cm^2/s for the 1:55 solution to 0.16 ± 0.01 x10^{-5} cm^2/s for the 1:11 solution. A significant difference in diffusion constant was not observed for solutions that had glucose with deuterium substitutions, further justifying the static approximation for glucose motion on DCS.

Both the glucose and water have similar degrees of change in the translational diffusion constants, reflecting the effect of hydrogen bonding on dynamics. Interaction with glucose thus disrupts the organization of the water molecules, as the retarding effect is observed for glucose to water ratio as low as 1:55. These results hint at the role that sugar may play in cryopreservation: in dry environments the binding of waters by sugar may prevent local dessication, while in cold environments the sugar disruption of the water network may prevent local destruction by favoring glass rather than ice formation.

References

[1] F. Franks Biophysics and Biochemistry at Low Temperatures; Cambridge University Press: Cambridge (1985).

[2] L. J. Smith, J. W. Brady, Z. Chowdhuri, D. L. Price and M.-L. Saboungi, submitted to J. Chem. Phys.

[3] C. Talon, L. J. Smith, J. W. Brady, J. R. D. Copley, D. L. Price, M.-L. Saboungi, submitted to J. Phys. Chem.

[4] J. Teixiera, M.-C. Bellisant-Funel, S.-H. Chen, and A. J. Dianoux, Phys. Rev. A. **31**, 1913 (1985).

L. J. Smith[1, 2], C. Talon[3], J. W. Brady[4], Z. Chowdhuri[5, 6], J. R. D. Copley[5], D. L. Price[7], M.-L. Saboungi[3]

[1] Argonne National Laboratory, Argonne, IL 60439

[2] Clark University, Worcester, MA 01610

[3] Centre de Recherche sur la Matière Divisée, 5071 Orléans Cédex 2, France

[4] Cornell University, Ithaca, NY 14853

[5] NIST Center for Neutron Research
National Institute of Standards and Technology
Gaithersburg, MD 20899-8562

[6] University of Maryland, College Park, MD 20742

[7] Centre de Recherche sur les Matériaux
à Haute Température
45071 Orléans Cédex 2, France

ATP-Induced Shape Change in a Model Protein Complexed in Chaperonins

The role of molecular chaperones in mediating and controlling intracellular, as well as *in vitro* protein folding, has broad implications for biotechnology. There is now considerable insight into the possible mechanisms whereby chaperone proteins recognize, stabilize, and release unfolded polypeptide chains in a manner whereby they are able to productively refold. However, there are a number of important, fundamental gaps in the understanding of chaperone action, which remain to be resolved. Among the growing list of chaperone families are the chaperonins GroEL (EL) and GroES (ES), which have been intensively studied. Knowledge of how misfolded protein substrates physically interact with EL should provide vital clues necessary to unravel the process by which EL mediates their proper folding. The ultimate goal is to determine the mechanism by which EL transforms its substrate proteins and then releases them in a form able to refold to their native conformation.

One of the key issues in establishing a molecular mechanism for EL is to describe in structural terms the conformations of polypeptide substrates when bound to various chaperonin complexes. For example, does a nonnative polypeptide substrate unfold further upon binding to EL? On the other hand, when a chain is released from EL in the presence of the co-chaperonin ES, does it adopt a more folded, or less folded conformation? These questions are difficult to resolve with naturally occurring proteins since they refold so readily when released from chaperonin complexes. One approach to address these issues, however, is to utilize a family of mutationally altered protein substrates that are unable to adopt their native conformation. The nonnative subtilisin variant, PJ9 (*p*), which is unable to refold when released, is one such system that is readily available [1].

Single-ring EL mutants have been shown to assist in the refolding of nonnative polypeptide chains [2, 3] and they form unusually stable complexes with ES upon the addition of nucleotides. Capitalizing on these properties, a single-ring EL variant (sEL) was used to trap *p* within EL by ES upon the addition of the nucleotides adenosine di- or tri-phosphate (ADP or ATP). Small angle neutron scattering (SANS) experiments were then performed to examine the structure of sEL/ES/*p* complexes and investigate changes in *p* conformation in the presence of both nucleotides.

p was 86 % deuterated (d*p*) so that it contrasted sufficiently with the chaperonin, allowing the contrast variation technique to be used to separate the scattering from the two components bound in the complex. The sEL mutant assured that d*p* and ES were each bound in a 1:1 stoichiometry with the sEL, providing an advantage over previous SANS experiments [4] which included mixed stoichiometries of EL and ES.

Unlike ATP, ADP does not cause dissociation of d*p* from EL. If d*p* is no longer covalently bonded to EL, would its location in the EL/ES complex change? To answer this question, two contrast variation series of measurements, one with ADP and the other with ATP present, were performed on the sEL/ES/d*p* complex [5]. Measurements were made in five D_2O buffers in each case, as shown in Fig. 1. The extensive $I(Q)$ data sets in Fig. 1 allow the separation of the scattering intensities from each of the components in the complex and also the cross-term intensity. Modeling is then used to try to reproduce these measured intensities.

Using this method, the location and approximate shape of d*p* in the sEL/ES/d*p* + ADP complex was determined as modeled in Fig. 2. The significant result is that the d*p* component has an asymmetric shape: part of the polypeptide must extend beyond the cavity inside the sEL ring up into the space surrounded by ES. The best fit to the data from both complexes (*i.e.*, with ADP or ATP) was

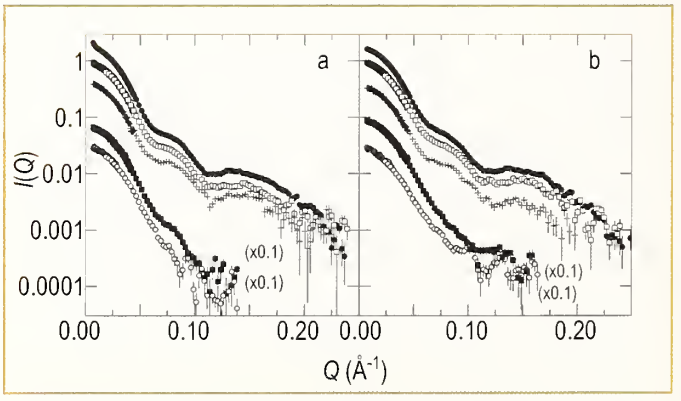

Fig. 1. Contrast variation data from sEL/ES/d*p* complexes a) + ADP and b) + ATP in 100 % (●), 85 % (□), 70 % (+), 20 % (O) and 0 % (■) D_2O solutions. The data in 20 % and 0 % D_2O solution are shifted by the factor 0.1, as indicated, for clarity.

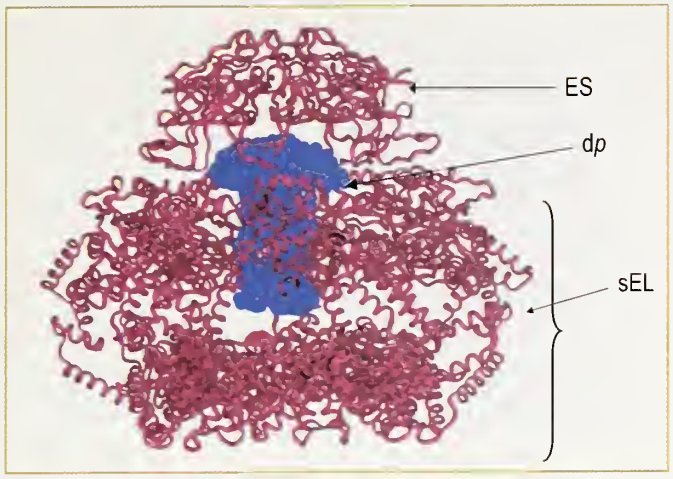

Fig. 2. Side view of a model for the sEL/ES/d*p* + ADP complex constructed from SANS contrast variation and crystallography data. The sEL/ES complex is represented by the red ribbon structure and the d*p* is represented by the blue spheres.

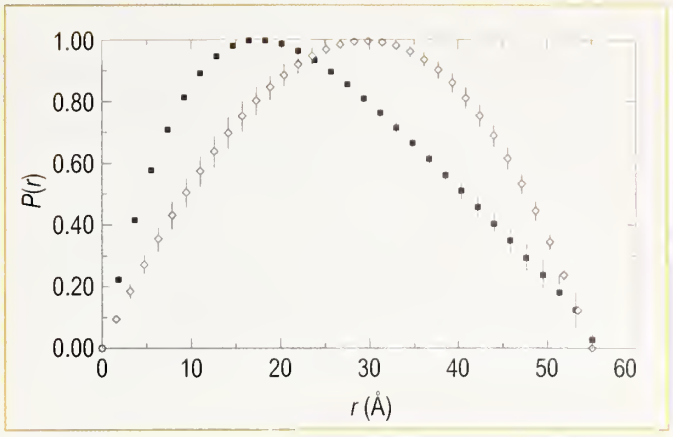

Fig. 3. Normalized distance distribution functions for d*p* bound to sEL/ES complexes + ADP (■) and + ATP (◇).

achieved using one ring of the EL/ES solution structure of Ref. 6 for the sEL/ES component of the complex, one ring of the x-ray structure for EL of Ref. 7 for the free sEL, and the x-ray structure for free ES of Ref. 8 in a ratio of 75:21:4 by mass.

The significant difference in the sEL/ES/d*p* complex formed from ATP is that the shape of the bound d*p* molecule changes from an asymmetric shape such as that shown in Fig. 2 to a more symmetric shape. Figure 3 shows the distance distribution functions obtained by Fourier inversion of the $I(Q)$ for bound d*p* in both the sEL/ES/d*p* + ADP and sEL/ES/d*p* + ATP complexes. The most probable distance increases from approximately 22 Å to 30 Å, with a similar increase in the radius of gyration, R_g, from 19.0 ± 0.5 Å to 21.0 ± 0.5 Å.

The shape of d*p* in the presence of ATP is clearly more symmetric, as indicated by the greater symmetry of the distance distribution function. This suggests that d*p* is transformed into a more expanded form in the ATP complex. However, the symmetry of this curve cannot be used to unambiguously assign a shape to d*p* in the ATP complex. Because the sEL/ES/d*p* complex dissociates in solution, which contains about 21 % of sEL/d*p* complex, it is possible that the distance distribution curve represents a composite of data from d*p* bound to sEL alone and to the sEL/ES complex formed from ATP. For the same reason, it is unclear from the data whether d*p* is still located partially in the sEL cavity. However, what is clear is that there has been a transformation in the shape of d*p* associated with the complex formed from ATP. The d*p* shape change was significant enough to be detected as a change in the shape of the scattering from this component, in spite of the fact that dissociation is likely to be present in the sample. A conformational change of d*p* either was not supported by the complex formed from ADP or was insufficient to generate a lasting change in shape in that case, and d*p* instead relaxed back to a form close to its original conformation. This important observation reflects the relative ability of ATP to promote refolding of protein substrates relative to ADP.

References

[1] Z. Lin and E. Eisenstein, Proc. Natl. Acad. Sci. USA **93**, 1977 (1996).

[2] I. S. Weissman, Chem. Biol. **2**, 255 (1995).

[3] S. G. Burston, J. S. Weissman, G. W. Farr, W. A. Fenton and A. L. Horwich, Nature **383**, 96 (1996).

[4] P. Thiyagarajan, S. J. Henderson, and A. Joachimiak, A, Structure **4**, 79 (1996).

[5] S. Krueger, S. K. Gregurick, J. Zondlo and E. Eisenstein, J. Struct. Biol. **141**, 240 (2003).

[6] R. Stegmann, E. Manakova, M. Rossle, H. Heumann, S. E. Nieba-Axmann, A. Pluckthun, T. Hermann, R. P. May and A. Wiedenmann, J. Struct. Biol. **121**, 30 (1998).

[7] K. Braig, Z. Otwinowski, R. Hegde, D. C. Boisvert, A. Joachimiak, A. L. Horwich and P. B. Sigler, Nature **371**, 578 (1994).

[8] J. F. Hunt, A. J. Weaver, S. J. Landry, L. Gierasch, and J. Deisenhofer, Nature **379**, 37 (1996).

S. Krueger
NIST Center for Neutron Research
National Institute of Standards and Technology
Gaithersburg, MD 20899-8562

S. K. Gregurick
University of Maryland, Baltimore County
Baltimore, MD 21250

J. Zondlo and E. Eisenstein
Center for Advanced Research in Biotechnology
University of Maryland Biotechnology Institute
Rockville, MD 20850

Phase Sensitive Neutron Reflectometry on a Water-Cushioned Biomembrane-Mimic

Biomimetic membranes have been developed as models of living cell membranes, and this has applications in the quest for biocompatibility of inorganic materials in biologically active mediums, such as coatings for artificial organs. A membrane consists of a lipid bilayer (two lipid layers) where hydrophobic carbon chains form the inside of the membrane and their polar head groups the interface with the aqueous surrounding medium. A supported membrane-mimic consists of a lipid-like bilayer, typically attached to a single-crystal substrate, with access to water only at the top surface [1, 2]. Here we use neutron reflectometry to study a system in which water has access to both sides of a membrane-mimic attached to such a substrate, thus making the system a closer mimic to a real cell membrane.

The system devised by Liu *et al.* [3] consists of a water-swellable polyelectrolyte that electrostatically binds to the substrate and acts as a "cushion" for the membrane, not unlike the cytoskeletal support found in actual mammalian cell membranes. The lower half of the membrane-mimic is a terpolymer that attaches to the polyelectrolyte. A phospholipid layer forms on top of the terpolymer and the bilayer is finally chemically crosslinked for added stability. The system is shown schematically in Fig. 1.

Neutron reflectivity measurements were performed at the NG-1 vertical stage reflectometer to obtain the compositional profile at every step of the assembling process of the membrane-mimic which consisted of three stages: a) polyelectrolyte multilayer (PE), b) polyelectrolyte multilayer plus terpolymer (PE+TER), and c) polyelectrolyte multilayer plus terpolymer plus phospholipid layer (PE+TER+PC) [4]. The spatial resolution attained was approximately 10 Å, about half the thickness of a membrane bilayer, making it possible to distinguish the two layers of a membrane but not the structure of a single layer.

A unique compositional profile of the biomimetic film with no a priori knowledge of the sample's composition is obtained by measuring the reflectivity of equivalent samples made onto two substrates [5]. The substrates used were single crystal silicon (Si) and sapphire (Al_2O_3) coated with chromium (Cr) and then a gold (Au) layer to allow the polyelectrolytes to bind to a similar surface on both wafers.

Figure 2 shows the compositional profiles for the PE, PE+TER and PE+TER+PC assemblies in a D_2O atmosphere at 92 % relative humidity. The figure shows that the hydration of the PE layer is almost unaffected by the addition of the terpolymer and the phospholipid layer. Also, upon the addition of the phospholipid layer to the PE+TER assembly, the composite PE+TER+PC assembly shows an increase in thickness of approximately 30 Å, consistent with the formation of a single phospholipid layer at the surface. It is also clear that the addition of a phospholipid layer onto the terpolymer layer rearranges this region

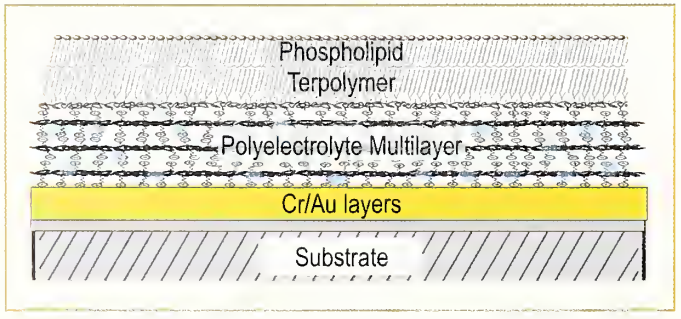

Fig. 1. Schematic diagram of a biomimetic membrane. The phospholipid layer at the top combines with the terpolymer layer to form a membrane-mimic that in turn resides on the water (blue dots) permeable "cushion" polyelectrolyte multilayer. The latter attaches electrostatically to the Au-capped substrate.

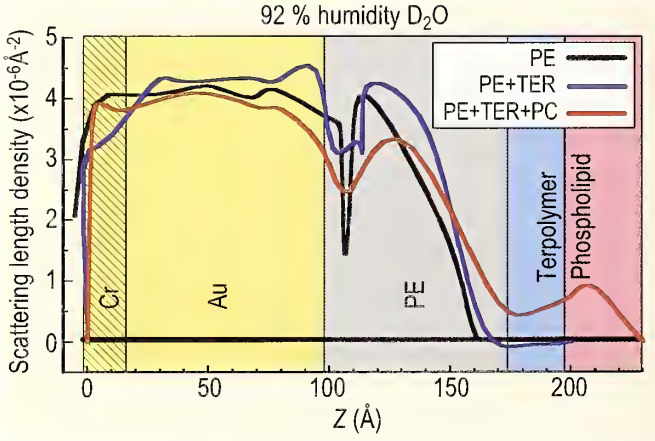

Fig. 2. Compositional profile of biomimetic membrane in a D_2O atmosphere at 92 % relative humidity at various stages of assembly on Au-capped substrate: only polyelectrolyte (PE), polyelectrolyte and terpolymer (PE+TER), polyelectrolyte, terpolymer and phospholipid (PE+TER+PC). The compositional profile is given by the scattering length density, SLD, profile when using neutrons.

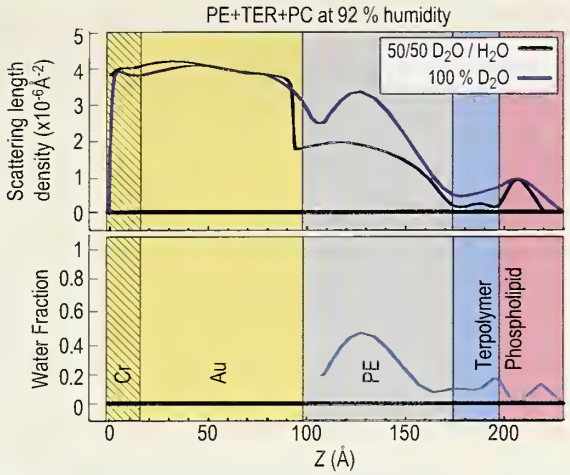

Fig. 3. Scattering length density profiles (top) and water fraction (bottom) for PE+TER+PC under indicated conditions.

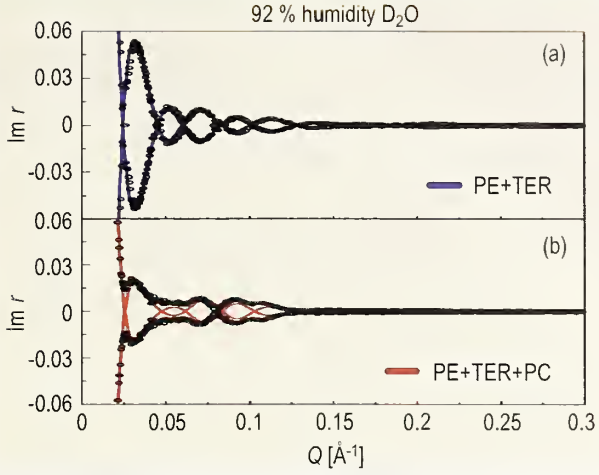

Fig. 4. Imaginary part of the complex reflectivity, Im $r(Q)$, data (symbols) and calculated curves (lines) obtained from the SLD profiles for the PE+TER and the PE+TER+PC assemblies shown in Fig. 2.

significantly, since the terpolymer layer only becomes apparent after the phospholipid layer is added. It is possible to verify with an independent technique (contact angle) that the terpolymer was in fact deposited because it forms a hydrophobic outer layer. The outer surface becomes hydrophilic once the phospholipid layer is deposited onto the terpolymer layer.

Figure 3 (top) shows the profile for the PE+TER+PC assembly under 92 % relative humidity in 100 % D_2O and in 50/50 D_2O/H_2O. The overall thickness change due to the intake of water, in going from dry (not shown) to 92 % relative humidity, was found to be 20 Å. Figure 3 (bottom) shows the water fraction in the assembly under 92 % relative humidity. This is obtained by assuming that the distribution of each component in the layers is unaffected by having either D_2O or 50/50 D_2O/H_2O. From the figure it can be seen that the polyelectrolyte multilayer has a 40 % water uptake. This is a significant amount of water, which suggests that the polyelectrolyte multilayer can work as a "cushion" for membrane-mimetic systems. The terpolymer and the phospholipid layers contain an average of 10 % water, which is also significant, suggesting that these layers are not tightly packed.

The method of making equivalent samples on two substrates to obtain a unique compositional profile has a built-in congruency test, particularly useful in checking the reproducibility of the samples as well as the quality of the films. The test is to compare the calculated imaginary part of the complex reflectivity from the obtained profile with the corresponding data, as is shown in Fig. 4 for the PE+TER and PE+TER+PC assemblies. From Fig. 4 it is concluded that the PE+TER samples are homogenous and essentially identical while for the PE+TER+PC assembly, the absence of true zeros, as indicated by the calculated curve, is suggestive of a small degree of sample inhomogeneity.

The system from Liu *et al.* has many characteristics desirable in a biomimetic membrane. It is a single membrane-mimic attached to a significantly hydrated soft "cushion" support that allows some membrane proteins to function. Thrombomodulin, a membrane protein relevant to blood-clotting, is being studied in this membrane-mimic environment to further develop biocompatible coatings for artificial organs [6].

References

[1] E. Sackmann, Science **271**, 43 (1996).

[2] A. L. Plant, Langmuir **15**, 5128 (1999).

[3] H. Liu, K. M. Faucher, X. L. Sun, J. Feng, T. L. Johnson, J. M. Orban, R. P. Apkarian, R. A. Dluhy, E. L. Chaikof, Langmuir **18**, 1332 (2002).

[4] U. A. Perez-Salas, K. M. Faucher, C. F. Majkrzak, N. F. Berk, S. Krueger, E. L. Chaikof, Langmuir **19**, 7688 (2003).

[5] C. F. Majkrzak, N. F. Berk, U. A. Perez-Salas Langmuir **19**, 1506 (2003).

[6] J. Feng, P. Y. Tseng, K. M. Faucher, J. M. Orban, X. L. Sun, E. L. Chaikof, Langmuir **18**, 9907 (2002).

U. A. Perez-Salas
NIST Center for Neutron Research
National Institute of Standards and Technology, Gaithersburg, MD 20899-8562

K. M. Faucher
Emory University School of Medicine, Atlanta, GA 30322

C. F. Majkrzak, N. F. Berk, S. Krueger
NIST Center for Neutron Research
National Institute of Standards and Technology
Gaithersburg, MD 20899-8562

E. L. Chaikof
Emory University School of Medicine
Atlanta, GA 30322

Biomaterials Constructed Via Designed Molecular Self-Assembly

We have been engaged in an interdisciplinary materials research effort to develop new classes of biomaterials that are constructed via designed molecular self-assembly [1]. These materials use specific polypeptides that are designed *a priori* to self-assemble into targeted nano- and microscopic structures. Using amino acids as the fundamental material building blocks, one can potentially engineer materials having targeted biological functions such as *in vivo* therapeutic delivery or tissue scaffolding. Materials can be designed whose morphology is responsive to specific environmental cues. The ability to actively manipulate material morphology can lead to "smart" materials whose structure and consequent biological function is responsive to environmental cues. Predictable control of material morphology would be a significant advance in the development of functional biomaterials because it would provide active control of biological properties that are dependent on an aggregate's shape or size. An example of molecular design for a specific application would be in the delivery of drugs and genes, where the shape of the delivery assembly favors selective interactions with different biological surfaces, *e.g.*, an active gating mechanism induced by a predicted external stimulus.

Polypeptides, composed of amino acids each of which imparts a unique structural and/or functional characteristic to the polymer molecule, provide an immense molecular toolbox from which one can construct functional materials via self-assembly. The primary tools exploited are the conformational propensities of individual amino acid residues to adopt desired secondary structures or shapes and the tendency of the appropriately designed secondary elements to self-associate (Fig. 1). It is now possible to design peptides that will fold into stable secondary structures such as α-helices (rod-like polymers that typically form nematic liquid crystals in solution and pack as hexagonal arrays of rods in the solid-state) and β-sheets (crystalline arrays of extended chains, mainly stabilized by H-bonding). It is also possible to design polypeptides that, in addition to intramolecular folding, undergo self-assembly to construct higher order structures.

Currently we are studying the self-assembly behavior of both charged and neutral amphiphilic di- and tri-block copolypeptides. Unlike membrane-forming lipids and surfactants, the neutral copolypeptides form robust bilayer membranes in aqueous solutions over a wide range of molecular weights and molar ratios. This has been observed in amphiphilic, nonionic, completely α-helical peptide block polypeptides at all of the molecular weights (20k g/mol to 60k g/mol) and molar ratios (ranging from 90/10 hydrophilic/hydrophobic to 60/40) studied. Diblocks of poly-L-lysine (K), with short ethylene glycol side chains

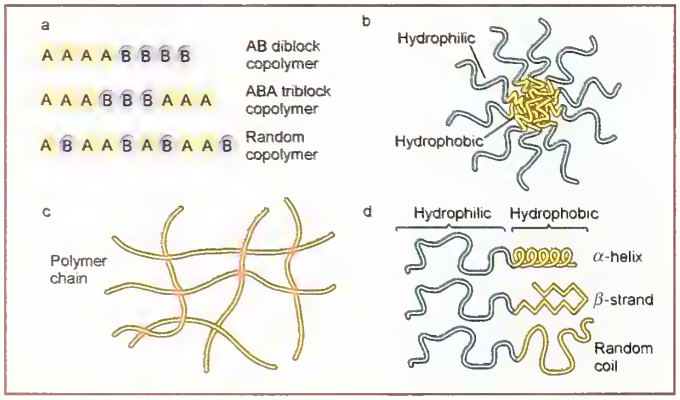

Fig. 1. a) Schematic of peptide monomers chemically bonded to form diblock, triblock and random copolymers; b) Amphiphilic copolypeptides self-assembled in micelles; c) Copolypeptides physically linked to form a hydrogel; and d) typical copolypeptide chain architectures [4].

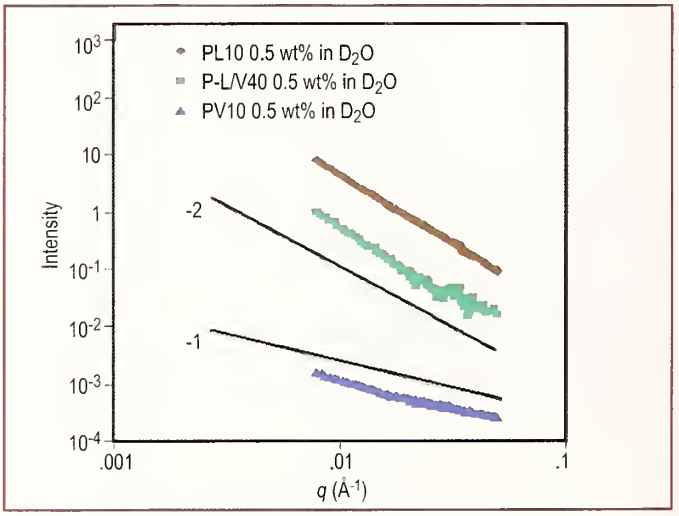

Fig. 2. SANS from amphiphilic diblock copolypeptides showing the change from threadlike morphology ($I(q) \sim q^{-1}$) when the hydrophobic block is an α-helix (lower curve), to sheetlike morphology ($I(q) \sim q^{-2}$) when the hydrophobic block is more like an extended β-sheet (upper two curves).

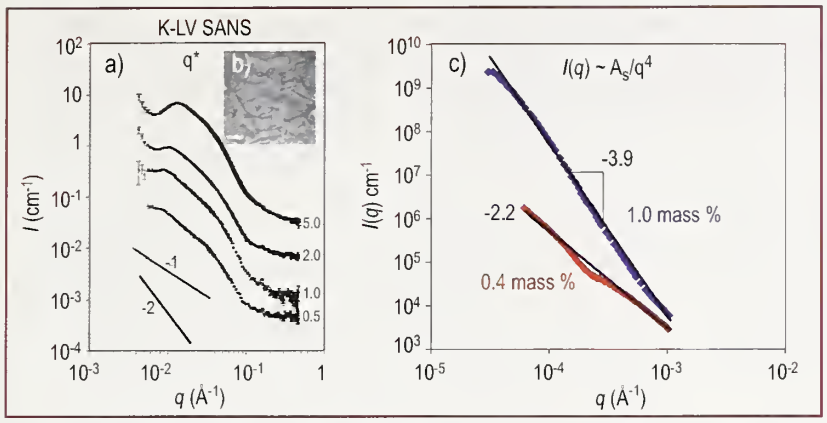

Fig. 3. a) SANS from hydrogels of diblock copolypeptides showing a diffraction peak corresponding to a regular repeat spacing in the self-assembled gel matrix; b) Cryo-TEM image of the .01 mass fraction hydrogel (the scale bar is 200 nm); c) USANS data showing the large drop in scattered intensity when the concentration of peptide falls below the gelation threshold (≈ 0.5 mass %).

(PEGLys) (P) as a nonionic block, joined with hydrophobic polyleucine (L) form fluid bilayers and also spontaneously form vesicles. On the other hand, PLP triblocks form extremely rigid, high aspect ratio membranes. Rigid membranes preclude use in therapeutic delivery assemblies but provide intriguing possibilities for synthetic biomaterial scaffolding in more concentrated suspensions.

A SANS study of secondary structure effects shows a large transition in the assembled structure induced by changing the minority hydrophobic block from an α-helix, polyleucine (L), to an extended β-sheet former, polyvaline (V). For the V-rich case the amphiphiles assemble into thread-like micelles with a large interfacial curvature between blocks. This is reflected in the blue curve of Fig. 2 with $I(q) \sim q^{-1}$. For the L-rich cases (green and red curves of Fig. 2) flat lamellar geometry in the membranes and vesicles is favored, with $I(q) \sim q^{-2}$. The result indicates that the interfacial area of the respective blocks (large for the leucine α-helix, small for the extended valine β-sheet) plays an important role in the interfacial curvature and the resultant structure formed, similar to what is observed in lipid self-assembly.

In addition to the bilayer/membrane forming nonionic polypeptides, hydrogel formation of charged, amphiphilic block polypeptides is observed. By removing the PEG side chain from poly-L-lysine, one obtains a polycationic lysine block at neutral pH. Block polypeptides of lysine and leucine form strong hydrogels at low molecular weights (20k g/mole) and concentrations (< 0.006 mass fraction), both an order of magnitude lower than observed in traditional polymeric hydrogel formation. The structural characterization of these unique gels is crucial to uncovering their gelation mechanism and in the design of new gel formers with the added control/environmental responsiveness discussed above. Gelation occurs with a variety of hydrophobic block secondary structures but with varying degrees of strength [2]. Both SANS and USANS measurements at the NCNR have been indispensible for probing the global nano- and microstructure of these porous hydrogel materials.

In some cases, the self-assembled gels exhibit a characteristic spacing in the underlying scaffold. An example of this is observed in Fig. 3 where the correlation peak shifts to lower q with decreasing concentration, indicating that the regular structure persists even as the characteristic spacing increases [3]. On the microscale, the hydrogels exhibit clear smooth surface scattering with $I(q) \sim q^{-4}$ as determined by USANS (Fig. 3c). When the peptide concentration drops below the gelation threshold (≈ 0.005 mass fraction) the material becomes a viscous liquid, and the USANS scattering drops significantly in slope indicating the loss of well-defined microstructure in the materials [3].

We have also investigated the dynamics of the gelation process [1]. In a rheometer, the gel structure was disrupted by large amplitude oscillations, but recovered 90 % of full strength within seconds of cessation of shear. The low mass fraction of material in the polypeptide hydrogels, combined with their recovery properties and microporous structure, allows them to fill an advantageous and unique niche between conventional polymer and surfactant hydrogels. Their peptide backbone also imparts to these materials some of the advantageous features of proteins (such as degradability and functionality), which makes them attractive for biomedical applications.

References

[1] A. P. Nowak, V. Breedveld, L. Pakstis, D. J. Pine, D. J. Pochan, T. J. Deming, Nature **417**, 424 (2002).

[2] J. P. Schneider, D. J. Pochan, B. Ozbas, K. Rajagopal, L. M. Pakstis, J. Gill, J. Am. Chem. Soc. **124**, 15030 (2002).

[3] D. J. Pochan, L. Pakstis, B. Ozbas, A. K. Nowak, T. J. Deming, Macromolecules, **35**, 5358 (2002).

[4] J. Kopeček, Nature **417**, 388 (2002).

D. J. Pochan, J. P. Schneider, L. Pakstis, B. Ozbas
University of Delaware, Newark, DE

A. P. Nowak and T. J. Deming
University of California at Santa Barbara
Santa Barbara, CA

Scattering Studies of the Structure of Colloid-Polymer Suspensions and Gels

The key step in assembling colloidal particles into useful structures for applications as coatings, viscosity modifiers, and gels, for example, lies in fine-tuning particle interactions to produce the desired microstructure. The distinct advantage of adding non-adsorbing polymer to a colloidal suspension (particles of radius R) lies in the ability to control the microstructure of the resulting dispersion with two independent variables — the molecular weight of the added polymer (radius of gyration R_g) which controls the range of particle interactions and the concentration of added polymer (c_p) which controls the strength of particle interactions. Recent studies [1, 2] have shown that a wide range of phase behavior can be observed in colloidal dispersions depending on the values of R_g/R and c_p/c_p^* (c_p^* is the polymer overlap concentration). For $R_g/R < 0.1$, the suspensions gel as more polymer is added to the system. For $0.1 < R_g/R < 0.3$, the colloids crystallize and for higher size ratios ($R_g/R > 0.3$) a liquid-liquid phase separation is thermodynamically favored. Standard theories in literature fail to predict the observed trends in phase behavior and we have recently shown that the only model that can qualitatively predict the observed experiments is the polymer reference interaction site model (PRISM) integral equation theory for colloid-polymer mixtures [1, 2].

In this work we report on Small Angle Neutron Scattering (SANS) and Ultra Small Angle X-Ray Scattering (USAXS) studies of the structures of model colloid-polymer suspensions over a wide range of R_g/R and c_p/c_p^*. Our aim in measuring the structure is twofold: to provide a test of different models especially PRISM for predicting the thermodynamics and structure of colloid-polymer mixtures; and to relate the observed microstructure to macroscopic flow properties (shear modulus, viscosity) especially under conditions where the suspensions gel.

The system used in this work consists of 100 nm diameter silica particles coated with octadecanol (1 nm to 2 nm hairs) and suspended in decalin. The particles in the absence of added polymer behave as hard spheres (no interactions except volume exclusion). The polymer used is polystyrene of different molecular weights to provide the appropriate R_g/R. Figures 1 and 2 are plots of the measured intensities and the calculated structure factors at an R_g/R of 0.06 and different values of c_p/c_p^*. The solid lines are comparisons with structure factors from PRISM theory for colloid-polymer mixtures. Agreement with theory and experiment is excellent for samples in the single- phase fluid region thus establishing the fact that PRISM accurately predicts the thermodynamics and structure of these suspensions in the q region of interest.

At a colloid volume fraction of 0.4 and R_g/R of 0.06, the suspensions gel at a c_p/c_p^* of 0.095. Shown in Fig. 2 is the measured structure factor in the gel phase at a c_p/c_p^* of 0.1. When particles become frozen in the gel state, they fall out of equilibrium and comparisons with theory worsen as is evident from Fig. 2. Another interesting characteristic about these gels is the high upturns in intensity at low angles. Fractal analysis gives an unphysical dimension of 3.4 that led us to propose a model of clusters of particles

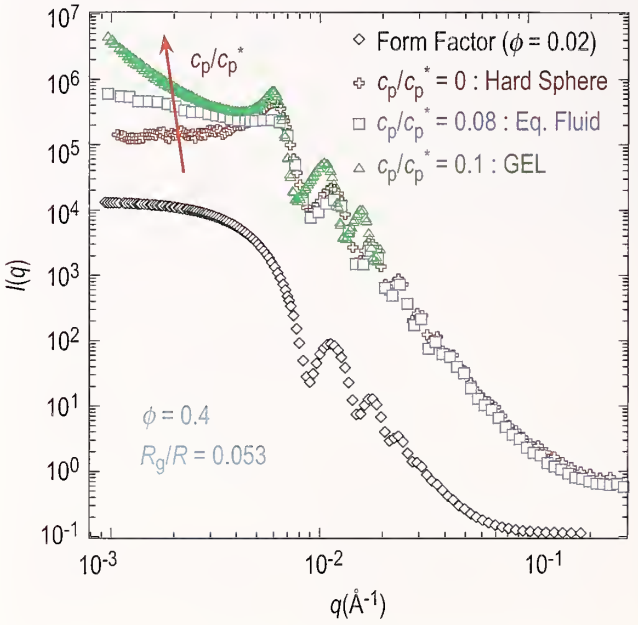

Fig. 1. Normalized scattering intensities $I(q)$ as a function of q (Å^{-1}) for samples with varying amounts of polymer quantified by the dimensionless polymer concentration c_p/c_p^*. The colloid volume fraction is fixed at $\phi = 0.40 \pm 0.01$, and $R_g/R = 0.053$. Data is shown for: $c_p/c_p^* = 0$ (hard spheres, crosses), 0.08 (equilibrium fluid, squares), and 0.1 (Gel, triangles). Experimental data (diamonds) for the form factor (single particle scattering) is also shown. As more polymer is added to the system, intensities at low angles increase indicating the presence of clusters/aggregates and an increased compressibility.

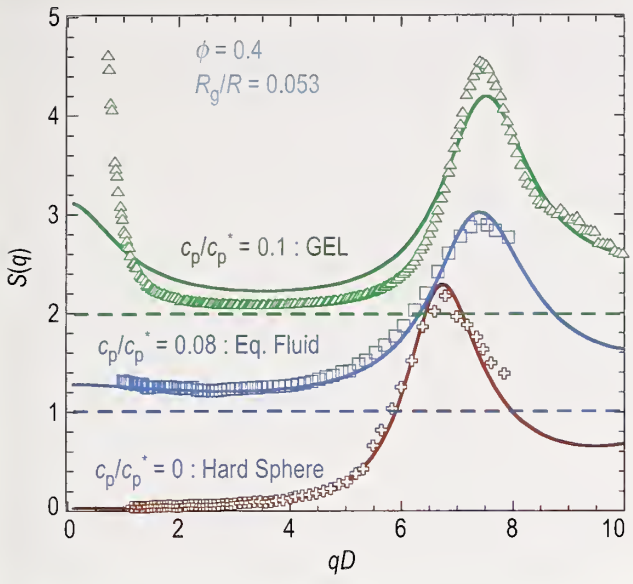

Fig. 2. Structure factor $S(q)$ as a function of the dimensionless wavevector qD (diameter D = 100 nm) for samples: c_p/c_p^* = 0.0 (hard spheres, crosses), 0.08 (equilibrium fluid, squares), and 0.10 (Gel, triangles), for the same ϕ and R_g/R as Fig. 1. Each subsequent data set is offset by 1 for clarity. Dotted lines show relevant baselines signifying $S(q)$ = 0 for each data set. Solid lines are the zero-adjustable parameter PRISM-mPY theory predictions. The structure factor which depicts the packing of particles with respect to each other in solution is calculated from the data of Fig. 1 by dividing the intensities of the respective suspensions by that of the form factor and then multiplying by the ratio of the volume fractions ($\phi_{FormFactor}/\phi_{Sample}$ = 0.02/0.4) [3, 4]. The location of the first peak (q^*) in the structure factor shifts to higher q's as more polymer is added to the system indicating that the particles are getting closer to each other on an average. When the suspension gels, the particles are frozen in space and q^* is constant with added polymer as one traverses deeper into the gel [3, 4]. The increased $S(0)$ for the gel sample is indicative of increased compressibility in the system due to clustering of particles (cluster size ≈ 5–8 particle diameters). The structure of the gels based on the calculated $S(q)$ is hypothesized to consist of clusters of particles with randomly distributes voids which gives rise to the steep upturns in $S(q)$ at low q [3, 4].

with randomly distributed voids throughout the gel sample (Debye-Bueche analysis). The cluster size in these samples is ≈ 5 to 8 particle diameters as calculated from the scattering curves. This finding has an important consequence when trying to predict the flow properties of these suspensions especially the elastic modulus as clusters reduce the ability to store energy compared to an open network of particles. More detailed discussions about the structure and its links to rheology can be found in references [3–5].

The above scattering experiments performed at the NCNR and at Argonne National Laboratory were the first systematic studies of the structure of a model colloid-polymer suspension. These experiments helped us validate the use of PRISM theory for colloid-polymer mixtures. We now have a predictive capability for the variety of interesting phenomena, such as phase transitions between qualitatively different glassy states and reentrant melting of colloidal crystals, observed in these colloid-polymer mixtures.

References

[1] S. Ramakrishnan, M. Fuchs, K. S. Schweizer and C. F. Zukoski, J. Chem. Phys. **106**, 2201 (2002).

[2] S. A. Shah, Y. L. Chen, K. S. Schweizer and C. F. Zukoski, J. Chem. Phys. **118**, 3350 (2003).

[3] S. A. Shah, S. Ramakrishnan, Y. L. Chen, K. S. Schweizer and C. F. Zukoski, Langmuir **19**(12), 5128 (2003).

[4] S. A. Shah, Y. L. Chen, S. Ramakrishnan, K. S. Schweizer and C. F. Zukoski, J. Phys. Condensed Matter **15**(27), 4751 (2003).

[5] S. A. Shah, Y. L. Chen, K. S. Schweizer and C. F. Zukoski, to be published in J. Chem. Phys.

S. Ramakrishnan, S. A. Shah, Y. L. Chen, K. S. Schweizer, and C. F. Zukoski
University of Illinois at Urbana-Champaign
Urbana, IL 61801

Spinons, Solitons, and Breathers in Spin-1/2 Chains

No matter how strong the nearest neighbor antiferromagnetic interactions, quantum fluctuations prevent static long-range order within an infinite line of spin-1/2 quantum moments. What at first blush appears to be the simplest possible antiferromagnet, thus turns out to be a unique correlated spin liquid [1]. The structures of two materials with this extraordinary brand of dynamic magnetism are illustrated above Figs. 2 and 3. Figs. 2(a) and 3(a) show *zero field* inelastic neutron scattering data from these materials as a function of energy transfer, $\hbar\omega$, and wave vector transfer, q. For conventional magnets such data feature a sharp sinusoidal ridge through the q-ω plane, which is evidence for coherent spin wave excitations. While a ridge is also visible in the present data, its energy width greatly exceeds the experimental resolution. The implication is that neutrons cannot create coherent excitations in spin-1/2 chains. This is a surprise given that mobile domain walls called spinons are known to be well-defined excited states carrying heat and momentum over macroscopic distances. The paradox is resolved by recognizing that a spinon is actually just half of a spin flip (see Fig. 1 (a)-(c)). Two spinons are needed to scatter a neutron, and the broadened spectrum reflects the range of energies for spinon pairs that can carry the linear momentum delivered by the neutron.

Spinons also lead to remarkable properties in a *non-zero* magnetic field. While a classical antiferromagnet develops magnetization through uniform canting of otherwise antiferromagnetic spins, the magnetization of a spin-1/2 chain is carried by a finite density of spinon like defects. The average distance between these magnetized defects defines a characteristic field dependent length scale which is manifest in the neutron scattering data as a q-shift in the longitudinal part of the zero field sinusoidal ridge of scattering. The result is a set of overlapping gapless continua. Predicted more than 20 years ago, the effect found its first experimental realization this year at the NCNR [2]. The data shown in Fig 2(b) were acquired under the same conditions as Fig. 2(a) though with the spin chain in a magnetized state induced by an external field. There is no complete theory for these data but it was recently shown that much of the spectral weight can be associated with the two-particle continuum of the high field version of spinons called psinons [4]. Comparison of the data in Fig. 2(b) to this theory however reveals that there is spectral weight close to $q = \pi$ that cannot be accounted for by psinons [2]. Theoretical work is now

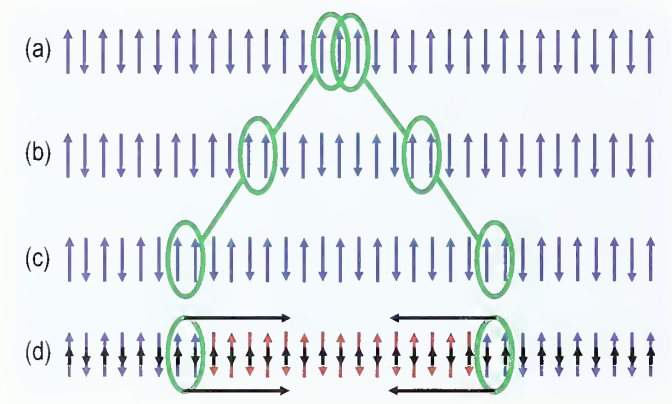

Fig. 1. Qualitative illustration of spinons in a spin-1/2 chain. (a) Shows a spin-flip excitation in an otherwise ordered segment of a spin chain. In the subsequent two frames the spin-flip is spatially separated into domain wall boundaries illustrating spinons that each carry half a spin flip. Separation of the walls costs no energy. (d) shows the situation when a staggered field (small black arrows) breaks the symmetry between even and odd sites of the lattice. Spinons now attract each other (separation costs energy) and can be expected to form bound states. Note that in a real spin-1/2 chain spinons are dynamic quantum degrees of freedom with a finite spatial extent.

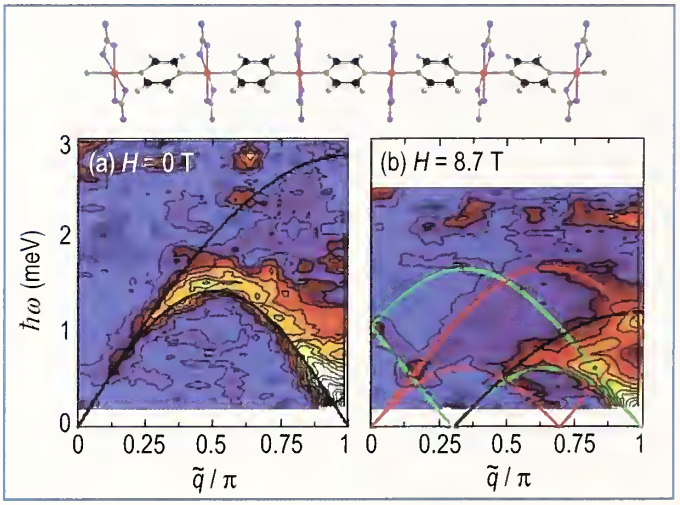

Fig. 2. False color image of SPINS neutron scattering data [2] from $Cu(C_4H_4N_2)(NO_3)_2$ (CuPzN) in zero and high field. Spin-1/2 copper atoms shown in red form uniform chains. The experiment provides evidence for a two-particle continuum from spin-1/2 particles with a field dependent chemical potential. The solid lines show boundaries for various types of continua determined through Bethe Ansatz and exact diagonalization.

under way to determine the nature of the corresponding excitations.

Static long-range order in the antiferromagnetic spin chain implies breaking the symmetry between odd and even sites of the lattice. As noted above, this does not occur spontaneously in a spin-1/2 chain but an applied field that alternates from site to site does break the symmetry and can therefore be expected to have a pronounced effect on both static and dynamic properties. Surprisingly, a staggered field is not hard to achieve. When even and odd sites along the spin chain have differently oriented atomic coordination environments, application of a uniform field induces an accompanying staggered field.

The molecular magnet $CuCl_2 \cdot 2$(dimethylsulfoxide) (CDC) has alternating coordination environments and Fig. 3(b) shows the dramatic effects on the neutron scattering spectrum in a field [3]. The zero field two spinon continuum coalesces into resolution limited modes with different energy gaps at $q = \pi$ and at the incommensurate wave vector. The staggered field breaks the domain symmetry (Fig. 1(d)), favoring antiferromagnetic domains that are aligned with the applied staggered field. If the domain between two spinons is out of phase with the staggered field the spinons attract each other. The strength of interaction grows with spinon separation resulting in asymptotically bound spinons. Because they consist of spinon pairs, these bound states can be created directly through neutron scattering.

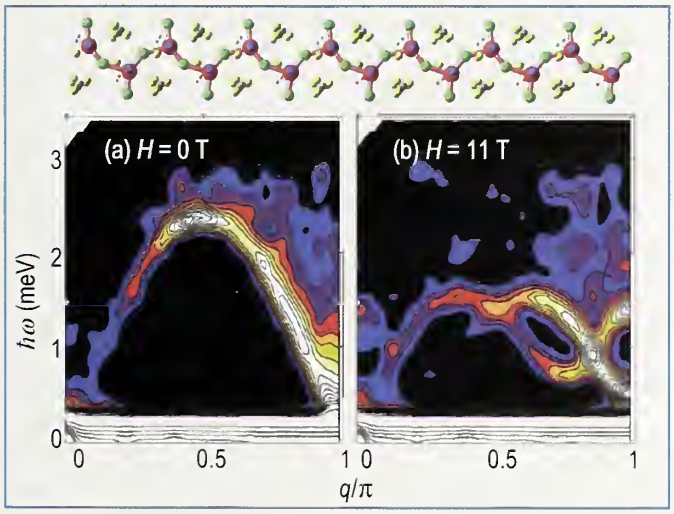

Fig. 3. False color image of DCS neutron scattering data [3] from $CuCl_2 \cdot 2$(dimethylsulfoxide) (CDC) in zero field and in a field of 11 Tesla. Spin-1/2 copper atoms shown in red form spin chains with alternating orientation of the coordinating environment, causing an effective staggered field in registry with the lattice in conjunction with the uniform field. The staggered field causes formation of soliton and breathers from spinons as evidenced by resolution limited modes with a finite energy gap.

Following the initial discovery of a field induced gap in a spin-1/2 chain at the NCNR [5], Affleck and Oshikawa showed that the relevant low energy field theory describing bound spinons is the quantum sine-Gordon model [6]. It can be shown that the excited states at the incommensurate wave vector in the spin-1/2 chain are topological excitations called solitons, while those at $q = \pi$ are soliton bound states called breathers. Identifying the lowest energy excitation at the incommensurate wave vector with a soliton, the quantum sine-Gordon model perfectly accounts for the energy of the two lower excitations at $q = \pi$ as being the corresponding breathers. The agreement between the observed excitation energies and the predictions of the quantum sine-Gordon model persists throughout the field range that we have accessed, which corroborates the identification of both excitations [3]. There is also detailed agreement between the experimental data and bound state structure factor calculations [7].

Despite its apparent simplicity, the spin-1/2 chain features a potpourri of complex many body physics that can be probed in exquisite detail using neutron spectroscopy. These experiments spur theoretical progress towards understanding strongly correlated electron systems and exemplify the close connection that is possible between theory and experiment in low dimensional quantum magnets.

References

[1] C. Broholm, *et al.*, pp 211-234 in "High Magnetic Fields – applications in condensed matter physics and spectroscopy" C. Berthier, L. P. Lévy, and G. Martinez, Eds. Springer Verlag (2002).

[2] M. B. Stone *et al.*, Phys. Rev. Lett., **91**, 037205 (2003).

[3] M. Kenzelmann *et al.*, cond-mat/0305476v1 submitted to Phys. Rev. Lett. (2003).

[4] M. Karbach *et al.*, Phys. Rev. B **66**, 054405 (2002).

[5] D. Dender *et al.*, Phys. Rev. Lett. **79**, 1750 (1997).

[6] M. Oshikawa *et al.*, Phys. Rev. Lett. **79**, 2883 (1997).

[7] F. H. L. Essler *et al.*, Phys. Rev. B **57**, 10592 (1998).

C. Broholm[1,2], Y. Chen[3], M. Kenzelmann[1,2], C. P. Landee[4], K. Lefmann[5], Y. Qiu[2,6], D. H. Reich[1], C. Rischel[7], M. B. Stone[8], and M. M. Turnbull[4]

[1] Johns Hopkins University, Baltimore, MD 21218

[2] NIST Center for Neutron Research
National Institute of Standards and Technology, Gaithersburg, MD 20899-8562

[3] Los Alamos National Laboratory, Los Alamos, NM 87545

[4] Clark University, Worcester, MA 01610

[5] Risø National Laboratory, DK-4000 Roskilde, Denmark

[6] University of Maryland, College Park, MD 20742

[7] Niels Bohr Institute, University of Copenhagen
DK-2100, Copenhagen, Denmark

[8] Pennsylvania State University
University Park, PA 16802

Structure and Properties of the Integer Spin Frustrated Antiferromagnet $GeNi_2O_4$

Spinels and pyrochlores are two of the most important crystal structures that are known to exhibit geometric magnetic frustration. In these materials there are three-dimensional networks of corner-sharing tetrahedra, a structural arrangement that leads to a high degree of magnetic frustration if the dominant nearest-neighbor interactions are antiferromagnetic. One interesting question that has not, to our knowledge, been addressed experimentally concerns whether half-integral spins exhibit fundamentally different behavior than integral spins in frustrated lattices. In order to address this issue we have been systematically investigating the magnetic and structural properties of spinels in which integer or half-integer-spin transition metal ions are located on the B-sublattice. In this report we describe the results [1] for an integer-spin (S = 1) frustrated magnet $GeNi_2O_4$.

$GeNi_2O_4$ is a normal spinel with the Ni^{2+} ions on the magnetically frustrated B-sites and the non-magnetic Ge^{4+} ions on the A-sites. $GeNi_2O_4$ becomes antiferromagnetic below a Néel temperature of $T_N \approx 12$ K. The crystal structure of $GeNi_2O_4$ has been refined, based upon neutron powder diffraction data from BT-1, in the cubic space group *Fd3m* at all temperatures. The structural refinements clearly demonstrate that there is no more than 1 % cation inversion (interchange of Ge^{4+} and Ni^{2+} ions between A and B sites), since Ge and Ni have very different neutron scattering lengths. This information cannot be obtained from x-ray diffraction due to the similar x-ray scattering strengths (atomic numbers) of Ge and Ni. In addition, we have verified that $GeNi_2O_4$ remains cubic below T_N using very high-resolution synchrotron x-ray powder diffraction at the Advanced Photon Source [1].

In Fig. 1 we show the crystal structure of $GeNi_2O_4$, with the relative spin orientations of the Ni^{2+} ions illustrated by plus and minus signs. The low temperature magnetic structure is a simple two-sublattice collinear structure in which the Ni^{2+} spins are aligned in ferromagnetic (111) planes, and the spin direction of the (111) planes alternates along the [111] direction [2]. Assuming this magnetic structure, we obtain a good fit to the magnetic peak intensities in our low temperature (T = 1.4 K) neutron diffraction pattern.

$GeNi_2O_4$ exhibits a surprising property, illustrated in Fig. 2 where we plot the intensity of the magnetic (½, ½, ½) Bragg reflection as a function of temperature. The Néel transition in $GeNi_2O_4$ clearly consists of two distinct transitions, the first located at 12.13 K and the second at 11.46 K. Such double Néel transitions have been observed in *one-dimensional* frustrated antiferromagnets [3], such as the chain Haldane magnet $CsNiCl_3$, but this is the first observation, to our knowledge, of such a transition in a *three-dimensional* frustrated magnet. The small splitting of the Néel transition shows that the Ni^{2+} ions in $GeNi_2O_4$ have very little magnetic anisotropy, and should thus be in the Heisenberg universality class.

The observation that $GeNi_2O_4$ remains cubic below T_N is in marked contrast with results for the transition metal oxide spinel $ZnCr_2O_4$ [4]. $ZnCr_2O_4$ undergoes a cubic-tetragonal structural phase transition at T_N. Such structural transitions have been described [5, 6] as three-dimensional analogs of the spin-Peierls transitions that occur in S = 1/2 one-dimensional antiferromagnets.

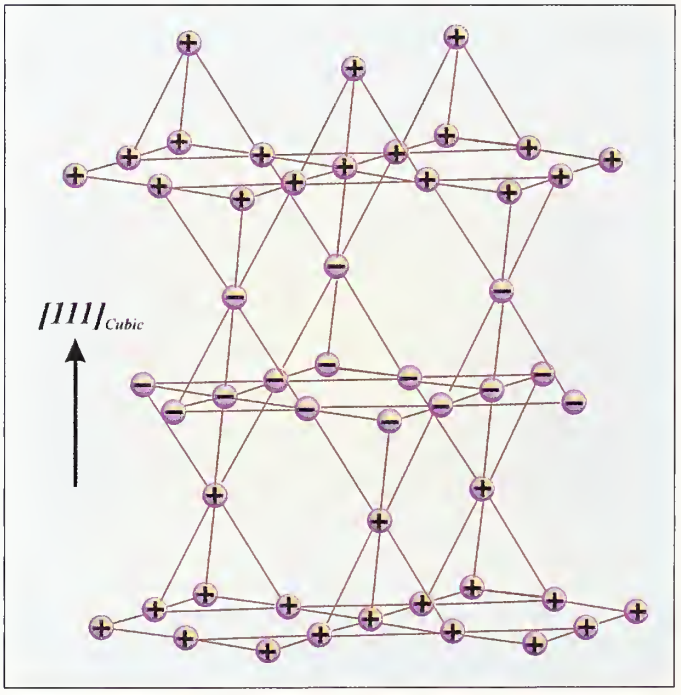

Fig. 1. A view of the crystal structure of $GeNi_2O_4$, illustrating the magnetically frustrated corner-sharing tetrahedra. The relative Ni^{2+} spin directions are shown by the plus and minus signs for the two collinear magnetic sublattices.

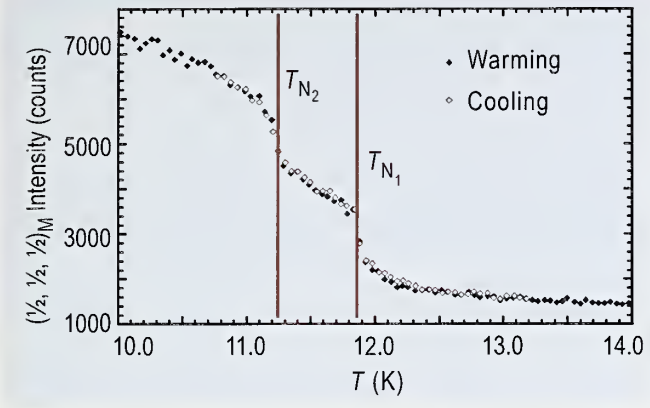

Fig. 2. The intensity of the (1/2,1/2,1/2) magnetic Bragg reflection versus temperature for $GeNi_2O_4$, measured on BT-7. The locations of the two Néel transitions, T_{N_1} and T_{N_2}, are shown.

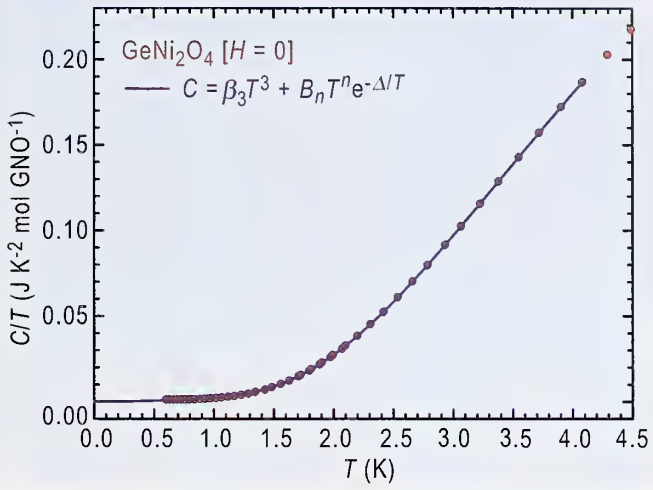

Fig. 3. Low temperature heat capacity of $GeNi_2O_4$ (red circles). A fit to the expression shown in the plot (blue line), assumes that both a gapless spin-wave term ($\beta_3 T^3$), and a gapped magnetic excitation term ($B_n T^n e^{-\Delta/T}$, with $n = 0$ and $\Delta = 11$ K), are present. It should be noted that the contribution to the T^3 term from the lattice (phonons) is about 8 times smaller than the magnetic contribution to this term at these low temperatures.

Furthermore, we have observed [1] the appearance of tetragonal distortions in two other spinels, $GeCo_2O_4$ ($S = 3/2$, effective spin 1/2 at low temperature) and $ZnFe_2O_4$ ($S = 5/2$), each of which has half-integer-spin transition metal ions. In both of these cases, the structural transitions are also closely associated with T_N, which suggests that distortions from cubic lattice symmetry generally occur at the Néel transitions in half-integer-spin magnetically frustrated spinels.

In light of these observations for half-integer-spin systems, it is interesting to speculate that the absence of a structural transition in $GeNi_2O_4$ may be a consequence of the integer-spin of the Ni^{2+} ion. In one-dimensional antiferromagnets, spin-Peierls transitions for spin-1 magnetic ions are prevented by the appearance of Haldane gaps, which render the chains rigid against dimerization [7]. This raises the question of whether a related phenomenon can also exist in a three-dimensional integer-spin *frustrated* lattice, which naturally leads us to measurements of the spin excitations in the Néel state of $GeNi_2O_4$.

In Fig. 3 we show the low temperature heat capacity of $GeNi_2O_4$. The data are superimposed with a fit including a contribution from gapless isotropic spin-waves and a gapped excitation located approximately $\Delta = 11$ K above the ground state. The gapped excitation in $GeNi_2O_4$ is a property of the Néel state *in the cubic structure*, and thus clearly requires a different explanation from the much higher energy excitation reported in *tetragonal* $ZnCr_2O_4$ [4, 6]. The absence of a structural phase transition in $GeNi_2O_4$ combined with the gapped magnetic excitation spectrum strongly suggests a direct connection between these phenomena and the integer spin of the Ni^{2+} ion.

References

[1] M. K. Crawford *et al.*, Phys. Rev. Lett., submitted; M. K. Crawford *et al.*, unpublished results.

[2] E. F. Bertaut *et al.*, J. Phys. **25**, 516 (1964).

[3] M. F. Collins and O. A. Petrenko, Can. J. Phys. **75**, 605 (1997).

[4] S.-H. Lee, C. Broholm, T. H. Kim, W. Ratcliff, and S.-W. Cheong, Phys. Rev. Lett. **84**, 3718 (2000).

[5] Y. Yamashita and K. Ueda, Phys. Rev. Lett. **85**, 4960 (2000).

[6] O. Tchernyshyov, R. Moessner, and S. L. Sondhi, Phys. Rev. Lett. **88**, 067203 (2002).

[7] F. D. M. Haldane, J. Appl. Phys. **57**, 3359 (1985).

M. K. Crawford, R. L. Harlow, R. Flippen
DuPont Co., Wilmington, DE 19880-0356

P. L. Lee, Y. Zhang
Advanced Photon Source
Argonne National Laboratory, Argonne, IL 60439

J. Hormadaly
Ben Gurion University of the Negev
Beer Sheeva, Israel

Q. Huang, J. W. Lynn
NIST Center for Neutron Research
National Institute of Standards and Technology
Gaithersburg, MD 20899-8562

R. Stevens, B. F. Woodfield, J. Boerio-Goates
Brigham Young University, Provo, UT 84602

R. A. Fisher
Lawrence Berkeley National Laboratory
University of California, Berkeley, CA 94720

Residual Stresses and Optimizing Machining Strategies for Aluminum Bars

Residual stresses have a major impact on the ability to fabricate dimensionally accurate machined components from aluminum wrought mill products. In addition, the ability to implement advanced assembly technologies such as determinant assembly, where parts are indexed to each other rather than to expensive assembly tooling, is compromised when the parts are not dimensionally accurate. An active research project on this subject is underway in which NCNR scientists are collaborating with Alcoa and Boeing. The current status of this project is outlined in this report.

In this work, finite element methods (FEM) are being used to predict residual stress profiles and to examine the influence of material processing and machining approaches on part distortion. However, although Alcoa is developing new destructive methods to estimate residual stresses in bulk materials, the neutron diffraction capabilities of the NCNR for characterizing residual stresses is key to validating both the FEM calculations and the measurement technique being developed at Alcoa. Ultimately, the goal is to understand the generation of residual stresses and how to control their effects in manufacturing and to correlate model predictions with actual experimental measurements. This information is critical in achieving optimization of the predictive capability utilizing new design tools that would enable much more efficient manufacturing approaches than are now employed.

The test system selected for the validation studies is a long rectangular extruded bar in which the longitudinal residual stress can vary as a function of position across the width and through the thickness, *i.e.*, $\sigma = \sigma(x,y)$. The material is aluminum alloy 2024 extruded using a 4-out die pattern, producing bars with a 63.5 mm by 63.5 mm cross section. For this study, four extrusions, each 1.83 m long, were cut from the parent extrusion for thermal processing at Alcoa and residual stress measurement and machining trials at NIST. Three 0.61 m long sections were cut from each extrusion. The twelve bars were attached in a vertical orientation to a hanging rack at a heat treatment furnace. All bars received a solution heat treatment (SHT) that is typical for a 2024 alloy. At the end of the SHT soak time, the material is quenched in 21 °C agitated tap water. Because of the vertical hanging orientation, each bar should experience the same quench on all four sides of the square cross section.

Residual stress measurements were made over the midplanes of three bars, randomly selected from the total, using the BT-8 stress diffractometer at the NCNR. A 5 mm by 5 mm by 5 mm sampling volume was used and the

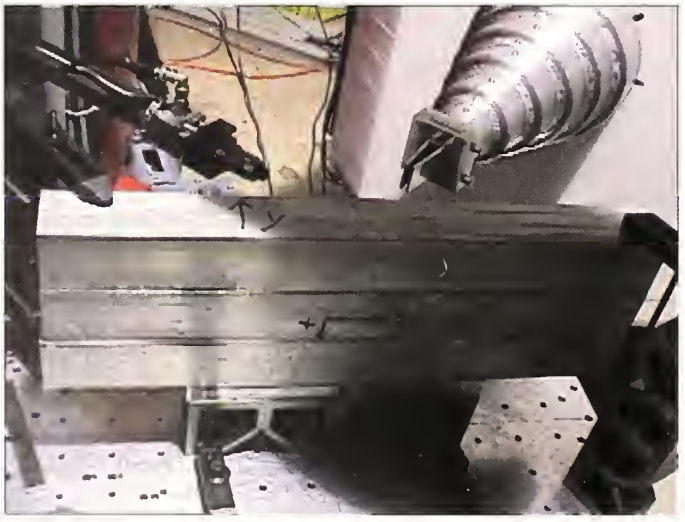

Fig. 1. The measurement configuration on the BT-8 instrument at the NCNR for residual stress determinations on three 2024 Al bars. Neutrons issuing from the collimated beam tube on the left are collected from the sample volume by the detector on the right. The sample is scanned by moving the mounting table.

Fig. 2. The effect of microstresses is minimized by utilizing 36 d_0 samples in which macrostresses are relaxed by the cross-cutting technique shown.

measurements made over a 9 x 9 mesh, 7.06 mm between centers. Because the material was composed of relatively large grains, the data were obtained by longitudinally averaging over a 90 mm long volume, extending ± 45 mm from the mid-plane. Since FCC metals are susceptible to grain-grain interaction microstresses, samples to provide the unstrained d spacing, d_0, representative of the whole cross-section were needed. These were obtained from a 25.4 mm by 63.5 mm by 63.5 mm piece cut from the end of a bar, and partially cut through the thickness in a 10 mm by 10 mm by 10 mm (6 x 6 mesh) pattern. The instrument and samples are shown in Figs. 1 and 2. Residual stresses were obtained from the measured d-spacings according to methods described previously [1].

The FEM is used to model the material and processing in order to guide the design of machining processes for optimal results. The initial objective of the FEM modeling is to obtain values for the level of quench-induced stress and to develop a simple final part geometry that exhibits widely varying distortion behavior as a function of machined part location. This involves a quenching simulation that predicts the thermal response of the aluminum to the quenchant, a mechanical simulation that predicts the quench-induced stress state and, finally, a machining simulation to predict the distortion. It is noted that the entire modeling process for identifying a machined part involves many FEM simulations and it is critical to have an efficient process for making changes to the input geometry and final part location [2].

In the upper part of Fig. 3 the three normal residual stress components determined by neutron diffraction are shown for one of the three bars studied. The distributions for the three bars were in reasonable agreement, but not identical — even within uncertainties. The lower part of Fig. 3 shows the FEM results for a bar.

The results, thus far, are encouraging although the minimum and maximum FEM-predicted residual stresses are somewhat too compressive for the xx and yy components. However, the real test of this project is in progress: that is, the capability to predict by a "machining" FE model the machined part distortion for a final part geometry and location chosen by the user utilizing the residual stress distribution previously calculated from the mechanical simulation. "L" shaped pieces will be machined from different positions in the three characterized bars. The FEM calculations predict significant differences in the amount of part distortion depending on the location of the "L" within the 63.5 mm by 63.5 mm cross section. The results are expected to be significant for a number of major applications.

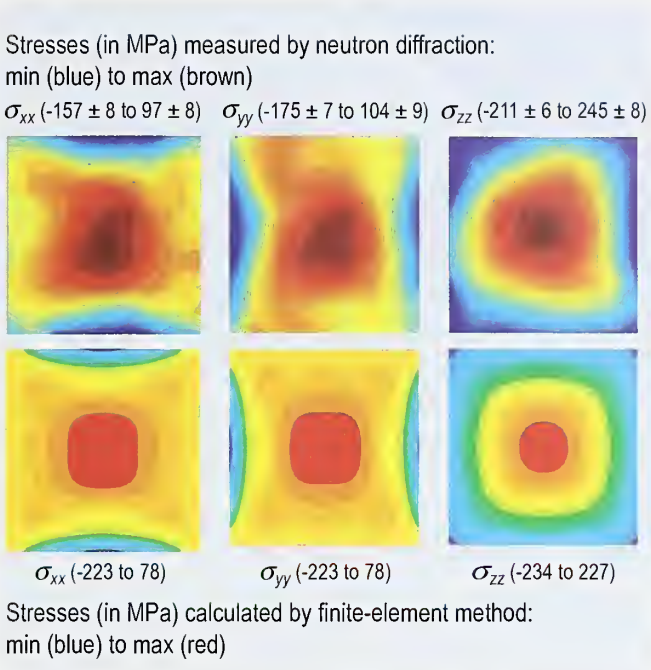

Fig. 3. Comparison of measured to calculated residual stresses. $\sigma_{ii} > 0$ is tensile; $\sigma_{ii} < 0$ is compressive. The upper panels represent the measurements while the lower panels show the comparable computed stresses.

References

[1] H. J. Prask and P. C. Brand, in Neutrons in Research and Industry, ed: G. Vourvopoulos, SPIE Proceedings Series, Vol. 2867, pp. 106-115 (1997), and references cited.

[2] M. A. Newborn and R. W. Schultz, The Influence of Residual Stress in Quenched 2024 Bar Stock on Machining Distortion, Alcoa Inc. internal publication, 2003.

T. Gnäupel-Herold
NIST Center for Neutron Research
National Institute of Standards and Technology
Gaithersburg, MD 20899-8562

and

University of Maryland
College Park, MD 20742

H. Prask
NIST Center for Neutron Research
National Institute of Standards and Technology
Gaithersburg, MD 20899-8562

R. Fields
Metallurgy Division
National Institute of Standards and Technology
Gaithersburg, MD 20899-8553

D. Bowden
Boeing Co.
St. Louis, MO 63166

E. Chu, M. Newborn, and R. Schultz
Alcoa, Inc.
Alcoa Center, PA 15069

Multicriticality in the Bragg-Glass Transition

The discovery [1] of a first-order solid-liquid transition in the vortex matter of a classic type-II superconductor niobium was widely regarded as an important result since it resolved a long-standing issue of whether a genuine order-disorder transition can take place in the vortex system in type-II superconductors, and whether the anomalous peak effect is indeed caused by a structural phase transition in the vortex matter. However, in a follow-up SANS experiment [2] on a Nb crystal which has a lower upper critical field, suggesting even less bulk disorder, neither the first-order transition nor the peak effect was found. These two seemingly contradictory results suggest either a trivial technical error in one of the two experiments, or something more profound and interesting in the physics of vortex matter, namely the existence of multicritical behavior in the Bragg-glass transition. We have now carried out a systematic study of the Nb crystal used in our original experiment, and have found such a multicritical point [3].

Our experiment was carried out on a Nb single crystal in which both the peak effect and the first-order Bragg-glass melting transition were observed at the same temperatures [1]. The sample has a zero-field T_c = 9.16 K, and an estimated Ginzburg-Landau parameter $\kappa(0)$ = 2.0. The experimental SANS configuration is shown in the inset of Fig.1 (a). The dc magnetic field was applied in the direction of the incoming neutron beam using a horizontal superconducting magnet. A coil was wound on the sample to allow *in situ* ac magnetic susceptibility measurements.

Fig.1(a) shows the SANS data at H = 0.3 T. The Gaussian widths are obtained from fitting the Bragg peaks (in intensity vs. azimuthal angle) to six Gaussian peaks evenly spaced 60° apart. It is clear that the azimuthal widths — a measure of orientational disorder in the vortex array — are strongly history dependent. Supercooling and superheating effects are observed for field-cooling (FC) and field-cooled-warming (FCW) paths, respectively. As reported previously [1], the disordered phase at $T > T_p$ and the ordered phase at $T < T_p$ are their respective thermodynamic ground states. The abrupt change in the structure factor $S(q)$ at the peak effect T_p depicts a symmetry-breaking phase transition from a vortex liquid with short-range order to a Bragg glass with quasi-long range order [1]. The phase transition is first order as evidenced by the strong thermal hysteresis in $S(q)$. Compared to that at higher fields, the metastability region for H = 0.3 T is smaller but still pronounced.

It was found that the thermal hysteresis of $S(q)$ observed in SANS is strongly field dependent, and the metastability region disappears completely at low fields.

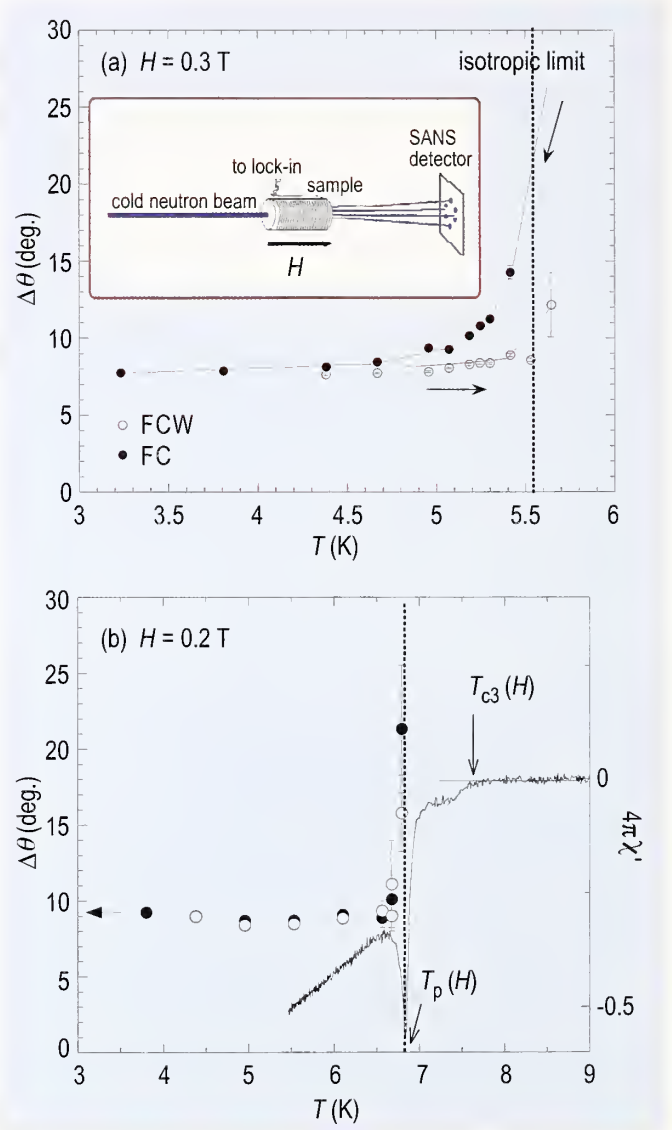

Fig. 1. (a) Temperature and history dependence of azimuthal widths of the (1,-1) diffraction peak at H = 0.3 T. The dashed line is the peak effect T_p at this magnetic field based on ac magnetic susceptibility measurements. Inset: experimental configuration. (b) Widths at H = 0.2 T. The ac susceptibility data are also shown for reference. Definitions of $T_p(H)$ and $T_{c3}(H)$ are shown.

Fig. 1 (b) shows the azimuthal width data for $H = 0.2$ T. For comparison, the real part $\chi'(T)$ of the ac magnetic susceptibility is also shown in Fig.1(b). The dip in $\chi'(T)$ is the well-established signature of the peak effect [1]. The history dependence of the Bragg-peak width is only detectable within 100 mK of the peak-effect temperature T_p. A similar trend is observable in the history dependence of the radial widths of the Bragg peaks. At 0.3 T, there is a pronounced thermal hysteresis in the radial widths. At 0.2 T, however, the hysteresis is barely discernable. At an even lower field of 0.1 T (data not shown), the thermal hysteresis in $S(q)$ is undetectable.

At $H = 0.1$ T, a very sharp peak effect (the onset-to-end width = 40 mK) is still present. Thus we believe the phase transition at 0.1 T is still first-order but the metastability region is too narrow to be resolved in SANS (the temperature resolution was $\approx$ 50 mK). Nevertheless, the diminishing hysteresis in the low-field regime suggests that the phase transition is becoming continuous and mean-field-like, namely there is a multicritical point on the phase boundary bordering the Bragg glass on the H-T phase diagram. We show that this multicritical behavior is directly related to the appearance and the disappearance of the peak effect.

Fig. 2 shows a three-dimensional plot of the $\chi'(T)$ as a function of temperature and magnetic field. At high fields, there is a pronounced peak effect, a characteristic dip in $\chi'(T)$. At higher temperatures above the peak-effect temperature $T_p(H)$ (or $H_p(T)$, used interchangeably), there is a smooth step in $\chi'(T)$. This step, $T_{c3}(H)$ (or $H_{c3}(T)$), defined in Fig.1 (b), is the onset of surface superconductivity. In the mean-field theory of Saint-James and de Gennes, $T_{c3}(H)$ is a continuous phase transition. The separation between $T_p(H)$ and $T_{c3}(H)$ grows larger with increasing magnetic field. Upon cooling, below $T_{c3}(H)$ and toward $T_p(H)$, the screening effect in $\chi'(T)$ increases gradually but there is no sharp feature to define another

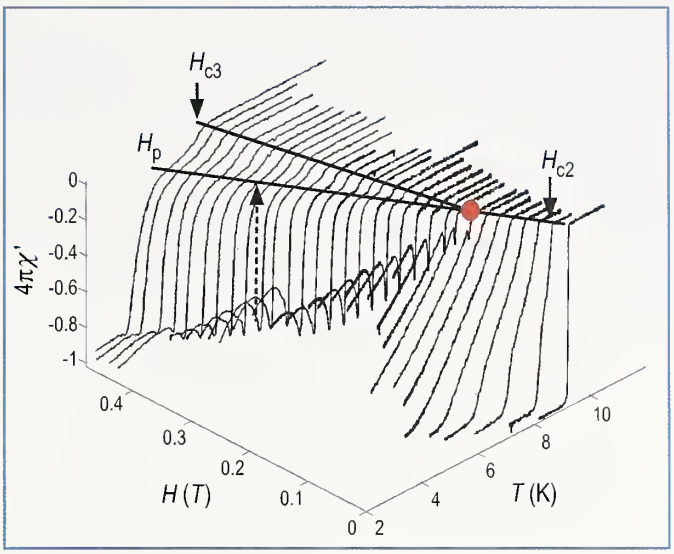

Fig. 2. Three-dimensional (3D) magnetic field and temperature dependence of the real part of the ac susceptibility $4\pi\chi'(T)$. Note that two values of ac fields were used in the measurements. For $H < 0.3$ T, $H_{ac} = 0.17$ mT, and for $H > 0.3$ T, $H_{ac} = 0.7$ mT, $f = 1.0$ kHz. The solid and dashed lines are guides to eyes. For the ac fields used, T_p is independent of the ac field amplitude.

temperature scale. With decreasing field, the peak effect becomes narrower and smaller. For $H < 0.08$ T, there is only a single kink in $\chi'(T)$ corresponding to the mean-field transition $T_{c2}(H)$ or $H_{c2}(T)$. There is no reentrant peak effect at low fields — the peak effect simply vanishes here. New theoretical studies are needed to elucidate the possible physical mechanisms of the multicritical point in a Bragg glass.

References

[1] X. S. Ling, S. R. Park, B. A. McClain, S. M. Choi, D. C. Dender, and J. W. Lynn, Phys. Rev. Lett. **86**, 712 (2001).

[2] E. M. Forgan, S. J. Levett, P. G. Kealey, R. Cubitt, C. D. Dewhurst, and D. Fort, Phys. Rev. Lett. **88**, 167003 (2002).

[3] S. R. Park, S.-M. Choi, D. C. Dender, J. W. Lynn, and X. S. Ling, submitted to Phys. Rev. Lett. (cond-mat-0305569).

S. R. Park and X. S. Ling
Brown University
Providence, RI 02912

S.-M. Choi
Korea Advanced Institute of Science and Technology
Taejon
South Korea

D. C. Dender and J. W. Lynn
NIST Center for Neutron Research
National Institute of Standards and Technology
Gaithersburg, MD 20899

Hidden Symmetries and Their Consequences in the t_{2g} Cubic Perovskites

The transition metal oxides have been the source of many fascinating physical phenomena such as high T_c superconductivity, colossal magnetoresistance, and orbiton physics [1]. These surprising and diverse physical properties arise from strong correlation effects in the *3d* bands. Most theoretical attempts to understand such systems are based on the Hubbard model. Here we report that for high symmetry transition metal oxides with threefold $\mathbf{t_{2g}}$ bands, this model possesses several novel hidden symmetries with many surprising consequences on the ground state properties [2, 3].

We consider cubic $3d^1$ perovskites (*i.e.*, ABO_3) where the five initially degenerate 3*d* states are split into a two-fold $\mathbf{e_g}$ manifold and a lower-energy threefold $\mathbf{t_{2g}}$ manifold with wavefunctions $d_{yz} \equiv X$, $d_{xz} \equiv Y$, and $d_{xy} \equiv Z$ (see Fig. 1). Keeping only the $\mathbf{t_{2g}}$ states, we base our discussion on the following generic three-band Hubbard Hamiltonian:

$$H = \sum_{i,\alpha,\sigma} \varepsilon_{i,\alpha} c^{+}_{i,\alpha,\sigma} c_{i,\alpha,\sigma} + \sum_{<ij>} \sum_{\alpha,\beta,\sigma} t_{i\alpha,j\beta} c^{+}_{i,\alpha,\sigma} c_{j,\beta,\sigma}$$
$$+ \sum_{i,\alpha,\beta,\sigma,\eta} U_{i\alpha,i\beta} \left(1 - \delta_{\alpha,\beta}\delta_{\sigma,\eta}\right) c^{+}_{i,\alpha,\sigma} c_{i,\alpha,\sigma} c^{+}_{i,\beta,\eta} c_{i,\beta,\eta}$$

Here $c^{+}_{i,\alpha,\sigma}$ creates a $\mathbf{t_{2g}}$ electron (or hole) on the i^{th} ion in the α spatial orbital (*i.e.*, $\alpha = X$, Y or Z) with spin σ, and $\varepsilon_{i,\alpha}$ is the on-site energy of the orbital at site i of a simple cubic lattice. $U_{i\alpha,i\beta}$ is the on-site Coulomb repulsion between orbitals α and β at site i. $t_{i\alpha,j\beta}$ is the effective hopping parameter from the α orbital at site i to the β orbital at its nearest neighbour site j.

As shown in Fig. 2, for cubic perovskites where the metal-oxygen-metal (*M-O-M*) bond is linear, the hopping parameter $t_{i\alpha,j\beta}$ is diagonal in the orbital indices α and β. This suggests that the total number of electrons in each orbital is a good quantum number. Furthermore $t_{i\alpha,j\beta}$ is zero along the "inactive" axis perpendicular to the orbital plane α, due to symmetry (Fig. 2). In other words an α-electron can only hop in α-plane. Thus, for the n^{th} plane perpendicular to the α-axis, the total number N_{n_α} of electrons in the α-orbital is conserved, *i.e.*, it is a good quantum number. Hence, one can consider the three dimensional lattice as a superposition of interpenetrating planes perpendicular to the *x*, *y*, and *z*-directions, each having a constant number of *X*, *Y*, and *Z* electrons, respectively, which are good quantum numbers (see Fig. 3(a)).

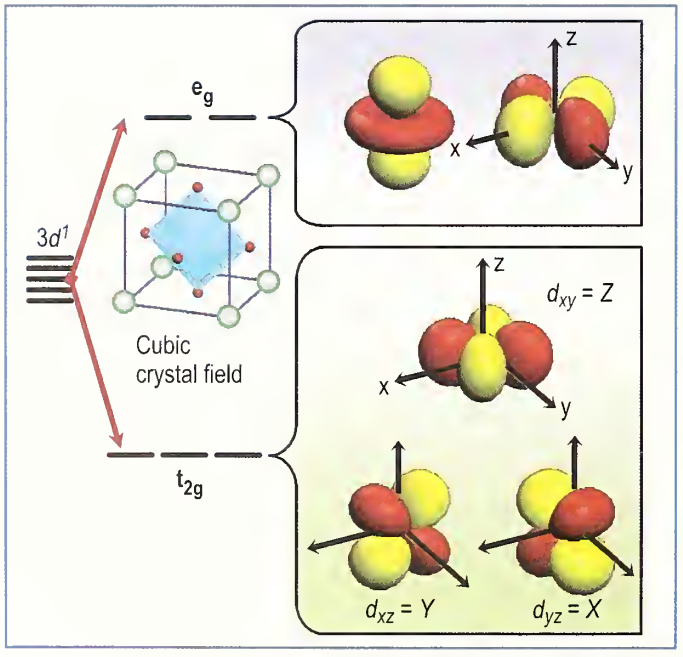

Fig. 1. A schematic view of the splitting of the five-fold *3d* orbitals under cubic crystal field. The transition metal is located at the center of the oxygen octahedra (shown in blue).

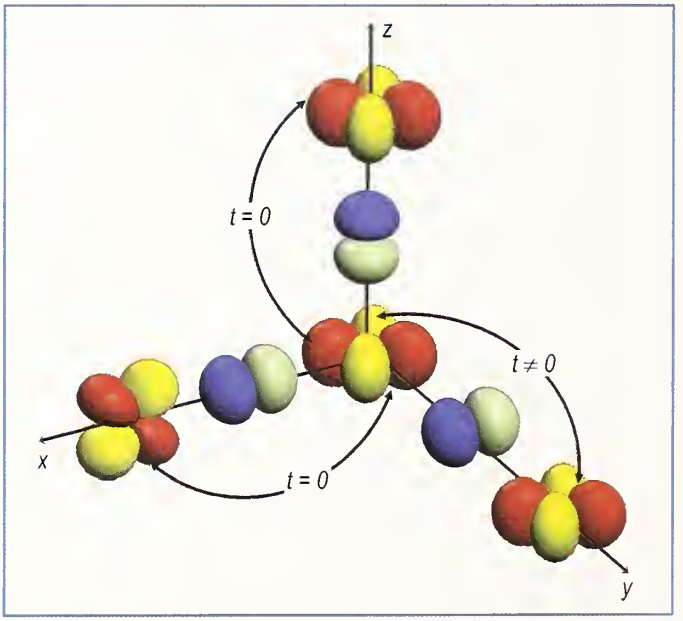

Fig. 2. A schematic view of the symmetry of the hopping parameter *t* via intermediate oxygen *p*-orbitals. Note that there is no hopping between different *d*-orbitals and no hopping along the *z*-axis for *Z*-orbitals due to symmetry.

In Ref. [3] we also show that the global rotation of the spins of α-orbital electrons *in any given plane* perpendicular to the α-axis leaves the Hubbard Hamiltonian given in Eq. (1) invariant. As a consequence of this rotational symmetry, one may conclude that both the Hubbard model and its 2nd order perturbation at order of t^2/U, the Kugel-Khomskii (KK) Hamiltonian, *cannot* support any long range spin order: if one *assumes* long-range spin order, the spins associated with α-orbitals within any given plane can be rotated at zero cost in energy, thereby destroying the supposed correlations among planes and/or among orbitals. and therefore the long-range order [2, 3]. The crucial conclusion here is that any credible theory of spin-ordering in these systems *cannot* be based solely on the KK Hamiltonian, as currently done in the literature.

The hidden symmetries discussed here are very useful in simplifying the exact numerical studies of small clusters. For example, to treat the simpler KK Hamiltonian for a cube of eight sites even using the conservation of the total spin (a widely used symmetry) requires the diagonalization of a matrix of dimensionality on the order of ½ million. Using the conservation laws applied to each face of the cube (see Fig. 3(a)), there is an astonishing numerical simplification. The ground state can be found from a Hamiltonian matrix within a manifold of just 16 states!! As seen in Fig. 3(b-d), these states are all products of four dimer states in each of which two electrons are paired into a spin zero singlet state. In this model a very unusual phenomenon occurs: when the electrons hop from site to site along active axes, they retain their membership in the singlet they started in. An example of this transformation is seen by comparing Figs. 3(c) and 3(d): pairs of electrons are tied together, as if by quantum mechanical rubber bands!

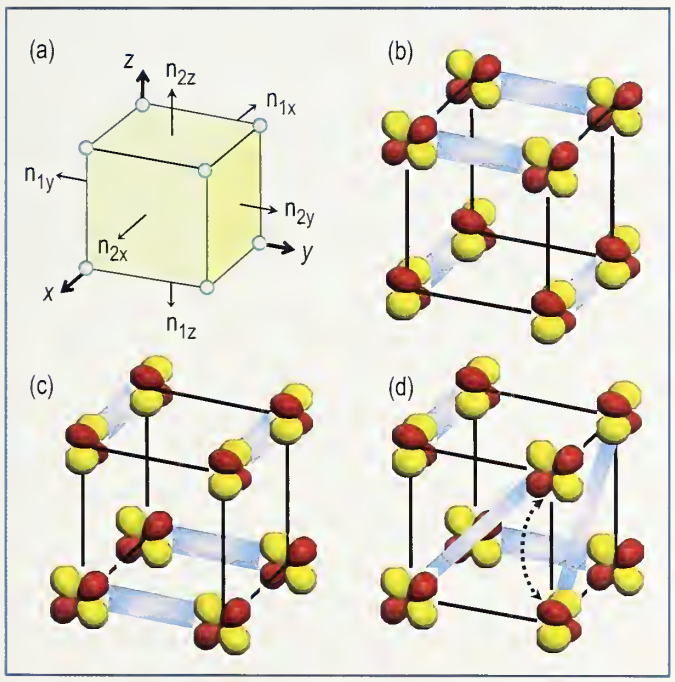

Fig. 3. (a) Six conserved quantum numbers as identified in the text, (b)-(c) Spin and orbital configurations for a cube of eight sites, indicating singlet spin dimers (as shown by thick blue lines) along the *x*-axis for *Y*-electrons and along *y*-axis for *X*-electrons. Configurations in (b) and (c) are the dominant ones in the ground state wavefunction. The less dominant configuration (d) is obtained from (c) by allowing the interchange of two *x*- and *y*- electrons along the *z*-axis, retaining their membership in the spin singlets.

In conclusion, we uncovered several novel symmetries of the Hubbard model for orthogonal $\mathbf{t_{2g}}$ systems. Using these symmetries, we rigorously showed that both the original Hubbard Hamiltonian [2] and the KK effective Hamiltonian [1] (without spin-orbit interactions) do not permit the development of long-range spin order in a three dimensional orthogonal lattice at nonzero temperature. It is important to take proper account of the symmetries identified here and to recognize that the observed long-range spin order can only be explained with the Hubbard or KK Hamiltonian providing suitable symmetry breaking terms are included. Such perturbations therefore play a crucial role in determining the observed behavior of these transition metal oxides. We hope that these results will inspire experimentalists to synthesize new $\mathbf{t_{2g}}$ transition metal oxides with tetragonal or higher symmetry. Such systems would have quite striking and anomalous properties.

References

[1] Y. Tokura and N. Nagaosa, Science **288**, 462 (2000) and references therein.

[2] A. B. Harris, T. Yildirim, A. Aharony, O. Entin-Wohlman, and I. Ya. Korenblit, Phys. Rev. Lett. (in press, 2003)(cond-mat/0303219).

[3] A. B. Harris, T. Yildirim, O. Entin-Wohlman, and A. Aharony, Phys. Rev. B (cond-mat/0307515).

T. Yildirim
NIST Center for Neutron Research
National Institute of Standards and Technology
Gaithersburg, MD 20899

A. B. Harris
University of Pennsylvania
Philadelphia, PA 19104

A. Aharony, O. Entin-Wohlman, and I. Ya. Korenblit
Tel Aviv University
Tel Aviv 69978, Israel

Structural Characterization of Acrylonitrile Catalysts

Acrylonitrile is not a household word, but products made from it are ubiquitous in our homes. Acrylic fibers made from acrylonitrile are used to make our clothing and carpets; they even reinforce paper products. Acrylonitrile-based plastics are often impact resistant and are used for computer and video-cassette cases. It is also formulated into nitrile rubber products, which are impervious to most solvents and thus are products of choice to contain gasoline or as protective gloves for lab use.

Worldwide, approximately 10 billion pounds of acrylonitrile are made each year through the reaction of ammonia and propylene. However, there is considerable interest in production of acrylonitrile from the reaction of ammonia and propane, since the latter compound is cheap enough to burn. Several multi-component mixtures have been tried as potential catalysts for this reaction, known as propane ammoxidation. The best of these mixtures contains molybdenum oxides doped with various transition metals. Neither the chemical structures nor the mechanism of operation of the various phases in the catalyst was previously understood.

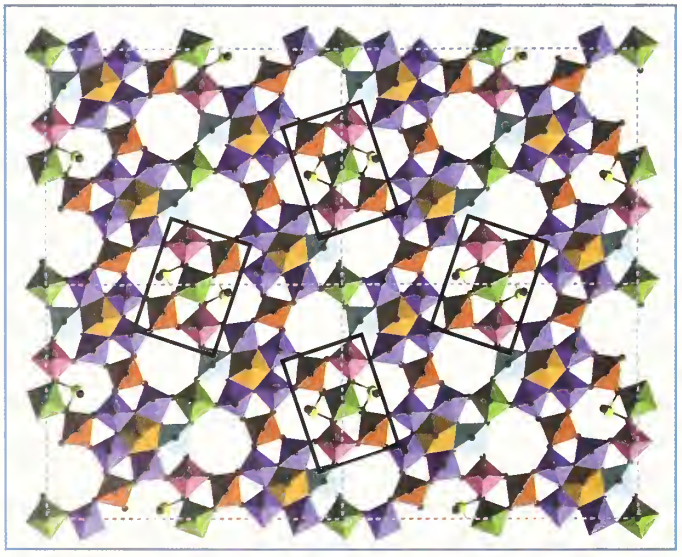

Fig. 1. A view of four unit cells of the M1 propane ammoxidation catalyst viewed along the *c*-axis. O atoms are shown as brown spheres and polyhedra are color coded by cation type: Mo^{6+} = purple, Mo^{5+} = pink, Mo^{6+}/ Mo^{5+} = light blue, Mo^{6+}/ V^{5+} = red, Mo^{5+}/V^{4+} = green, Te^{4+} = yellow. The regions believed to be active sites for catalysis are shown in rectangular boxes [3].

In 2001, workers at CNRS and Elf Atochem, both in France, used electron microscopy to study the most effective known propane ammoxidation catalyst, a (Mo, V, Nb, Te) oxide, and determined that it was composed of two chemical phases, an orthorhombic phase, labeled M1 and a hexagonal phase, known as M2. [1] They were even able to propose schematic structures for these materials. These models, however, do not indicate which cation is found at a particular site and thus provide no knowledge of cation coordination or valence state. Thus, these schematic structures provide little insight into the catalysis function of the materials.

The M1 and M2 compounds are not simple phases. They have large unit cells and do not form single crystals. Therefore, detailed structural information can come only from powder diffraction studies. However, materials of this form, with 40+ atoms in the asymmetric unit are at the limit of where powder diffraction can be used to resolve individual atoms. Further, deviations from crystallinity are seen readily in the electron microscope. The presence of these "errors" in crystallization reduces the long-range ordering in the material and degrades the diffraction pattern, which reduces the amount of structural information that can be obtained. Structural analysis from a mixture of the M1 and M2 phases is not possible. With the advent of combinatorial synthesis, collaborators at Symyx Technologies, Inc. were able to find ways to synthesize the M1 and M2 phases separately. [2] With reasonably pure phases it becomes possible to consider structure determination to learn how the materials function. With those questions answered, there is hope to create even better catalysts, that will further improve the industrial production of acrylonitrile from the desired starting materials.

The usefulness of x-ray diffraction for structure elucidation for these phases is also limited, because the scattering from O is almost negligible in the presence of heavy elements such as Mo, Nb and Te. For that matter, Mo and Nb are virtually indistinguishable with x-rays. With neutron powder diffraction, however, O scattering is comparable to the other atom types and Mo and Nb can potentially be distinguished. However at natural abundance, V is invisible to neutron diffraction.

Due to the complexity of these structures, even with neutron and x-ray powder diffraction data combined, it

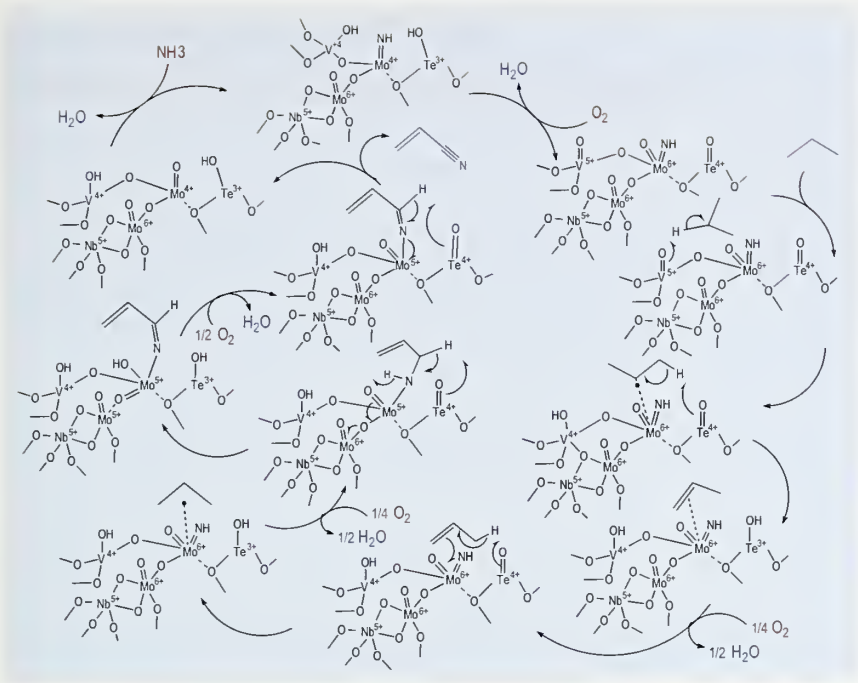

Fig. 2. A schematic mechanism for propane ammoxidation by the M1 catalyst that details the cation centers believed to be responsible for reactive process [3].

would still be very difficult and perhaps impossible to determine the structures *ab initio*. However, using unit cell dimensions and schematic models from electron microscopy, it was possible to build and test atomistic models against the neutron and x-ray powder diffraction data sets individually and in final stages, the two data sets combined. Using this approach, the structure of the M1 phase was determined (see Fig. 1). Work on the structure of the M2 phase, which turns out to be also orthorhombic, is nearly complete.

The result for the M1 phase shows that the material has a layer structure with two sets of channels, one approximately hexagonal, the other roughly heptagonal. The channels allow for the accommodation of large metal cations. This is where the large Te^{4+} cation atom sits. The large channel provides access to the cation's lone pair electrons, which is likely quite important in the ammoxidation reaction. Structural results also provide details of the metal atom coordination, which can then be used to determine the most likely oxidation state for each atom, as is indicated in the figure. Based on these structural results, it becomes possible to explore how the catalyst functions, as is outlined in Fig. 2 [3]. The active sites for propane oxidation to propylene are most likely the bridging lattice oxygen between V^{5+} cations and neighboring V^{4+} or Mo^{5+}. The subsequent addition of ammonia then occurs at a Mo^{6+} cation that neighbors the sites where propane is converted to propylene. Presumably, abstraction of hydrogen is carried out at Te^{4+} centers. The chemical function of the M2 phase will be more clear when the structure of that material is fully determined. However, it is clear that the M2 phase plays a role in the conversion of incompletely reacted intermediates that desorb from the M1 catalyst prior to the completion of the propane ammoxidation reaction.

Predicted oxidation states of V and Mo in M1 from the refined structure are consistent with those observed in XPS and EPR studies. The Te environment is consistent with those observed by Millet *et al.* using EXAFS in mixed-phase samples [4].

Only with the combination of numerous techniques was it possible to solve this propane ammoxidation catalyst puzzle. Neutron powder diffraction was essential for refinement of metal and oxygen coordinates and determination of metal-oxygen bond lengths, which was pivotal to calculating cation oxidation states and characterizing the chemical nature of the surrounding oxygen atoms.

References

[1] M. Aouine, J. L. Dubois, and J. M. M. Millet, Chem. Commun. **13**, 1180 (2001).

[2] P. DeSanto Jr, D. J. Buttrey, R. K. Grasselli, C. G. Lugmair, A. F. Volpe Jr., B. H. Toby and T. Vogt, Topics in Catalysis, **23** (1-4), 23-38 (2003).

[3] R. K. Grasselli, J. D. Burrington, D. J. Buttrey, P. DeSanto Jr, C. G. Lugmair, A. F. Volpe Jr., and T. Weingand, Topics in Catalysis, **23** (1-4), 5-22 (2003).

[4] J. M. M. Millet, H. Roussel, A. Pigamo, J. L. Dubois, and J. C. Jumas, App. Cat. A: Gen. **232** (1-2), 77 (2002).

P. DeSanto Jr., D. J. Buttrey and R. K. Grasselli
University of Delaware
Newark, DE 19716

C. G. Lugmair and A. F. Volpe Jr.
Symyx Technologies, Inc.
Santa Clara, CA 95051

B. H. Toby
NIST Center for Neutron Research
National Institute of Standards and Technology
Gaithersburg, MD 20899-8562

and

T. Vogt
Brookhaven National Laboratory
Upton, NY 11973

Serving the Science and Technology Community

The past year has been perhaps the best ever for users at the NCNR, in terms of numbers of participants, and the diversity and quality of their research activities at our facility. Nearly all of the originally envisioned instruments have been operational for several years, and forefront science, as represented by the highlight articles in this report, is being produced at a steady rate. Although it is fair to say that the NCNR has reached a mature state of development, new instruments are still being developed and brought on line. The CNBT reflectometer (AND/R) is being completed during the summer of 2003, and the MACS cold-neutron triple-axis and an upgraded 10 m SANS diffractometer will be made available in the near future.

The User Program

Making the NCNR accessible to a diverse community from academia, government and industry requires continual effort. Efficient proposal handling, fair and thorough review, and timely allocation of instrument time are essential to our user community. For the past year, our proposal process, including proposal review as well as submission, has been entirely Internet-based, resulting in a significant shortening in the time between proposal deadline and beamtime allocation. Despite increased security, physical access to our facility has been significantly delayed in only a handful of cases. User demand has remained very strong, with research participation (see Fig. 1) and the number and quality of proposals at an all-time high.

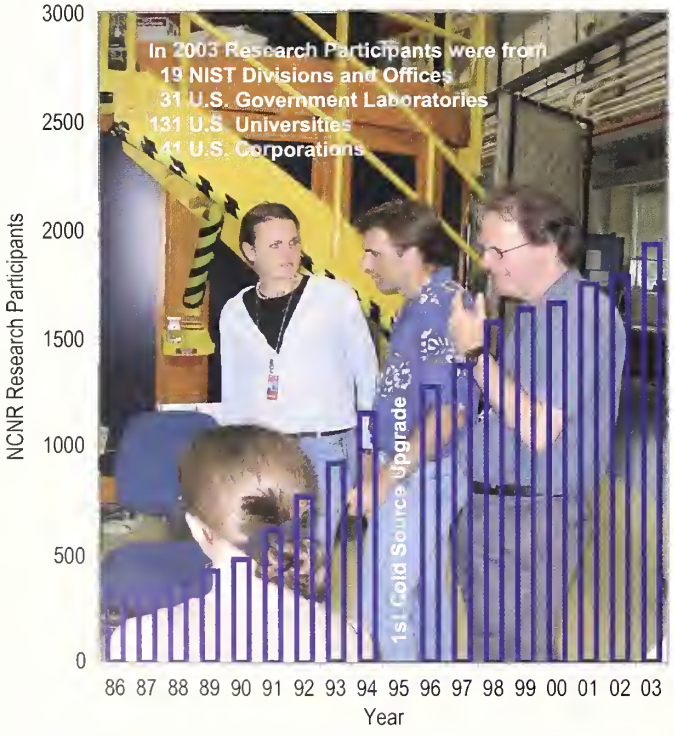

Fig.1. Numbers of NCNR Research Participants over time.

While there are several ways in which users access NCNR instrumentation, the most important is through our formal proposal process. At approximately six-month intervals, users may submit proposals for beam time. After each proposal has received written reviews from external referees, our Program Advisory Committee (PAC) allocates beam time to the best proposals, based on the reviews, their own judgment, and technical input from NCNR staff. Current PAC members include Andrew Allen (NIST Ceramics Division), Robert Briber (Maryland), Michael Crawford (DuPont), Sossina Haile (Cal Tech), Kenneth Herwig (Oak Ridge), Yumi Ijiri (Oberlin), Michael Kent (Sandia), Sanat Kumar (Rensselaer), Robert Leheny (Johns Hopkins), Dieter Schneider (Brookhaven), and John Tranquada (Brookhaven). Over the course of a year, the PAC allocated more than 1100 instrument-days to more than 290 experiments. In doing so, it had to make some difficult choices, since a total of more than 2400 days were requested in more than 380 proposals. The proposal system applies to only about half the instruments at the NCNR, but these are our most advanced ones, supported at a high level by NCNR staff and all our available resources. Although the other instruments are not offered through proposals, most of the time on the latter is also allocated to users through direct collaborations with local staff, or through more formal collaborative research consortia, as detailed below. For example, short- and long-term collaborations account for most of the beam time scheduled on the thermal triple-axis spectrometers.

A New Voice for Users

A separate advisory committee has recently been formed to represent our user community. At monthly conference call meetings, members of the NCNR Users' Committee discuss users issues, sometimes with the

participation of NCNR staff and management. The current membership includes Nitash Balsara (UC Berkeley, chair), Collin Broholm (Johns Hopkins), Paul Butler (Oak Ridge), Tonya Kuhl (UC Davis), Robert Leheny (Johns Hopkins) (liaison to the PAC), and Paul Sokol (Penn State). Among recent topics of discussion were software for data analysis, sample environments, the proposal process, and obtaining feedback from users. The committee welcomes comments from users at any time. Please see http://www.ncnr.nist.gov/NCNR_Users_Commitee.html for the members' email addresses.

Center for High Resolution Neutron Scattering

The Center (CHRNS) is a most important component of user participation at our facility. Funded by the National Science Foundation (NSF) and NIST, it offers a suite of instruments unmatched in North America for the investigation of the structure and dynamics of solids by neutron scattering, probing length scales from 1 nm to ≈ 10 μm and energies from ≈ 30 neV to ≈ 100 meV. Most of the proposals we receive ask for time on one of the CHRNS instruments, which include two 30 m SANS diffractometers, a high-resolution USANS diffractometer, a backscattering spectrometer, a neutron spin echo spectrometer, and a cold-neutron triple-axis spectrometer. An upgraded 10 m SANS diffractometer will be included among the CHRNS instruments in the near future.

Cold Neutrons for Biology and Technology

A new instrument for structural biology, the Advanced Neutron Diffractometer/Reflectometer, AND/R, has recently been completed. (See highlight on page 6 of this report.) This instrument and other facilities dedicated to studies of biological membrane systems are part of the Cold Neutrons for Biology and Technology (CNBT) program, funded by the National Institutes of Health (NIH), with contributions from NIST, the University of California at Irvine and the University of Pennsylvania. In addition to the above-mentioned institutions, the CNBT partnership consists of investigators from Johns Hopkins University, Rice, Carnegie Mellon, and Duke University. Other collaborators are from UC San Diego, the Los Alamos National Laboratory, and NIH. Other facilities at NCNR dedicated to CNBT include 10 % of the time on the NG-7 30 m SANS diffractometer, a fully equipped biology laboratory, and a state of the art computer facility for molecular dynamics computations. The combination provides a powerful set of capabilities for U.S. researchers interested in structural biology investigations by neutron scattering.

NOBUGS 2002

A conference on scientific computing at user facilities was hosted by NIST on November 4–6, 2002, addressing both software and hardware issues at neutron and synchrotron x-ray user facilities. The 77 participants represented nearly all the world's major scattering laboratories. The 2002 conference, organized by NCNR staff, was the fourth in the biennial NOBUGS series, providing an opportunity for those involved to compare notes, discuss techniques and results, and establish collaborations in the area of computing and data acquisition infrastructure for research, a field not normally covered by traditional scientific conferences. Among the topics highlighted at NOBUGS 2002 were Data Acquisition and Instrument Control Methods, Data Formats, Data Reduction, Visualization and Analysis, Collaborative Initiatives and Distributed Computing, and Computer Security at User Facilities.

Ninth Annual Summer School

More than 30 students from 23 different institutions traveled to the Gaithersburg, MD campus of the National Institute of Standards and Technology to attend the ninth annual summer school on neutron scattering during the week of June 9–13, 2003. The school was organized by the NCNR and CHRNS with support from the National Science Foundation, and involved students from 18 states and Canada with diverse backgrounds ranging from chemistry, physics, and materials science, to polymer science, nuclear engineering, and biophysics. The summer school alternates every year between the two central themes of diffraction and spectroscopy. This year's school focused on four different dynamical studies using the NCNR's Disk Chopper Spectrometer (DCS), High-Flux Backscattering Spectrometer (HFBS), Neutron Spin Echo (NSE) spectrometer, and Spin Polarized Inelastic Neutron Scattering (SPINS) spectrometer. Most of the students' efforts were directed to hands-on experiments, a direction that we have followed for several years. Course materials about the experiments and underlying principles were made available through our website prior to the school. Small groups of students rotated among the instruments, performing illustrative experiments, and analyzing their data with the aid of our software and the advice of our staff. Among the experiments was the study of the diffusion of surfactant micelles and shape fluctuations of

microemulsions using the NSE spectrometer, and quantum rotations in methyl iodide using the HFBS. On the final day, each of the student groups presented the results of their studies to the rest of the school. According to evaluations, the school was highly effective in introducing the students to the various methods and applications of neutron spectroscopy.

Theory, Modeling, and Neutron Scattering

Modern materials research relies heavily on developing models that explain and predict behavior under a variety of conditions. Because of the relatively simple nature of the interaction between neutrons and materials and the wide dynamical and spatial ranges that can be probed, neutron scattering is an important method for testing the validity of these theoretical models. To promote a fruitful exchange between theory and experiment, NCNR's Taner Yildirim, Seung-Hun Lee and Dan Neumann organized a workshop entitled Theory, Modeling and Neutron Scattering co-sponsored by the NCNR and NIST Center for Theoretical and Computational Materials Science. This workshop brought experts from around the world on both theoretical and modeling methods and neutron scattering measurements to the NCNR for a three-day meeting in August 2003. Invited presentations covering a wide range of materials from proteins to nanotubes to magnetic perovskites sparked an intense discussion among the more than 50 attendees on how combining these techniques offers key insights into a remarkable variety of phenomena in materials.

Independent Programs

The Neutron Interactions and Dosimetry Group (Physics Laboratory) provides measurement services, standards, and fundamental research in support of NIST's mission as it relates to neutron technology and neutron physics. The national and industrial interests served include homeland defense, neutron imaging, scientific instrument calibration, nuclear-electric power production, radiation protection, defense nuclear energy systems, radiation therapy, and magnetic resonance imaging. The group's research may be represented as three major activities. The first is Fundamental Neutron Physics including magnetic trapping of ultracold neutrons, operation of a neutron interferometry and optics facility, development of neutron spin filters based on laser polarization of ^{3}He, measurement of the beta decay lifetime of the neutron,

Fig. 2. Daniel Phelan, Souleymane Omar Diallo, Hui Wu and Seth Jonas analyze results of a backscattering spectrometry experiment at the ninth annual Summer School on Neutron Scattering.

and investigations of other coupling constants and symmetries of the weak interaction. This project involves a large number of collaborators from universities and national laboratories. The second is Standard Neutron Fields and Applications using both thermal and fast neutron fields for materials dosimetry in nuclear reactor applications, neutron spectrometry development, and for personnel dosimetry in radiation protection. These neutron fields include thermal neutron beams, "white" and monochromatic cold neutron beams, a thermal-neutron-induced ^{235}U fission neutron field, and ^{252}Cf fission neutron fields, both moderated and unmoderated. The third is Neutron Cross Section Standards, including experimental advancement of the accuracy of such standards, as well as their evaluation, compilation and dissemination.

The **Smithsonian Center for Materials Research and Education's (SCMRE) Nuclear Laboratory for Archeological Research** has chemically analyzed over 26,600 artifacts by INAA at the NCNR over the last 26 years. SCMRE's research programs draw extensively upon the collections of the Smithsonian, as well as those of national and international institutions. The chemical analyses provide a means of linking these diverse collections together to study continuity and change involved in the production of ceramic objects. INAA data are used to determine if groups of ceramics have been made from the same or different raw materials. The ceramics can then be attributed to geographic regions, specific sources, workshops and even individual artists. The ability to use chemical composition to link specific pottery groups to specific production locations through the analysis of less portable fired tiles and bricks has shown that nearly all individual California missions were producing earthenware ceramics for their own use soon after their founding. Moreover, potters at five missions had mastered the technologically demanding process of glazing and were also producing Pb glazed pottery previously thought to have all been imported from Mexico.

The **Nuclear Methods Group** (Analytical Chemistry Division, Chemical Sciences and Technology Laboratory) develops and applies nuclear analytical techniques for the determination of elemental compositions, striving for improvements in accuracy, sensitivity, and selectivity. The group has pioneered the use of cold neutrons as analytical probes in two methods, prompt-gamma activation analysis (PGAA) and neutron depth profiling (NDP). In PGAA, the amount of a particular analyte is measured by detecting characteristic gamma-rays emitted by the sample while it is being irradiated in an intense cold-neutron beam. NDP is another in-beam method that can characterize the concentration of several elements as a function of depth in the first few microns below a surface. It accomplishes this by energy analysis of the charged particles emitted promptly during neutron bombardment. In addition to NDP and PGAA, the group has a high level of capability in two more conventional methods, instrumental and radiochemical neutron activation analysis (INAA and RNAA). In aggregate, the techniques used by the group are a powerful set of complementary tools for addressing analytical problems for both in-house and user programs, and are used to help certify a large number of NIST Standard Reference Materials.

The **Center for Food Safety and Applied Nutrition**, U.S. Food and Drug Administration (FDA), directs and maintains a neutron activation analysis (NAA) facility at the NCNR. This facility provides agency-wide analytical support for special investigations and applications research, complementing other analytical techniques used at FDA with instrumental, neutron-capture prompt-gamma, and radiochemical NAA procedures, radioisotope x-ray fluorescence spectrometry (RXRFS), and low-level gamma-ray detection. This combination of analytical techniques enables diverse multi-element and radiological information to be obtained for foods and related materials. The NAA facility supports agency quality assurance programs by developing in-house reference materials, by characterizing food-related reference materials with NIST and other agencies, and by verifying analyses for FDA's Total Diet Study Program. Other studies include the development of RXRFS methods for screening food ware for the presence of Pb, Cd and other potentially toxic elements, use of instrumental NAA to investigate bromate residues in bread products, use of prompt-gamma NAA to investigate boron nutrition and its relation to bone strength, and the determination of the elemental compositions of dietary supplements.

The **ExxonMobil Research and Engineering Company** is a member of the Participating Research Team (PRT) that operates, maintains, and conducts research at the NG-7 30 m SANS instrument and the NG-5 Neutron Spin Echo Spectrometer. Their mission is to use those instruments, as well as other neutron scattering techniques available to them at NCNR, in activities that complement research at ExxonMobil's main laboratories as well as at its affiliates' laboratories around the world. The aim of these activities is to deepen understanding of the nature of ExxonMobil's products

and processes, so as to improve customer service and to improve the return on shareholders' investment. Accordingly, and taking full advantage of the unique properties of neutrons, most of the experiments use SANS or other neutron techniques to study the structure and dynamics of hydrocarbon materials, especially in the fields of polymers, complex fluids, and petroleum mixtures. ExxonMobil regards its participation in the NCNR and collaborations with NIST and other PRT members not only as an excellent investment for the company, but also as a good way to contribute to the scientific health of the nation.

The NCNR provides its resources to a large number of researchers from US universities and colleges, and the latter in turn have provided substantial aid to the construction of NCNR instruments and participation in collaborative research programs. For example, **the Johns Hopkins University** has taken a leading role in the development of the MACS spectrometer, and conducts extensive studies of magnetism and soft condensed matter, involving several faculty members, as well as engineering staff. The **University of Maryland** is likewise heavily involved at the NCNR, maintaining several researchers at our facility. Other institutions that have noteworthy long-term commitments at the NCNR are the **University of Minnesota** (member of the participating research teams, or PRTs, for the NG7 SANS instrument and the NG7 reflectometer). **UC Irvine**, **Johns Hopkins, Penn**, **Rice**, **Duke**, and **Carnegie-Mellon University** are all members of the CNBT collaboration. The **University of Pennsylvania** is also a member of the PRT for the FANS spectrometer.

The **U.S. Army Research Laboratory** has sponsored a scientific program based at the NCNR for three decades. Among its accomplishments are investigations of materials at high pressure, determinations of crystal structure of molecular solids, and the initiation of residual stress measurements at the NCNR.

The NIST neutron source operated for 255 full power (20 MW) days or approximately 100 % of the scheduled time. A typical operating year consists of seven cycles. A cycle has 38 days of continuous full power operation, followed by 11 days of shutdown maintenance, refueling, and startup preparations. The number of operating days in this fiscal year has increased significantly over the previous year because of improvements to the physical systems. The new shim arm seals have reduced leakage as expected and a sample of seal material undergoing testing has exhibited no noticeable corrosion. The new cooling tower has performed well, allowing full power operation through all of the summer of 2002. All work has been completed on the Thermal Column Tank Cooling System, fulfilling the design requirement to provide cooling without drawing water or helium from the main heavy water systems. A second pump was added and a purification loop was installed, with purification of the system heavy water achieved using particulate filters and an ion exchanger column. The system has had no adverse affect on the operating schedule: a replacement tank has been fabricated for future installation. Other upgrades accomplished in FY2003 include the permanent addition of camera equipment for monitoring refueling operations and replacement of the electronics for both intermediate range nuclear channels. These new electronics have worked well and are also serving as an evaluation platform to determine the type of replacement instrument for all of the nuclear channels.

Recently licensed as NCNR operators are: (left photo) Randy Strader, and (right photo) Greg Heller and Chris Grant. Jim Moody (far right) is in training as an operator.

All security measures requested by the U. S. Nuclear Regulatory Commission for the facility have been implemented fully. Items necessary for 20 more years of operation, such as secondary cooling water pumps and motors, control rods, heavy water, and a new operating console, have been acquired, are in production, or are in various stages of planning.

Data Analysis, Visualization, and Modeling Software Developments

This has been an exciting year in the area of data visualization and analysis software development with numerous additions to the NCNR's growing suite of software tools as well as many enhanced capabilities in the existing software. Version 1.0 of DAVE (the Data Analysis and Visualization Environment), is a comprehensive set of software tools developed for the interpretation of inelastic neutron scattering data, and was released last year (see Fig. 1). DAVE is a feature-rich application under extensive development as its user base grows and additional requests are accommodated. Some of the new capabilities added this year include enhancements in visualization with fully customizable plots in one and two dimensions, proper handling for single crystal time-of-flight data, new capabilities for exploring and analyzing multiple datasets, and a new module allowing users to fit parameterized models of $S(Q,\omega)$ to 2-dimensional data. These additions are currently undergoing extensive beta testing and are available in the current development version of DAVE (http://www.ncnr.nist.gov/dave/).

The *Igor Pro*-based SANS data reduction and analysis software developed at the NCNR has proven to be very popular with facility users. The Ultra Small-Angle Neutron Scattering (USANS) instrument at BT-5 extends the lowest momentum transfer Q reached by SANS by nearly two orders of magnitude. In response to users' needs, *Igor Pro*-based software has been developed to allow user-friendly reduction of USANS data sets. The software allows experimenters to inspect raw USANS data and to interactively reduce them into a fully corrected USANS data set (see Fig. 2).

A team from the NCNR, the University of Maryland, Baltimore County, and from Los Alamos National Laboratory (LANL) are developing a SANS-Modeler software package. This package is a web-based (http://sans.chem.umbc.edu/) molecular modeling tool to aid users performing Small Angle Neutron Scattering experiments on biological macromolecules. The web site is a compilation of software developed over the years at both the NIST Center for Neutron Research and LANL.

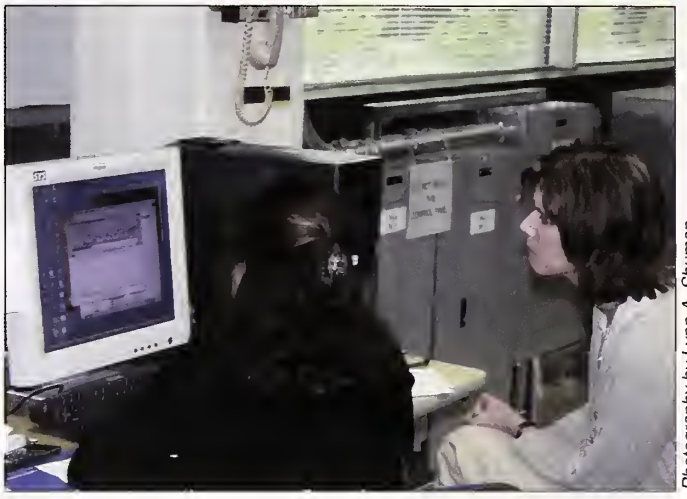

Photography by Lynn A. Shuman

Fig. 1. Victoria Garcia-Sakai and Janna Maranas (Pennsylvania State University) inspect some of their DCS data using the DAVE software package.

Currently users can calculate the contrast factor for nucleic acids and proteins as well as for protein/nucleic acid complexes, simulate a molecular structure using simple shapes such as spheres, cylinders and helices and generate model SANS data, and align two macromolecular structures from which the model SANS data can be calculated. Furthermore users can calculate model SANS data from high-resolution x-ray crystallography or NMR structures that are written in the format recognized by the Research Collaboratory for Structural Bioinformatics (RCSB) Protein Data Bank (PDB). In addition to the on-line modeling capabilities SANS-Modeler also allows 3-D visualization of protein structures. Currently, SANS-Modeler is being tested and planned release to the general SANS community is scheduled for later this year.

Over the past year our reflectometry fitting software has been greatly refined and it is now available for different operating system platforms, including Linux, Windows, Mac OS/X, and SGI's IRIX. Installation is as simple as dragging a single file onto the desktop. With its context sensitive help facility and graphical user interface it is easy for novice users to analyze their data. With access to the underlying scripting language, it is a powerful and flexible tool for experts. This software is gaining wide acceptance in the NCNR reflectivity user community as the standard tool for data reduction and analysis. From the NOBUGS

2002 conference in November and from presentations inside NIST, we are now interacting with other US neutron facilities to further improve the software and explore the possibility for broader use.

EXPGUI, the NCNR-developed graphical interface to the Los Alamos GSAS crystallography package continues to impact the Rietveld community. In the past year, the software was downloaded well over a thousand times and the web pages were viewed more than one hundred thousand times. The user-friendly nature of the EXPGUI package is attractive to students and the program has now been integrated into a number of university courses. It has also been widely taught in workshops, for example at the recent Oak Ridge National Lab's NICEST workshop, the Georgia Tech Advanced Rietveld Short Course and the American Crystallographic Society's annual summer crystallography course. Requests for program enhancements, as well as new features added to the software, are tracked on the NCNR website (www.ncnr.nist.gov/xtal/software/expgui/wishlist.html). In FY2003, requests outstripped the Crystallography team's ability to respond. The major new features added to the code were:

- CIF: The IUCr's standard format, the crystallographic information file (CIF), including the powder diffraction extensions (pdCIF) have been implemented.

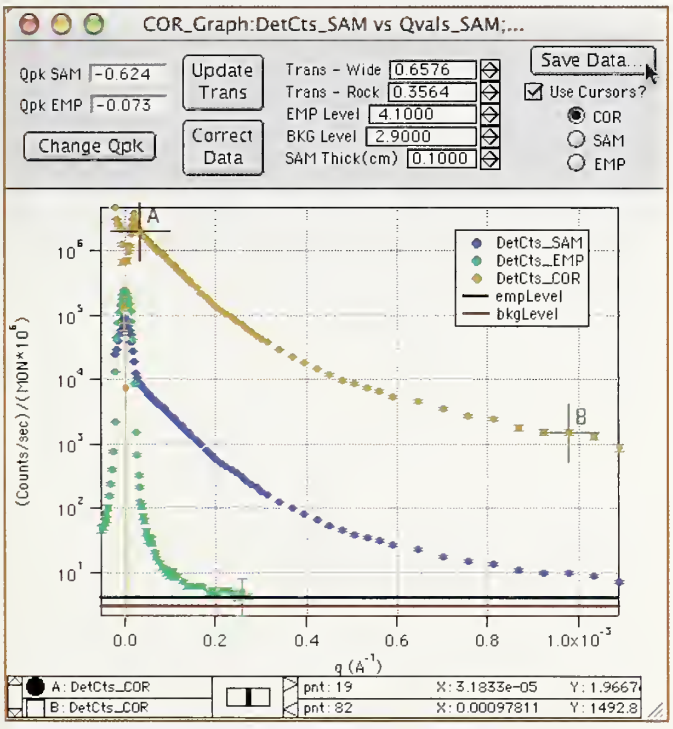

Fig. 2. A screenshot of USANS data reduction software, showing the raw scattering of the sample and empty cell, and the (rescaled) corrected USANS data. The user can override any of the automatically determined parameters, and the effects are directly visualized in the graph.

[Toby, B. H., Von Dreele, R. B. & Larson, A. C. "Reporting of Rietveld Results Using pdCIF: *GSAS2CIF*," J. Appl. Cryst. **36**, 1290 (2003).]

- Instrument parameter file editor: GSAS instrument parameter files describe the diffraction instrument and provide a starting point for the refinement. While users at the NCNR receive an accurate file for BT-1, building or finding an appropriate file for many other instruments has been a major trouble spot for many other users. The new editor shows the contents of the file and the options in an easy-to-understand fashion. It can also be used to create new instrument parameter files "from scratch."
- POWPREF warning: The POWPREF program is used in GSAS to map reflections to the powder diffraction data points. It must be rerun when the data range changes or if phases are added. Neophyte (and occasionally experienced) users may run into problems when they fail to run this program. EXPGUI now tracks these types of actions and reminds users to run the POWPREF program before attempting a refinement.
- Other enhancements include: new data and coordinate export abilities, ability to read in multiple datasets in a single step. Also, all reported bugs were fixed.

Data Acquisition and Instrument Control

Nearly every NCNR instrument relies on motors to position neutron optical elements and to orient the sample. The NCNR is in the process of replacing the motor control hardware with a new architecture to improve the serviceability and reliability of these critical systems (Fig. 3). The new architecture employs VME-based computers and motor indexers with an NCNR-designed chassis for multiple motor driver modules. Extensive use is made of commercial, off-the-shelf components through vendor-neutral interfaces. The chassis system features standardized connectors, jumpers and dip-switches to facilitate configuring the motor control system in the field. The complete system is capable of controlling up to 64 encoder-equipped motors using a full spectrum of motion control features. The new system has been deployed on the BT-8 DARTS instrument and on the NG-7 reflectometer.

Another major standardization effort has been the development of a standard control and readout interface for linear and area neutron detectors. This system is a PC-based histogrammer that interfaces with the detectors through either vendor-

supplied electronics or through standard NIM hardware using a high-speed digital I/O bus that is controlled over Ethernet using a simple, NCNR-designed protocol. Over the past year, this system has been successfully used on the NG-1 reflectometer, NG-1 SANS, and the NG-5 Neutron Spin Echo Spectrometer.

Sample Environment Equipment

There have been a number of improvements made to the equipment pool and support infrastructure for sample environments at the NCNR. The 9 Tesla horizontal field superconducting magnet with single crystal windows has been customized for SANS and USANS studies (Fig. 4). A pulse tube refrigerator capable of temperatures in the range of 4 K to 300 K has been integrated into the BT-1 powder diffractometer as a dedicated unit. A new closed-cycle refrigerator was added for general purpose use providing sample temperatures over a wide range: 7 K to 800 K. A new liquid helium cryostat, designed especially for the DCS instrument, was purchased and provides temperatures in the range of 1.5 K to 300 K. New support equipment includes: needle valve heaters for clearing blocked liquid helium cryostats, helium transfer stations at key locations, a new equipment preparation area at the north end of the Guide Hall, and new or updated user manuals for most of the equipment.

BT-7 Double Focusing Triple Axis Spectrometer Development

A new double focusing triple axis spectrometer for BT-7, is at an advanced stage of development, with installation planned for early next year. Highlights from this year's activities include delivery of the monochromator drum shields, completion of the double focused monochromator using Cu(311) and PG(002), installation of the instrument shutter system and incident beam collimation system, completion of the sample goniometer "bucket," and final testing of the air pad floor system. Final design, fabrication and testing are currently underway for the new analyzer system and for the data acquisition and instrument control system.

Photography by Lynn A. Shuman

Fig. 3. Doris Kendig (NCNR) adjusts motor drivers on the new motor control system.

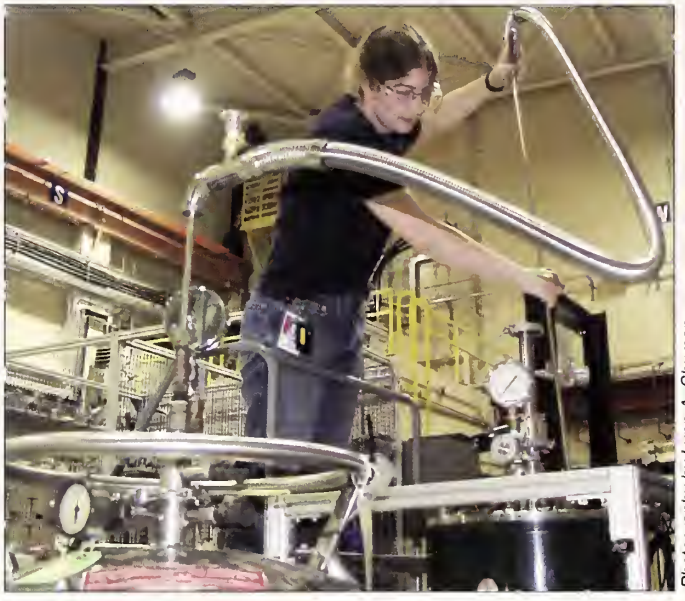

Photography by Lynn A. Shuman

Fig. 4. Rachel Anderman (NCNR) fills the new 9T horizontal field superconducting magnet with helium.

Publications

Abdurashitov, J. N., Gavrin, V. N., Girin, S. V., Gorbachev, V. V., Gurkina, P. P., Ibragimova, T. V., Kalikhov, A. V., Khairnasov, N. G., Knodel, T. V., Mirmov, I. N., Shikhin, A. A., Veretenkin, E. P., Vermul, V. M., Yants, V. E., Zatsepin, G. T., Bowles, T. J., Teasdale, W. A., Nico, J. S., Cleveland, B. T., Elliott, S. R., Wilkerson, J. F., "Solar Neutrino Flux Measurements by the Soviet-American Gallium Experiment (SAGE) for Half the 22-Year Solar Cycle," Jour. Exp. Th. Phys. **95** (2), 181 (2002).

Adams, C. P., Lynn, J. W., Smolyaninova, V. N., Biswas, A., Greene, R. L., Ratcliff, W., Cheong, S.-W., Mukovskii, Y. M., Shulyatev, D. A., "First-Order Nature of the Ferromagnetic Phase Transition in (La-Ca)MnO_3 Near Optimal Doping," Phys. Rev. B, in press.

Agamalian, M., Iolin, E., Kaiser, H., Rehm, C., Werner, S. A., "A New Dynamical Diffraction-Based Technique of Residual Stress Measurements in Thin Films," Appl. Phys. A **74**, S1686 (2002).

Allen, A. J., Berk, N. F., Ilavsky, J., Long, G. G., "Multiple Small-Angle Neutron Scattering Studies of Anisotropic Materials," Appl. Phys. A **74**, S937 (2002).

Allen, J. W., Aronson, M., Boebinger, G. S., Broholm, C., Lance Cooper, S., Crow, J. E., Hammel, P. C., Lander, G., "Future Probes in Materials Science," Physica B **318**, 12 (2002).

Anderson, D. L., Mackey, E. A., "Improvements in Food Analysis by Thermal Capture Prompt Gamma-ray Spectrometry," J. Radioanal. Nucl. Chem., in press.

Angell, C. A., Yue, Y.-Z., Wang, L.-M., Copley, J. R. D., Borick, S., Mossa, S., "Potential Energy, Relaxation, Vibrational Dynamics and the Boson Peak, of Hyperquenched Glasses," J. Phys. Condens. Matter **15**, S1051 (2003).

Annis, B. K., Kim, M.-H., Brown, C., "Comparison of Boson Peaks in Polypropylenes," Macromol. **36** (2), 520 (2003).

Azuah, R. T., Glyde, H. R., Scherm, R., Mulders, N., Fak, B., "Bose-Einstein Condensation in Liquid He-4 in Vycor," J. Low Tem. Phys. **130** (5-6), 557 (2003).

Baklanov, M. R., Kondoh, E., Lin, E. K., Gidley, D. W., Lee, H.-J., Mogilnikov, K. P., Sun, J. N., "Comparative Study of Porous SOG Films with Different Non-Destructive Instrumentation," in *Proceedings of the National Interconnect Technology Conference*, in press.

Bao, W., Trevino, S. F., Lynn, J. W., Pagliuso, P. G., Sarrao, J. L., Thompson, J. D., Fisk, Z., "Effect of Pressure on Magnetic Structure in Heavy Fermion $CeRhIn_5$," Appl. Phys. A **74**, S557 (2002).

Berk, N. F., Majkrzak, C. F., "Wavelet Analysis Neutron Reflectivity," Langmuir, in press.

Bhatia, S., Barker, J., Mourchid, A., "Scattering of Disk-Like Particle Suspensions: Evidence for Repulsive Interactions and Large Length Scale Structure from Static Light Scattering and Ultra-Small-Angle Neutron Scattering," Langmuir **19** (3), 532 (2003).

Biggs, S., Walker, L. M., Kline, S. R., "The Formation of an Irreversibly Adsorbed and Organized Micelle Layer at the Solid-Liquid Interface," Nanoletters **2** (12), 1409 (2002).

Bishop, R. L., Blackman, M. J., "Instrumental Neutron Activation Analysis of Archaeological Ceramics: Scale and Interpretation," Acc. Chem. Res., in press.

Black, T. C., Huffman, P. R., Jacobson, D. L., Snow, W. M., Schoen, K., Arif, M., Kaiser, H., Lamoreaux, S. K., Werner, S. A., "Precision Neutron Interferometric Measurement of the n-d Coherent Neutron Scattering Length and Consequences for Models of Three-Nucleon Forces," Phys. Rev. Lett. **90**, 192502 (2003).

Blackman, M. J., Redford, S., "Northern Syrian Luster and Fruitware: Petrographic and Chemical Implications for Productions and Distribution," Antiquity, in press.

Blasie, J. K., Kneller, L. R., Majkrzak, C. F., "Neutron Interferometry of Vectorially-Oriented Single Monolayers of Membrane Proteins and Their Artificial Synthetic Maquettes," Abstr. Pap. Am. Chem. Soc. **224**, 123 (2002).

Böni, P., Clementyev, E., Stadler, C. H., Roessli, B., Shirane, G., Werner, S. A., "Fincher-Burke Excitations in Single-Q Chromium," Appl. Phys. A **74**, S716 (2002).

Bordallo, H. N., Chapon, L. C., Cook., J. C., Copley, J. R. D., Goremychkin, E., Kern, S., Lee, S.–H., Yildirim, T., Manson, J. L., "Spin Excitations in 3D Molecular Magnets Probed by Neutron Scattering," Appl. Phys. A **74**, S634 (2002).

Borgoul-Maciejczyk, P., Ondov, J. M., "Heterogenous Nature of Metallic Components in Baltimore Particulate Matter," Environ. Sci. Technol., in press.

Borodin, O., Douglas, R., Smith, G. D., Trouw, F., Petrucci, S., "MD Simulations and Experimental Study of Structure, Dynamics, and Thermodynamics of Poly(ethylene oxide) and Its Oligomers," J. Phys. Chem. B **107**, 6813 (2003).

Bossev, D. P., Ferdinand, S., Paulaitis, M. E., "Effect of Pressure on Microstructure in Water-in-Oil and Oil–in-Water Microemulsions for $C_{12}E_5$ n-Octane/D_20 Mixtures," Langmuir, in press.

Boukari, H., Allen, A. J., Long, G. G., Ilavsky, J., Wallace, J. S., Berndt, C. C., Herman, H., "Small-Angle Neutron Scattering Study of the Role of Feedstock, Particle Size on the Microstructural Behavior of Plasma-Sprayed Yttria-Stabilized Zirconia Deposits," J. Mater. Res. **18** (3), 624 (2003).

Broholm, C., Aeppli, G., "Dynamic Correlations in Quantum Magnets," to appear in Strong Interactions in Low Dimensions, edited by D. Baeriswyl. and L. Degiorgi, (Kluwer), in press.

Brown, C. M., Manson, J. L., "Solid State Ligand Dynamics in Interpreting Mn[N(CN)2]2(pyrazine): A Neutron Spectroscopy Study," J. Amer. Chem. Soc. **124** (42), 12600 (2002).

Caffrey, P. F., Ondov, J. M., "Dry Deposition of Elemental Aerosol Constituents to Lake Michigan Surface Waters, by Size and by Source," Environ. Sci. Technol., in press.

Caffrey, P. F., Ondov, J. M., "Dry Removal of Elemental Aerosol Particulate Constituents in Near Shore Gradient of Southern Lake Michigan," Environ. Sci. Tech., in press.

Campbell, B. J., Sinha, S. K., Osborn, R., Rosenkranz, S., Vasiliu-Doloc, L., Mitchell, J. F., Islam, Z., Seeck, O. H., Lynn, J. W., "Polaronic Orbital Polarization in a Layered Colossal Magnetoresistive Manganite," Phys. Rev. B **67**, R020409 (2003).

Cappelletti, R. L., "MSEL, FY2002 Programs and Accomplishments," NIST IR, 6908 (2002).

Cappelletti, R. L., "NCNR 2002 NIST Center for Neutron Research Accomplishments and Opportunities," NIST SP 993 (2002).

Cava, R. J., DiSalvo, F. J., Brus, L. E., Dunbar, K. R., Gorman, C. B., Maile, S. M., Interrante, L. V., Musfeldt, J. L., Navrotsky, A., Nuzzo, R. G., Pickett, W. E., Wilkinson, A. P., Ahn, C., Allen, J. W., Burns, P. C., Ceder, G., Chidsey, C. E. D., Clegg, W., Coronado, E., Dai, H., Deem, M. W., Dunn, B. S., Galli, G., Jacobson, A. J., Kanatzidis, M., Lin, W., Manthiram, A., Mrksich, M., Norris, D. J., Nozik, A. J., Peng, X., Rawn, C., Rolison, D., Singh, D. J., Toby, B. H., Tolbert, S., Wiesner, U. B., Woodward, P. M., Yang, P., "Future Directions in Solid State Chemistry: Report of the NSF-Sponsored Workshop," Progr. Solid State Chem. **30**, 1 (2002).

Chakoumakos, B. C., Rawn, C. J., Rondinone, A. J., Marshall, S. L., Stern, L. A., Circone, S., Kirby, S. H., Jones, C. Y., Toby, B. H., Ishii, Y., "The Use of Rigid Body Constraints in Rietveld Refinements of Neutron Diffraction Data of Clathrate Hydrates," in *Proceeding of the 4th International Conference on Gas Hydrates*, (Yokohama, Japan, 2002), in press.

Chakoumakos, B. C., Rawn, C. J., Rondinone, A. J., Stern, L. A., Circone, S., Kirby, S. H., Ishii, Y., Jones, C. Y., Toby, B. H., "Temperature Dependence of Polyhedral Cage Volumes in Clathrate Hydrates" Can. J. Phys. **81** (1-2), 183 (2003).

Chen, S.-H., Chen, W.-R., Mallamace, F., "The Glass-to-Glass Transition and Its End Point in a Copolymer Micellar System," Science, **300,** 619 (2003).

Chen, S.-H., Mallamace, F., Faraone, A., Gambadauro, P., Lombardo, D., Chen, W. R., "Observation of a Re-Entrant Kinetic Glass Transition in a Micellar System with Temperature-Dependent Attractive Interaction," Eur. Phys. J. E **9**, 283 (2002).

Chen, W. C., Bailey, C., Borchers, J. A., Farrow, R. F. C., Gentile, T. R., Hussey, D. H., Majkrzak, C. F., O'Donovan, K. V., Remmes, N., Snow, W. M., Thompson, A. K., "Polarized ^{3}He Analyzers for Neutron Reflectometry," Physica B **335**, 196 (2003).

Cheng, X., Fisher, J. W., Yen, B. T., Roy, S., Prask, H. J., Gnäupel-Herold, T., "Residual Stress Modification by Post-Weld Treatment and Its Beneficial Effect on Fatigue Strength of Welded Structures," ASM Matls. Solutions Conf. & Show, (Columbus, OH, 2002), in press.

Chen-Mayer, H. H., Lamaze, G. P., Coakley, K. J., Satija, S. K., "Two Aspects of Thin Film Analysis: Boron Profile and Scattering Length Density Profile," Nucl. Inst. Meth. A **505**, 531 (2003).

Choi, E. J., Foster, M. D., Daly, S., Tilton, R., Przbycien, T., Majkrzak, C. F., Witte, P., Menzel, H., "Effect of Flow on Human Serum Alumin Adsorption to Self-Assembled Monolayers of Varying Packing Density," J. Colloid Interf. Sci., in press.

Choi, H. D., Firestone, R. B., Lindstrom, R. M., Molnar, G. L., Reddy, A. V. R., Tan, V. H., Zhou, C. M., Paviottia-Corcuera, R. A., Trkov, A., "Development of a Database for Prompt Gamma-Ray Neutron Activation Analysis," J. Nucl. Sci. Tech., in press.

Choi, E. J., Foster, M. D., Daly, S., Tilton, R., Przbycien, T., Majkrzak, C. F., Witte, P., Menzel, H., "Effect of Flow on Human Serum Alumin Adsorption to Self-Assembled Monolayers of Varying Packing Density," Langmuir **19** (13), 5464 (2003).

Chong, K. P., Sung, L., VanLandingham, M. R., "Solid Micromechanics: Research and Challenges," in *Proceedings of the 13th Micromechanics Europe (MME 2002) Workshop*, (Sinaia, Romania, Oct. 6-8, 2002), in press.

Chowdhuri, Z., Hansen, G., Snow, W. M., Keith, C. D., Thompson, A. K., Dewey, M. S., Gilliam, D. M., Nico, J. S., Wietfeldt, F. E., Lozowski, W. M., Jane, V., Greene, G. L., "A Cryogenic Radiometer for Absolute Neutron Rate Measurement," Rev. Sci. Instrum., in press.

Clarke, W. B., Guscott, R., Lindstrom, R. M., "Binding of Lithium and Boron to Human Plasma Proteins II: Results for a Bipolar Not on Lithium Therapy," Biol. Trace Element Res., in press.

Coakley, K. J., Chowdhuri, Z., Snow, W. M., Richardson, J. M., Dewey, M. S., "Estimation of Neutron Mean Wavelength From Rocking Curve Data," Meas. Sci. Technol. **14** (1), 131 (2003).

Copley, J. R. D., "An Acceptance Diagram Analysis of the Contaminant Pulse Removal Problem with Direct Geometry Neutron Chopper Spetrometers," Nucl. Inst. Meth. A, in press.

Copley, J. R. D., Cook, J. C., "The Disk Chopper Spectrometer at NIST: A New Instrument for Quasielastic Neutron Scattering Studies," Chem. Phys. **292**, 477 (2003).

Cranswick, L. M. D., Mumme, W. G., Grey, I. E., Roth, R. S., Bordet, P., "A New Octahedral Tilt System in the Perovskite Phase $Ca_3Nb_2O_8$," J. Solid State Chem. **172**, 178 (2003).

Dag, S., Gulseren, O., Ciraci, S., Yildirim, T., "Electronics Structure of the Contact Between Carbon Nanotube and Metal Electrodes," Appl. Phys. Lett., in press.

Dag, S., Gulseren, O., Yildirim, T., Ciraci, S., "Oxidation of Carbon Nanotubes: Structure and Energetics," Phys. Rev. B **67**, 165424 (2003).

Dattelbaum, A., He, L., Tsui, F., Martin, J. D., "Synthesis and Characterization of Cu_2ZrCl_6: A Thermochromic, Van Vleck Paramagnet," J. Alloys and Comp. **338,** 173 (2002).

DeBruyn, H., Gilbert, R. G., White, J. W., Schulz, J. C., "Characterization of Electrosterically Stabilized Polystyrene Latex; Implications for Radical Entry Kinetics," Polymer **44** (16), 4411 (2003).

DeBruyn, H., Gilbert, R. G., White, J. W., Schulz, J. C., "SANS Study of Electrosterically Stabilized Polystyrene Latex," Langmuir, in press.

DeSanto, P., Buttrey, J., Grasselli, R. K., Lugmair, C. G., Volpe, A. F., Toby, B. H., Vogt, T., "Structural Characterization of the Orthorhombic Phase M2 in MoVNbTeO Propane Ammoxidation Catalyst," Topics in Catalysis, in press.

DeWall, J., Dimeo, R. M., Sokol, P. E., "Slow Diffusion of Molecular Hydrogen in Zeolite 13X," J. Low Temp. Phys. **129** (3-4), 171 (2002).

Dimeo, R. M., "Visualization and Measurement of Quantum Rotational Dynamics," Am. J. Phys., **71** (9), 885 (2003).

Dimeo, R. M., Chowdhuri, Z., Meyer, A., Gehring, P. M., Neumann, D. A., "The NIST High-Flux Backscattering Spectrometer," Appl. Phys. A **74**, S311 (2002).

Dimeo, R. M., Neumann, D. A., "The Effects of Confinement on Rotational Tunneling," Appl. Phys. A **74**, S1382 (2002).

DiNoia, T. P., Van Zanten, J. H., Fetters, L. J., Wright, P. J., Kline, S. R., Garach-Domech, A., McHugh, M. A., "Impact of Supercritical Fluid Solvent Quality on Polymer Conformation in Semidilute Solutions: SANS Data for Poly(ethylene-co-1-butene) in Dimethyl Ether to Kilobar Pressures," Macromol., in press.

Divita, F., Terry, J., Kidwell, C. A., Ondov, J. M., Pandis, S., "Characterization of Primary Aerosol Emissions from a Municipal Incinerator Via Ground-Level Sampling with a Micro-Orifice Impactor." Atmos. Environ., in press.

Downing, R. G., Iyengar, G. V., "Methodological Issues in the Analytical Determination of Boron," Environ. Health Perspect., in press.

Dubsky, J., Prask, H. J., Matejicek, J., Gnäupel-Herold, T., "Stresses in Plasma Sprayed Cr_2O_3 Coatings Measured by Neutron Diffraction," Appl. Phys. A **74**, S1115 (2002).

Duckham, A., Zhang, D. Z., Liang, D., Luzin, V., Cammarata, R. C., Leheny, R. L., Chien, C. L., Weihs, T. P., "Temperature Dependent Mechanical Properties of Ultra-Fine Grained FeCo-2V," Acta Mater. **51** (14), 4083 (2003).

Dullo, A. R., Ruddy, F. H., Seidel, J. G., Adams, J. M., Nico, J. S., Gilliam, D. M., "The Neutron Response of Miniature Silicon Carbide Semiconductor Detectors," Nucl. Instrum. Meth. A. **498** (1-3), 415 (2003).

Durgun, E., Dag, S., Bagci, V. M. K., Gulseren, O., Yildirim, T., Ciraci, S., "Systematic Study of Adsorption of Single Atoms on a Carbon Nanotube," Phys. Rev. B **67**, 201401 (2003).

Eitouni, H. B., Hahn, H., Balsara, N. P., Pople, J. A., Hempenius, M. A., "Thermodynamic Interactions in Organometallic Block Copolymers: Poly(styrene-*block*-ferrocenyldimethylsilane)," Macromol. **35**, 7765 (2002).

Elliot, J., Meuse, V., Silin, V., Krueger, S., Woodward, J. T., Petralli-Mallow, T. P., Plant, A. L., "Biomedical Membranes on Metal Supports: Opportunites and Challenges," in *Proceedings of the Biomolecular Films: Design, Function, and Application*, edited by J. Rusling (New York, Marcel Dekker, Inc., 2003), p. 99.

Faraone, A., Liu, L., Mou, C.-Y., Shih, P.-C., Brown, C. M., Copley, J. R. D., Dimeo, R. M., Chen, S.-H., "Dynamics of Supercooled Water in Mesoporous Silica Matrix MCM-48-S," Eur. Phys. J. E, in press.

Faraone, A., Liu, L., Chen, S.-H., Mou, C.-Y., Shih, P.-C., Copley, J. R. D., "Translational and Rotational Dynamics of Water in Mesoporous Silica Materials: MCM-41-S and MCM-48-S," J. Chem. Phys. **119,** 3963 (2003).

Garvey, C. J., Parker, I. H., Simon, G. P., Whittaker, A. K., Knott, R. B., "An Experimental Study by NMR and SANS of the Ambient Hydration of Paper," in *Proceedings of the 12th Fundamental Research Symposium*, (Pulp and Paper Fundamental Research Society, Oxford), in press.

Gaulin, B. D., Mao, M., Wiebe, C. R., Qiu, Y., Shapiro, S. M., Broholm, C., Lee, S.-H., Garrett, J. D., "Spin and Lattice Excitations in the Heavy Fermion Superconductor UNi_2Al_3," Phys. Rev. B **66** (17), 174520 (2002).

Gawrys, K. L., Spiecker, P. M., Kilpatrick, P. K., "The Role of Asphaltene Solubility and Chemistry on Asphaltene Aggregation," Petroleum Science and Technology **21**, 461 (2003).

Gehring, P. M., "Summer School on Methods and Applications of Neutron Spectroscopy Held at NIST," Neutron News, in press.

Geissler, E., Hecht, A. M., Rochas, C., Horkay, F., Bley, F., Livet, F., "Structure and Dynamics of Silica-Filled Polymers by SANS and Coherent SAXS," Macromol. Symp. **190,** 23 (2002).

Gentile, T. R., Hayden, M. E., Barlow, M. J., "Comparison of Metastability Optical Pumping Sources," J. Opt. Am. B. in press.

Gibson, W. M., Schultz, A. J., Chen-Mayer, H. H., Mildner, D. F. R., Gnäupel-Herold, T., Miller, M. E., Prask, H. J., Vitt, R., Youngman, R., Carpenter, J. M., "Polycapillary Focusing Optic for Small Sample Neutron Crystallography," J. Appl. Cryst **35** 677 (2002).

Gilliam, D. M., Thompson, A. K., Nico, J. S., "A Neutron Sensor For Detection of Nuclear Materials In Transport," *AIP Conference Proceedings*, (Unattended Radiation Sensor Systems for Remote Applications), edited by J. I. Trombka, D. P. Spears, and P. H. Solomon, **632,** 0-7354-0087 (American Institute of Physics), p. 291.

Glagolenko, I. Y., Carney, K. P., Kern, S., Goremychkin, E. A., Udovic, T. J., Copley, J. R. D., Cook, J. C., "Quantitative Analysis of UH_3 in U Metal and UO_2 Matrices by Neutron Vibrational Spectroscopy," Appl. Phys. A **74**, S1397 (2002).

Glinka, C. J., "Summer School on SANS and Reflectometry Held at NIST," Neutron News **13** (4), 6 (2002).

Gnäupel-Herold, T., "Single Crystal Elastic Constants From Powder Measurements," in *Proceedings of Accuracy in Powder Diffraction. III* (NIST Special Publication), in press.

Gnäupel-Herold, T., Prask, H. J., Biancaniello, F. S., "Residual Stresses and Elastic Constants in Thermal Deposits", in Recent Advances in Experimental Mechanics – In Honor of Isaac M. Daniel, edited by E.E. Gdoutos, (Kluwer Academic Publishers, Dordrecht 2002), in press.

Goodrich, R. G., Young, D. P., Hall, D., Fisk, Z., Harrison, N., Betts, J., Migliori, A., Woodward, F. M., Lynn, J. W., "New Aspects of the Temperature - Magnetic Field Phase Diagram of CeB_6," Phys. Rev. B, in press.

Granado, E., Huang, Q., Lynn, J. W., Gopalakrishnan, J., Greene, R. L., Ramesha, K., "Spin-Orbital Ordering and Mesoscopic Phase Separation in the Double Perovskite Ca_2FeReO_6," Phys. Rev. B **66** (6), 064409 (2002).

Granado, E., Ling, C. D., Neumeier, J. J., Lynn, J. W., Argyriou, D. N., "Inhomogeneous Magnetism in La-doped $CaMnO_3$: (I) Nanometric-Scale Spin Clusters and Long-Range Spin Canting," Phys. Rev. B, in press.

Granado, E., Martinho, H., Sercheli, M. S., Pagliuso, P. G., Jackson, D., Torelli, M., Lynn, J. W., Rettori, C., Fisk, Z., Oseroff, S. B., "Unconventional Metallic Magnetism in $LaCrSb_3$," Phys. Rev. Lett. **89** (10), 107204 (2002).

Grohol, D., Huang, Q., Toby, B., Lynn, J. W., Lee, Y. S., Nocera, D. G., "Powder Neutron Diffraction Analysis and Magnetic Structure of Kagomé type Vanadium Jarosite $NaV_3(OD)_6(SO_4)_2$," Phys. Rev. B **68**, 094404 (2003).

Gruell, H., Sung, L., Karim, A., Douglas, J. F., Satija, S. K., Han, C. C., "Surface Segregation of a Symmetrical Segregating Polymer Blend Film Above and Below the Critical Point of Phase Separation," Europhys. Lett., in press.

Gu, X., Raghavan, D., Ho, D. L., Sung, M. R., VanLandingham, M. R., Nguyen, T., "Nanocharacterization of Surface and Interface of Different Epoxy Network," in *Proceedings of the MRS Fall 2001 Meeting*, edited by Frank, C. W., in press.

Gu, X., Sung, L., Ho, D. L., Michaels, C. A., Nguyen, D., Jean, Y. C. Nguyen, T., "Surface and Interface Properties of PVDF/ Acrylic Copolymer Blends Before and After UV Exposure," in *Proceedings of the 80th Annual Meeting Technical Program* (Oct. 30-Nov.1, New Orleans, LA, 2002), in press.

Guàrdia, E., Martí, J., Padró, J. A., Saiz, L., Komolkin, A. V., "Dynamics in Hydrogen Bonded Liquids: Water and Alcohols," J. Molec. Liq. **96-97**, 3 (2002).

Gulseren, O., Yildirim, T., Ciraci, S., "Effects of Hydrogen Adsorption on Single Wall Carbon Nanotubes: Metallic Hydrogen Decoration,: Phys. Rev. B **66**, 121401 (2002).

Gulseren, O., Yildirim, T., Ciraci, S., "Formation of Quantum Structures on a Single Nanotube by Modulation Hydrogen Adsorption," Phys. Rev. B, in press.

Gulseren, O., Yildirim, T., Ciraci, S., Kilic, C., "Reversible Band-Gap Engineering in Carbon Nanotubes by Radical Deformation," Phys. Rev. B **65**, 155410 (2002).

Guo, H. K., Tao, R. B., Lin, M. Y., "Quantitative Analysis of Rod Like Micelle Solutions Viscosity Using Microscopic Parameters," Int. J. Mod. Phys. B **17** (1-2), 119 (2003).

Hammouda, B., Ho, D., Kline, S., "SANS from Poly(ethylene oxide) Water Systems," Macromol. **35**, 8578 (2002).

Hanley, H. J. M., Muzny, C. D., Ho, D. L., Glinka, C. J., "A Small-Angle Neutron Scattering Study of a Commercial Organoclay Dispersion," Langmuir **19**, 5575 (2003).

Harris, A. B., Aharony, A., Entin-Wholman, O., Korenblit, I. Ya., Yildirim, T., "Landau Expansion for the Kugel-Khomskii t_{2g} Hamiltonian," Phys. Rev. B, in press.

Harris, A. B., Yildirim, T., Aharony, A., Entin-Wohlman, O., Korenblit, I. Ya., "Hidden Symmetries and Their Consequences in t_{2g} Cubic Perovskites," Phys. Rev. B, in press.

Harris, A. B., Yildirim, T., Aharony, A., Entin-Wohlman, O., Korenblit, I. Ya., "Unusual Symmetries in the Kugel-Khomskii-Hamiltonian," Phys. Rev. Lett., in press.

Harris, S. P., Heller, W. T., Greaser, M. L., Moss, R. L., Trewhella, J., "Solutions Structure of Heavy Meromyosin by Small Angle Scattering," J. Bio. Chem. **278**, 6034 (2003).

Hase I., Ikeda S. I., Shirakawa N., Stalick J. K., "Electronic Structure of Sr_2MoO_4," J. Low. Temp. Phys. **131** (3-4), 269 (2003).

Hassan, P. A., Fritz, G., Kaler, E. W., "Small Angle Neutron Scattering Study of Sodium Dodecyl Sulfate Micellar Growth Driven by Addition of a Hydrotropic Salt," J. Coll. Interface Sci. **257** (1), 154 (2003).

Hayashi, M., Hashimoto, T., Weber, M., Gruell, H., Esker, A., Han, C. C., Satija, S. K., "Transient Interface Instability in Bilayer Polymer Films as Observed by Neutron Reflectivity Studies," Macromol., in press.

Heath, C. H., Streletzky, K., Wyslouzil, B. E., Wolk, J., Strey, R., "H_2O-D_2O Condensation in a Supersonic Nozzle," J Chem. Phys. **117** (13), 6176 (2002).

Heath, C. H., Streletzky, K. A., Wyslouzil, B. E., Wolk, J., Strey, R., "Small Angle Neutron Scattering From D_2O-H_2O Nanodroplets and Binary Nucleation Rates in a Supersonic Nozzle," J. Chem Phys. **118** (12), 5465 (2003).

Hecht, A. M., Horkay, F., Geissler, E., "Thermal Fluctuations in Polymer Gels Investigated by Neutron Spin Echo and Dynamic Light Scattering," Macromol. **35**, 8552 (2002).

Hedden, R. C., Bauer, B. J., "Structure and Dimensions of PAMAM/PEG Dendrimer-Star Polymers," Macromol. **36** (6), 1829 (2003).

Hedden, R. C., Lee, H. J., Bauer, B. J., Soles, C. L., Wu, W. L., Lin, E. K., "Measurement of Pore Size and Matrix Characteristics in Low-k Dielectrics by Neutron Contrast Variation," in *Proceedings of the International Conference on Characterization and Metrology for ULSI Technology,* (March, 2003, Austin TX), in press.

Heller, W. T., Anusamhadneh, E., Finley, N., Rosevear, P. R., Trewhella, J., "The Solution Structure of a Cardiac Troponin C- Troponin I- Troponin T Complex Shows a Somewhat Compact Troponin C Interacting with an Extended Troponin I- Troponin T Component," Biochem. **41**, 15654 (2002).

Henrickson, R. C., Vandiver, P. B., Blackman, M. J., "Lustrous Black Fine Ware at Gordion, Turkey: A Distinctive Sintered Slip Technology," in *Materials Research Society Symposium Proceedings,* Materials Issues in Art and Archaeology VI, edited by P. B. Vandiver, M. Goodway, and J. L. Mass. **712** (2002), p. 391.

Hentze, H. P., Raghavan, S. R., McKelvey, C. A., Kaler, E. W., "Silica Hollow Spheres by Templating of Catanionic Vesicles," Langmuir **19** (4), 1069 (2003).

Ho, D. L., Glinka, C. J., "Effects of Solvent Solubility Parameters on Organclay Dispersions," Chem. Mater. **15** (6), 1309 (2003).

Ho, D. L., Hammouda, B., Kline, S. R., "Clustering of Poly(ethylene oxide) in Water Revisited," J. Poly. Sci.: Part B: Poly. Phys. **41**, 135 (2003).

Hoffman, A., Seo, J. W., Fitzsimmons, M. R., Siegwart, H., Fompeyrine, J., Locquet, J.-P., Dura, J. A., Majkrzak, C. F., "Induced Magnetic Moments at a Ferromagnet-Antiferromagnet Interface," Phys. Rev. B **66** (22), 220406 (2002).

Horkay, F., Hecht, A. M., Grillo, I., Basser, P. J., Geissler, E., "Experimental Evidence for Two Thermodynamic Length Scales in Neutralized Polyacrylate Gels." J. Chem. Phys. **117** (20), 9103 (2002).

Huang, Q. Z., Karen, V. L., Santoro, A., Kjekshus, A., Linden, J., Pietari, T., Karen, P., "Substitution of Co^{3+} in $YBa_2Fe_3O_8$," J. Solid State Chem. **172** (1), 73 (2003).

Huffman, P. R., "An Experiment to Search for Parity-Conserving Time Reversal Invariance Using Epithermal Neutrons From the Spallation Neutron Source," in *Astrophysics, Symmetries, and Applied Physics at Spallation Neutron Sources,* (World Scientific Publishing Co. Pte. Ltd.) **156** (2002).

Huffman, P. R., Arif, M., Dewey, M. S., Gentile, T. R., Gilliam, D. M., Jacobson, D. L., Nico, J. S., Thompson, A. K., "The Fundamental Neutron Physics Facilities at NIST," *AIP Conference Proceedings,* Application of Accelerators in Research and Industry: Seventeenth International Conference on the Application of Accelerators in Research and Industry, edited by J. L. Duggan, (Denton, Texas, 12-16 November 2002), **680** (2003).

Huffman, P. R., Coakley, K. J., Dzhosyuk, S. N., Golub, R., Korobkina, E., Lamoreaux, S. K., Mattoni, C. E. H., McKinsey, D. N., Thompson, A. K., Yang, G. L., Yang, L., Doyle, J. M., "Progress Towards Measurement of the Neutron Lifetime Using Magnetically Trapped Ultracold Neutrons," in *Proceedings for the "Quark-mixing, CKM Unitarity,"* (Heidelberg, 19-20 September 2002), in press.

Hussey, D., Fan, S., Neff, B., Bailey, C., Snow, W. M., Rich, D., Thompson, A. K., Gentile, T. R., Te Velthuis, S. G. E., Felcher, G. P., "Simultaneous Polarization Analysis of Zeeman Splitting in Polarized Neutron Reflectometry Using a Polarized ^{3}He Neutron-Spin Filter," Appl. Phys. A **74**, S234 (2002).

Ishii, Y., Jones, C. Y., Marshall, S. L., Rawn, C. J., Chakomakos, B. C., "Structure Study of Tetrahydrofuran Deuterate by Neutron Powder Diffraction," JAERI Review, Progress Report on Neutron Scattering Research (April 1, 2001 – March 31, 2002), edited by S. Katano, S. Koizumi, M. Matsuda (2002), in press.

Jeng, U.-S., Lin, T.-L., Wang, L. Y., Chiang, L. Y., Ho, D. L., Han, C. C., "SANS Structural Characterization of Fullerenol-Derived Star Polymers In Solutions," Appl. Phys. A **74**, S487 (2002).

Jeon, H. S., Dixit, P. S., Yim, H., Kent, M. S., Shin, S., Satija, S. "Interfacial Structure and Properties in Polystyrene/Epoxy Bilayer Films," J. Polym. Sci. Pol. Phys. **40** (23), 2653 (2002).

Jones, C. Y., Marshall, S. L., Chakoumakos, B. C., Rawn, C. J., Ishii, Y., "Structure and Thermal Expansivity of Tetrahydrofuran Deuterate Determined by Neutron Powder Diffraction." J. Phys. Chem. B **107** (25), 6026 (2003).

Jones, R. L., Hu, T. J., Prabhu, V. M., Soles, C. L., Lin, E. K., Wu, W. L., Goldfarb, D. L., Angelopoulos, M., "Form of Deprotection in Chemically Amplified Resists," in *Proceedings of the International Conference on Characterization and Metrology for ULSI Technology,* (March, 2003, Austin, TX), in press.

Jones, R. L., Hu, T. J., Prabhu, V. M., Soles, C. L., Lin, E. K., Wu, W. L., Goldfarb, D. L., Trinque, B. C., Willson, C. G., "Deprotection Volume Characteristics and Line Edge Morphology in Chemically Amplified Resists," in *Proceedings of the SPIE: Advances in Resist Technology and Processing XX,* (March, 2003, Austin, TX), **5039** (2003), p. 1031.

Jones, R. L., Hu, T., Lin, E. K., Wu, W. L., Casa, D. M., Orji, N. G., Vorburger, T. V., Bolton, P. J., Barclay, G. G., "Sub-Nanometer Wavelength Metrology of Lithographically Prepared Structures: A Comparison of Neutron and X-ray Scattering," in *Proceedings of the SPIE: Metrology, Inspection, and Process Control for Microlithography XVII,* (February, 2003, Santa Clara, CA), in press.

Jones, R. L., Kumar, S. K., Grull, H., Han, C. C., Briber, R. M., Russell, T. P., "Experimental Phase Behavior of Ultrathin Film Polymer Mixtures," in press.

Jones, R. L., Prabhu, V. M., Goldfarb, D. L., Lin, E. K., Soles, C. L., Lenhart, J. L., Wu, W. L., Angelopoulos, M., "Correlation of the Reaction Front with Roughness in Chemically Amplified Photoresists," in *Symposia of the American Chemical Society,* (American Chemical Society, Washington, DC), in press.

Jones, R. L., Soles, C. L., Starr, F. W., Lin, E. K., Lenhart, J. L., Wu, W. L., Goldfarb, D. L., Angelopolous, M., "Chain Conformation in Ultrathin Polymer Films," in *Proceedings of the SPIE: Advances in Resist Technology and Processing XIX,* (March, 2002, Santa Clara, CA) **4690** (2003), p. 342.

Jones, R. L., Starr, F. W., Soles, C. L., Lin, E. K., Lenhart, J. L., Wu, W. L., Goldfarb, D., Angelopoulos, M., "Chain Conformation in Ultrathin Polymer Resists," in *Proceedings of the SPIE Conference*, **4689** (2002).

Jones, T. D., Chappin, K. A., Bates, F. S., Annis, B. K., Hagaman, E. W., Kim, M.-H., Wignall, G. D., Fan, W., Waymouth, R., "Effect of Tecticity on Coil Dimensions and Thermodynamics Properties of Polypropylene," Macromol. **35**, 5061 (2002).

Kang, H. J., Dai, P., Lynn, J. W., Matsuura, M., Thompson, J. R., Zhang, S.-C., Argyriou, D. N., Onose, Y., Tokura, Y., "Antiferromagnetic Order as the Competing Ground State in Electron Doped $Nd_{1.85}Ce_{0.15}CuO_4$," Nature **423**, 522 (2003).

Karen, P., Kjekshus, A., Huang, Q., Karen, V. L., Lynn, J. W., Rosov, N., Natali-Sora, I., Santoro, A., "Neutron Powder Diffraction Study of Nuclear and Magnetic Structures of $Yba_2Fe_3O_{8+\omega}$ ($-0.24 < \omega < 0.11$)," J. Solid State Chem., in press.

Karim, A., Yurekli, K., Meredith, C., Amis, E., Krishnamoorti, R., "Combinational Methods for Polymer Materials Science: Phase Behavior of Nanocomposite Blend Films," Polym. Eng. Sci. **42** (9), 1836 (2002).

Karlsson, E. B., Abdul-Redah, T., Udovic, T. J., Hjörvarsson, B., Chatzidimitriou-Dreismann, C. A., "Short-lived Proton Entanglement in Yttrium Hydrides," Appl. Phys. A **74**, S1203 (2002).

Karunadasa, H., Huang, Q., Ueland, B. G., Schiffer, P., Cava R. J., "Ba_2LnSbO_6 and Sr_2LnSbO_6 (Ln = Dy, Ho, Gd) Double Perovskites: Lanthanides in the Geometrically Frustrating fcc Lattice," in *Proceedings of the National Academy of Sciences of the United States* **100** (14), 8097 (2003).

Keller, T., Wagner, W., Allen, A., "Characterisation of Thermally Sprayed Metallic NiCrAlY Deposits by Multiple Small-Angle Scattering," Appl. Phys. A **74**, S975 (2002).

Kelly, R. W., Murphy, K. E., Becker, D. A., Mann, J. L., "Determination of Cr in Certified Reference Material HISS-1, Marine Sediment, by Cold Plasma Isotope Dilution ICP-MS and INAA: Comparison of Microwave Versus Closed (Carius) Tube Digestion," J. Anal. At. Spectrom. **18**, 166 (2003).

Kent, M., "A Quantitative Study of Tethered Chains in Various Solution Conditions Using Langmuir Diblock Copolymer Monolayers," Macromol., in press.

Kenzelmann, M., Chien, Y., Broholm, C., Reich, D. H., Qiu, Y., "Field Dependence of Solitons and Breathers in an Antiferromagnetic S=1/2 Chain," Phys. Rev. Lett., in press.

Kenzelmann, M., Xu, G., Zaliznyak, I. A., Broholm, C., DiTusa, J. F., Aeppli, G., Ito, T., Oka, K., Takagi, H., "Structure of End States for a Haldane Spin Chain," Phys. Rev. Lett. **90** (8), 087202 (2003).

Kepa, H., Kutner-Pielaszek, J., Twardowski, A., Majkrzak, C. F., Story, T., Sadowski, J., Giebultowicz, T. M., "Polarized Neutron Reflectometry Studies of GaMnAs/GaAs Superlattices," Appl. Phys. A **74**, S1526 (2002).

Kepa, H., Majkrzak, C. F., Sipatov, A. Y., Giebultowicz, T. M., "Polarized Neutron Reflectometry Studies of Magnetic Semiconductor Superlattices," Physica B, in press.

Kepa, H., Springholz, G., Giebultowicz, T. M., Goldman, K. I., Majkrzak, C. F., Kacman, P., Blinowski, J., Holl, S., Krenn, H., Bauer, G., "Magnetic Interactions in EuTe Epitaxial Layers and EuTe/PbTe Superlattices," Phys. Rev. B, in press.

Kepa, H., Van Khoi, L., Brown, C. M., Sawicki, M., Furdyna, J. K., Giebultowicz, T. M., "Probing Hole-Induced Ferromagnetic Exchange in Magnetic Semiconductors by Inelastic Neutron Spectroscopy," Phys. Rev. Lett., in press.

Khalifah, P., Osborn, R., Huang, Q., Zandergen, H. W., Jin, R., Liu, Y., Mandrus, D., Cava, R. J., "Orbital Ordering Transition in $La_4Ru_2O_{10}$," Science **297** (5590), 2237 (2002).

Khaykovich, B., Birgeneau, R. J., Chou, F. C., Erwin, R. W., Kastner, M. A., Lee, S.-H., Lee, Y. S., Smeibidl, P., Vorderwisch, P., Wakimoto, S., "Effect of a Magnetic Field on Long-Range Magnetic Order in Stage-4 and Stage-6 Superconducting La_2CuO_{4+y}," Phys. Rev. B **67** (5), 054501 (2003).

Kidwell, C. B., Ondov, J. M. "Elemental Analysis of Sub-Hourly Ambient Aerosol Collections," Aersol. Sci. Technol., in press.

Kim, H., Huang, Q. Z., Lynn, J. W., Kauzlarich, S. M., "Neutron Diffraction Study of the Ternary Metal Zintl Compound $Ca_{14}MnSb_{11}$," J. Solid. State. Chem. **168** (1), 162 (2002).

Kim, H.-C., Volksen, W., Miller, R. D., Huang, E., Yang, G., Briber, R. M., Shin, K., Satija, S., "Neutron Reflectivity on Nanoporous Poly(Methysilsesquioxane) Thin Films," Chem. Mater. **15** (3), 609 (2003).

Kline, S. R., Hammouda, B., "Corrective Refractive Optics Sharpens Focus of SANS Instruments," J. Res. Natl. Inst. Stand. Technol., in press.

Kodibagkar, V. D., Browning, C. D., Udovic, T. J., Conradi, M. S., "Deuterium NMR Study of Structure and Motion in LuD_3," Phys. Rev. B **67**, 174115 (2003).

Koga, T., Seo, Y. S., Zhang, Y., Shin, K., Kusano, K., Nishikawa, K., Rafailovich, M. H., Sokolov, J. C., Chu, B., Peiffer, D., Occiogrosso, R., Satija, S. K., "Density-Fluctuation-Induced Swelling of Polymer Thin Films in Carbon Dioxide," Phys. Rev. Lett. **89** (12), 125506 (2002).

Koga, T., Seo, Y.-S., Hu, X., Shin, K., Zhang, Y., Rafailovich, M. H., Sokolov, J. C., Chu, B., Satija, S., "Dynamics of Polymer Thin Films in Supercritical Carbon Dioxide," Europhys. Lett. **60** (4), 559 (2002).

Koga, T., Seo, Y.-S., Shin, K., Zhang, Y., Rafailovich, M. H., Sokolov, J. C., Chu, B., Satija, S. K., "The Role of Elasticity in the Anomalous Swelling of Polymer Thin Films in Density Fluctuating Supercritical Fluids," Macromol. **36**, 5236 (2003).

Koga, T., Shin, K., Zhang, Y., Seo, Y.-S., Rafailovich, M. H., Sokolov, J., Chu, B., Satija, S. K., "Polymer Thin Films in Supercritical CO_2," in *Proceedings of the ASR-2000*, J. Phys. Soc. Japan., in press.

Kreyssig, A., Stockert, O., Reznik, D., Woodward, F. M., Lynn, J. W., Bitterlich, H., Souptel, D., Behr, G., Loewenhaupt, M., "Magnetic Excitations of RNi_2B_2C Single Crystals with R=Tb and Ho," Physica C., in press.

Krishnamurthy, V. V., Bhandar, A. S., Piao, M., Zoto, I., Lane, A. M., Nikles, D. E., Wiest, J. M., Mankey, G. J., Porcar, L., Glinka, C. J., "Shear and Magnetic Field Induced Ordering in Magnetic Nanoparticles Dispersions from Small Angle Neutron Scattering," Phys. Rev. E **67** (5), 051406 (2003).

Krueger, S. K., Gregurick, S., Shi, Y., Wang, S., Wladkowski, B. D., Schwartz, F. P., "Entropic Nature of the Interaction Between Promoter Bound CRP Mutants and RNA Polymerase," Biochemistry **42** (7), 1958 (2003).

Krueger, S. K., Gregurick, S., Zondlo, J., Eisenstein, E., "Interaction of GroEL and GroES/GroES Complexes with a Non-Native Subtilisin Variant: A Small-Angle Neutron Scattering Study," J. Struc. Biology **141**, 240 (2003).

Kucera, J., Zeisler, R., "Low-Level Determination of Silicon in Biological Materials Using Radiochemical Neutron Activation Analysis," J. Radioanal. Nucl. Chem., in press.

Kulkarni, A., Wang, Z., Nakamura, T., Sampath, S., Goland, A., Herman, H., Allen, J., Ilavsky, J., Long, G., Frahm, J., Steinbrech, R. W., "Comprehensive Microstructural Characterization and Predictive Property Modeling of Plasma-Sprayed Zirconia Coatings," Acta Mater. **51** (9), 2457 (2003).

Kutteruf, M. R., Brown, C. M., Iwaki, L. K., Cambell, T. M., Korter, T. M., Heilweil, E. J., "Terahertz Spectroscopy of Short-Chain Polypeptides," Chem. Phys. Letts. **375** (3-4), 337 (2003).

Kuzmanovic, D. A., Elashvili, I., Wick, C., O'Connell, Krueger, S., "Spatial Distribution Analysis and Molecular Weight Determination of Bacteriophage MS2 by Small Angle Neutron Scattering and a Novel Concentration Determination Method," Structure, in press.

Lamaze, G. P., Chen-Mayer, H. H., Becker, D. A., Vereda, F., Goldner, R. B., Haas, T., Zerigian, P., "Cold Neutron Depth Profiling of Lithium Battery Materials," J. Power Sources **119**, 680 (2003).

Lee, A. S., Butun, V., Vamvakaki, M., Armes, S. P., Pople, J. A., Gast, A. P., "Structure of pH-Dependent Block Copolymer Micelles: Charge and Ionic Strength Dependence", Macromol. **35** (22), 8540 (2002).

Lee, H. J., Lin, E. K., Bauer, B. J., Wu, W. L., Hwang, B. K., Gray, W. D., "Characterization of Chemical-Vapor-Deposited Low-k Thin Films Using X-Ray Porosimetry," Appl. Phys. Lett. **82**, 1084 (2003).

Lee, H. J., Soles, C. L., Liu, D. W., Bauer, B. J., Wu, W. L., "Pore Size Distributions in Low-k Dielectric Thin Films from X-ray Porosimetry," Journal of Polymer Science Part B-Polymer Physics **40**, 2170-2177 (2002).

Lee, J. H., Balsara, N. P., Chakraborty, A. K., Krishnamoorti, R., Hammouda, B., "Thermodynamics and Phase Behavior of Block Copolymer/Homopolymer Blends with Attractive and Repulsive Interactions," Macromol. **35** (20), 7748 (2002).

Lee, S.-H., Broholm, C., Ratcliff, W., Gasparovic, G., Huang, Q., Kim, T. H., Cheong, S. W., "Emergent Excitations in a Geometrically Frustrated Magnet," Nature, **418**, 856 (2002).

Lefebvre, A. A., Lee, J. H., Balsara, N. P., Vaidyanathan, C., "Determination of Critical Length Scales and the Limit of Metastability in Phase Separating Polymer Blends," J. Chem. Phys. **117**, 9063 (2002).

Lefebvre, A. A., Lee, J. H., Balsara, N. P., Vaidyanathan, C., "Fluctuation Mediated Phase Separation in Polymer Blends Near the Limit of Metastability," J. Chem. Phys. **117**, 9074 (2002).

Levin, I., Amos, T. G., Nino, J. C., Vanderah, T. A., Randall, C. A., Lanagan, M. T., "Structural Study of an Unusual Cubic Pyrochlore $Bi_{1.5}Zn_{0.92}Nb_{1.5}O_{6.92}$," J. Solid State Chem. **168** (1), 69 (2002).

Li, Z. G., Harlow, R. L., Foris, C. M., Li, H., Ma, P., Vickery, R. D., Maurin, M. B., Toby, B. H., "New Applications of Electron Diffraction in the Pharmaceutical Industry: Polymorph Determination by Using a Combination of Electron Diffraction and Synchrotron X-ray Powder Diffraction Techniques," Microscopy and Microanalysis **8**, 134 (2002).

Lin, E. K., Lee, H. J., Bauer, B. J., Wang, H., Wetzel, J. T., Wu, W. L., "Structure and Property Characterization of Low-k Dielectric Porous Thin Films Determined by X-ray Reflectivity and Small-angle Neutron Scattering," in *Low Dielectric Constant Materials for IC Applications*, edited by P. S. Ho, J. Leu, and W. W. Lee (Springer Publishing Inc), in press.

Lin, E. K., Soles, C. L., Goldfarb, D. L., Trinque, B. C., Burns, S. D., Jones, R. L., Lenhart, J. L., Angelopoulos, M., Willson, C. G., Satija, S. K., Wu, W.-L., "Measurement of the Spatial Evolution of the Deprotection Reaction Front with Nanometer Resolution Using Neutron Reflectometry," in *Proceedings of SPIE Conference (2002)*.

Lin, Y., Alexandridis, P., "Self-Assembly of an Amphiphilic Siloxane Graft Copolymer in Water," J. Phys. Chem. B **106**, 10845 (2002).

Lin. Y., Alexandridis, P., "Small-Angle Neutron Scattering Characterization of Micelles Formed by Poly(dimethyl-siloxane)-graft-polyether Copolymers in Mixed Polar Solvents," J. Phys. Chem. B **106**, 12124 (2002).

Lin, Y., Alexandridis, P., "Temperature-Dependent Adsorption of Pluronic F127 Block Copolymers onto Carbon Black Particles Dispersed in Aqueous Media," J. Phys. Chem. B **106**, 10834 (2002).

Lin, Z., Wu, C., Heller-Zeisler, S., Ondov, J. M., "Chemical Mass Balance of Primary Aerosol Constituents in Baltimore Air," Atmos. Environ, in press.

Lindstrom, R. M., "An Improved Radiochemical Neutron Activation Analysis Procedure for Trace Mercury," J. Radioanal. Nucl. Chem., in press.

Lindstrom, R. M., Blaauw, M., Unterweger, M., and Lucas, L. "The Half-Lives of ^{24}Na, ^{42}K, and ^{198}Au.," J. of Radioanal. Nucl. Chem., in press.

Ling, C. D., Granado, E., Neumeier, J. J., Lynn, J. W., Argyriou, D. N., "Inhomogeneous Magnetism in La-Doped $CaMnO_3$: (II) Phase Separation due to Lattice-Coupled Ferromagnetic Interactions," Phys. Rev. B, in press.

Ling, X. S., Park, S. R., Choi, S. M., Dender, D. C., Lynn, J. W., Reply to Comment on "Direct Observation on Superheating and Supercooling of Vortex Matter Using Neutron Diffraction," Phys. Rev. Lett. **89** (25), 259702 (2002).

Lin-Gibson, S., Schmidt, G., Kim, H., Han, C. C., Hobbie, E. K., "Shear-Induced Mesostructure in Nanoplatelet-Polymer Gels," J. Chem. Phys., in press.

Liu, Q. T., Diamond, M. L., Gingrich, S. E., Ondov, J. M., Maciejczyk, P., Stern, G. A. "Accumulation of Metals, Trace Elements and Semi-Volatile Organic Compounds in Films on an Urban Impervious Surface," Environ. Pollut. **122**, 51 (2003).

Livingston, R. A., Bumrongjaroen, W., Neumann, D. A. "Inelastic Neutron Scattering Measurements of Pozzolan Performance in Portland Cement," Nondestructive Characterization of Materials XI, edited by R. E. Green, B. B. Djordjevic, and M. P. Hentschel, (Springer, Berlin, Germany) **615** (2003).

Luzin, V., Brokmeier, H. G., "Attenuation Corrections in Neutron Texture Experiment," Mater. Sci. Forum **408**, 191 (2002).

Luzin, V., Gnäupel-Herold, T., Prask, H. J., "Evaluation of Local and Global Elastic Properties of Textured Polycrystals Means of FEM," Mater. Sci. Forum **408**, 407 (2002).

Lynn, G., Dadmun, M. D., Lin, E. K., Wallace, W. E., Wu, W., "Neutron Reflectivity Studies on a Small Molecules Liquid Crystal/Polymer Interface," Liquid Crystal **29**, 551 (2002).

Lynn, J. W., "Polaron Glass in Colossal Magnetoresistive Oxides Researched," J. Res. Natl. Inst. Stand. Technol. **107**, 480 (2002).

Lynn, J. W., Huang, Q., Brown, C. M., Miller, V. L., Foo, M. L., Schaak, R. E., Jones, C. Y., Mackey, E. A., Cava, R. J., "Structure and Dynamics of Superconducting Na_xCoO_2 Hydrate and Its Unhydrated Analog," Phys. Rev. B, in press.

Maciejczyk, P. B., Zeisler, R., Hwang, J. S., Thurston, G. D., Chen, L. C., "Characterization of Size-Fractioned World Trade Center Dust and Estimation of Relative Dust Contribution to Ambient Concentrations," ACS Symposium Series, in press.

Mackay, M. E., Dao, T. T., Tuteja, A., Ho, D. L., Van Horn, B., Kim, H.-C., Hawker, C. J., "Nanoscale Effects Leading to Non-Einstein-like Behavior – Reduction in Polymer Melt Viscosity by the Addition of Nanometer-sized Particles," Nature Materials, in press.

Mackay, M. E., Hong, Y., Jeong, M., Tande, B. M., Wagner, N. J., Hong, S., Gido, S. P., Vestberg, R., Hawker, C. J., "Microphase Separation of Hybrid Dendron-Linear Diblock Copolymers into Ordered Structures," Macromol. **35**, 8391 (2002).

Mackey, E. A., Oflaz, R. D., Epstein, M. S., Buehler, B., Porter, B. J., Rowles, T., Wise, S. A., Becker, P. R., "Elemental Composition of Liver and Kidney Tissues of Rough-Toothed Dolphins (Steno Bredanensis)," Archives of Environ. Contamination and Toxicology **44** (4), 523 (2003).

Majewski, J., Smith, G. S., Burgess, I., Zamlynny, V., Szymanski, G., Lipkowski, J., Satija, S. K., "Neutron Reflectivity Studies of Electric Field Driven Structural Transformations of Surfactants," Appl. Phys. A **74**, S364 (2002).

Majkrzak, C. F., Berk, N. F., "Advances in Specular Neutron Reflectometry," J. Appl. Phys. A **74**, S67 (2002).

Majkrzak, C. F., Berk, N. F., "Phase Sensitive Reflectometry and the Unambiguous Determination of Scattering Length Density Profiles," Physica B, in press.

Majkrzak, C. F., Berk, N. F., Perez-Salas, U. A., "Phase-Sensitive Neutron Reflectometry," Langmuir, in press.

Manson, J. L., Bordallo, H. N., Lynn, J. W., Huang, Q., Feyerherm, R., Loose, A., Chapon, L., Argyriou, N., "Magnetic Ordering and Spin Excitations in $Mn(dca)_2(pyz)$ [dca = $N(CN)^-_2$; pyz = pyrazine]," Appl. Phys. A **74**, S722 (2002).

Marazano, B. J., Wagner, N. J., "Flow-Small Angle Neutron Scattering Measurements of Colloidal Dispersion Microstructure Through the Shear Thickening Transition," J. Chem. Phys. **117** (22), 10291 (2002).

Marshall, J. C., Cosgrove, T., Jack, K., Howe, A., "Small-angle Neutron Scattering of Gelatin/Sodium Dodecyl Sulfate Complexes at the Polystyrene/Water Interface," Langmuir **18** (25), 9668 (2002).

Martinho, H., Granado, E., Moreno, N. O., Garcia, A., Toniani, I., Rettori, C., Neumeier, J. J., Oseroff, S. B., "Strong Charge Carrier Effect on the Magnetic Coupling of La-doped $CaMnO_3$," Physica B, in press.

Martter, T. D., Foster, M. D., Yoo, T., Xu, S., Lizzaraga, G., Quirk, R. P., Butler, P. D., "Nonuniversal Behavior of the Thermodynamic Interaction Parameter in Blends of Star and Linear Polybutadiene," Macromol. **35** (26), 9763 (2002).

Mason, T. G., Lin, M. Y., "Time-Resolved Small Angle Neutron Scattering Measurements of Asphaltene Nanoparticle Aggregation Kinetics in Incompatible Crude Oil Mixtures," J. Chem. Phys. **119**, 565 (2003).

Mason, T. G., Lin, M. Y., "Asphaltene Nanoparticle Aggregation in Mixtures of Incompatible Crude Oils," Phys. Rev. E **67**, 050401(2003), in press.

Matějíček, J., Sampath, S., Gnäupel-Herold, T., Prask, H. J., "Residual Stress in Sprayed Ni+5% Al Coatings Determined by Neutron Diffraction," Appl. Phys. A **74**, S1692 (2002).

McGuire, S. C., Samuel, M. J., Sulcer, J. D., Lamaze, G. P., Chen-Mayer, H. H., "Neutron Depth Profiling of Boron-Doped Ni_3Al Coatings," American Laboratory, in press.

McKinsey, D. N., Dzhosyuk, S. N., Golub, R., Habicht, K., Huffman, P. R., Mattoni, C. E. H., Yang, L., Doyle, J. M., "Detecting Ionizing Radiation in Liquid Helium Using Wavelength Shifting Light Collection," Nucl. Intrum. Meth. A, in press.

McKinsey, D. N., Dzhosyuk, S. N., Huffman, P. R., Mattoni, C. E. H., Yang, L., Doyle, J. M., Golub, R., Habicht, K., "The Time Dependence of Liquid Helium Fluorescence," Phys. Rev. A **67**, 044005 (2003).

Meyer, A., Dimeo, R. M., Gehring, P. M., Neumann, D. A., "The High-Flux Backscattering Spectrometer at the NIST Center for Neutron Research," Rev. Sci. Instrum. **74** (5), 2759 (2003).

Mildner, D. F. R., Chen-Mayer, H. H., Gibson, W. M., "Focusing Neutrons with Tapered Capillary Optics," J. Appl. Phys. **92**, 6911 (2002).

Mildner, D. F. R., Chen-Mayer, H. H., Gibson, W. M., Schultz, A. J., "A Monolithic Polycapillary Focusing Optic for Polychromatic Neutron Diffraction Applications," in *Proceedings of the SPIE Conference, "Advanced In Neutron Scattering Instrumentation*, edited by I. S. Anderson, B. Guérard (July 2002. Seattle, WA) **4785**, (2002), p. 43.

Mook, H. A., Dai, P., Hayden, S. M., Hiess, A., Lynn, J. W., Lee, S.-H., Dogan F., "Magnetic Ordering in $YBa_2Cu_3O_{6+x}$ Superconductors," Phys. Rev. B **66** (14), 144512 (2002).

Moyer, R. O., Toby, B. H., "Ca_2IrD_5- An Order-Disorder Transition," J. Alloys Comp., in press.

Mukherjee, S., Cohen, R. E., Gulseren, O., "Vacancy Formation Enthalpy at High Pressure in Tantalum," Phys. Rev. B, in press.

Nair, S., Tsapatsis, M., "Infared Reflectance Measurements of Zeolite Film Thickness, Refractive Index and Other Characteristics," Micro. Meso. Mater. **58**, 81 (2003).

Nakatani, A. I., "Chain Dimensions in Polysilicate-Filled Poly (Dimethyl Siloxane)," in *Proceedings of the International Journal of Thermophysics, 14th Symposium on Thermophysical Properties*, (Boulder, CO), in press.

Narehood, D. G., Grube, N., Dimeo, R. M., Brown, D. W., Sokol, P. E., "Inelastic Neutron Scattering of H_2 in Xerogel," J. Low. Temp. Phys. **132** (3-4), 223 (2003).

Narehood, D. G., Pearce, J. V., Eklund, P. C., Sokol, P. E., Lechner, R. E., Pieper, J., Copley, J. R. D., Cook, J. C., "Diffusion of H_2 Adsorbed on Single Walled Carbon Nanotubes," Phys. Rev. B **67**, 205409 (2003).

Natali-Sora, I., Santoro, A., Huang, Q., "Oxidation States of Fe in $YBa_2Fe_3O_8$ From a Bond Valence Analysis of the Structure," J. Solid State Chem., in press.

Noakes, D. R., Arrott, A. S., Belk, M. G., Deevi, S. C., Huang, Q. Z., Lynn, J. W., Shull, R. D., Wu, D., "Incommensurate Spin Density Waves in Iron Aluminides," Phys. Rev. Lett., in press.

Norman, B. R., Iyengar, G. V., "Further Applications of Pre-Irradiation Combustion and Neutron Activation Analysis Technique for the Determination of Iodine in Food and Environmental Reference Materials: Merits and Demerits," Fresen. J. Anal. Chem., in press.

O'Donovan, K. V., Borchers, J. A., Majkrzak, C. F., Hellwig, O., Fullerton, E. E., "Extracting Buried Twists With Polarized Neutron Reflectometry," Appl. Phys. Lett. A **74**, S1544 (2002).

Olin, J. S., Blackman, M. J., Mitchem, J. E., Waselkov, G. A., "Compositional Analysis of Glazed Earthenwares from Eighteenth-Century Sites on the Northern Gulf Coast," J. Hist. Arch. **36** (1), 79 (2002).

Olin, J. S., Blackman, M. J., Waselkov, G., "Databases for the Analysis of European Ceramics in American Archaeology," in Patterns and Process: A Festschrift in Honor of Dr. Edward V. Sayre, Edited by Lambertus van Zelst, (Smithsonian Center for Materials Research and Education, Suitland, Maryland) p. 65.

Ondov, J. M., Caffrey, P. F., Suarez, A. E., Borgoul, P. V., Holsen, T., Paode, R. D., Sofuoglu, S. C., Sivadechathep, J., Lu, J., Kelly, M. J., Church, T., Scudlark, J., "Atmospheric Deposition of Trace Elements to Lake Michigan: Influence of Urban and Industrial South Shore Sources," Aerosol. Sci. Technol., in press.

Otano-Rivera, W., Messier, R., Pilione, L. J., Santiago, J. J., Lamaze, G. P., "Effect of Al Additions and AlN Interlayers on the Stablization of cBN Sputtered Thin Films," J. Diamond & Rel. Matls., in press.

Ou-Yang, W.-C., Chen, H.-L., Ho, D. L., Tsao, C.-C., Yang, G., Peng, K.-Y., Chen, S.-A., Han, C., "Solution Structure of Electroluminescent Semiconducting Polymers MEH-PPV Studied by SANS," Phys. Rev. Lett., in press.

Park, S.-H., Gies, H., Toby, B. H., Parise, J. B., "Characterization of a New Microporous Lithosilicate with ANA Topology," Chem. Mater. **14**, 3187 (2002).

Paul, R. L., Chen-Mayer, H. H., Myneni, G. R., "Determination of Hydrogen in Niobium by Cold Neutron Prompt Gamma-ray Activation Analysis and Neutron Incoherent Scattering," in Hydrogen in Materials and Vacuum Systems, edited by G. R. Myneni, S. Chattopadhyay (American Institute of Physics) *AIP Conference Proceedings* **671** (Melville, NY 2003) p. 151.

Paul, R. L., Simons, D. S., "Calibration of Phosphorus Implantation Dose in Silicon by Radiochemical Neutron Activation Analysis," in: Silicon Front-End Junction Formation Technologies, *MRS Symposium Proceedings*, edited by D. F., Downey, M. E. Law, A. Claverie, M.J. Rendon, Matls. Res. Soc., **717** (Warrendale, PA, 2002), p. 291.

Paul, R. L., Simons, D. S., "Radiochemical Neutron Activation Analysis for Certification of Ion-Implanted Phosphorus in Silicon," Anal. Chem., in press.

Perez-Salas, U., Briber, R. M., Rafailovich, M. H., Sokolov, J., "Interfacial Fracture Toughness Between Glassy Polymer Networks," J. of Polym. Sci. Part B: Poly. Phys. **41** (16), (2003).

Perez-Salas, U., Faucher, K. M., Majkrzak, C. F., Berk, N. F., Chaikof, E. L., Krueger, S., "Characterization of a Biomimetic Polymeric Lipid Bilayer by Phase Sensitive Neutron Reflectometry," Langmuir, in press.

Perez-Salas, U., Briber, R. M., Hamilton, W. A., Rafailovich, M. H., Sokolov, J., Nasser, L., "Polystyrene Network-Network Interdiffusion," Macromol. **35** (17), 6638 (2002).

Phair, J. W., Schulz, J. C., Aldridge, L. P., Smith, J. D., "Small-Angle Neutron Scattering (SANS) and Rheological Characterization of AluminosilicateHydrogels," J. Am. Cer. Soc., in press.

Phair, J. W., Schulz, J. C., Bertram, W. K., Aldridge, L. P., VanDeventer, J. S. J., "Investigation of the Microstructure of Alkali Activated Cements by Neutron Scattering," Cem. Conc. Res., in press.

Popov, G., Lobanov, M. V, Tsiper, E., Greenblatt, M., Caspi, E. N., Lynn, J. W., "Neutron Diffraction Study of the Sr_2MnReO_6 Double Perovskite," J. Phys. C, in press.

Porcar, L., Hamilton, W. A., Butler, P. D., Warr, G. G., "Scaling of Membrane Phase Dynamics," *NCNR Highlights*, 30 (2002).

Porcar, L., Hamilton, W. A., Butler, P. D., Warr, G. G., "Scaling of Shear-Induced Transformations in Membrane Phases," Phys. Rev. Lett. **89**, 168301 (2002).

Porcar, L., Hamilton, W. A., Butler, P. D., Warr, G. G., "Scaling of Structural and Rheological Response of L3 Sponge Phases in the "Sweetened" Cetylpyridinium-Hexanol/dextrose-brine System," Langmuir, in press.

Prabhu, V. M., Jones, R. L., Lin, E. K., Soles, C. L., Wu, W. L., Goldfarb, D. L., Angelopoulos, M., "Polyelectrolyte Effects in Model Photoresist Developer Solutions: Roles of Base Concentration and Added Salts," in *Proceedings of the SPIE, Advances in Resist Technology and Processing XX* **5039** (February, 2003, Santa Clara, CA), p. 404.

Prabhu, V. M., Jones, R. L., Lin, E. K., Wu, W. L., "Polyelectrolyte Effects in Model Photoresist Developer Solutions," J. of Vacuum Sci. Tech. B **21**, 1403 (2003).

Prask, H. J., Gnäupel-Herold, T., Luzin, V., Fisher, J. W., Cheng X., Roy, S., "Residual Stress Modification and Fatigue Life Enhancement," in *Trends in Welding Research*, edited by S. A. David et al. (ASM International, Materials Park, OH, 2003), p. 897.

Prask, H. J., Gnäupel-Herold, T., Fisher, J. W., Cheng, X., Stuart, J. T., "Residual Stress Modification by Means of Ultrasonic Impact Treatment," in *Proceedings of the SEM Annual Conference on Experimental and Applied Mechanics*, (June, 2001, Porland, Oregon), p. 551.

Pugh, D. V., Dursun, A., Corcoran, S. G., "Formation of Nanoporous Platinum by Selective Dissolution of Cu From $Cu_{0.75}$ $Pt_{0.25}$," J. Mater. Res. **18** (1), 216 (2003).

Qiu, Y., Broholm, C., Ishiwata, S., Azuma, M., Takano, M., Bewley, R., Buyers, W. J. L., "Spin Trimer Antiferromagnetism in $La_4Cu_3MoO_{12}$," Phys. Rev. B, in press.

Radlinski, A. P., Ioannidis, M. A., Hinde, A. L., Hainbuchner, M., Baron, M., Rauch, H., Kline, S. R., "Angstrom to Millimeter Characterization of Sedimentary Rock Microstructure," Phys. Rev. Lett., in press.

Raphael, M. P., Ravel, B., Huang, Q., Willard, M. A., Cheng, S. F., Das, B. N., Stroud, R. M., Bussmann, K. M., Claassen, J. H., Harris, V. G., "Presence of Antisite Disorder and its Characterization in the Predicted Half-Metal Co_2MnSi," Phys. Rev. B **66**, 104429 (2002).

Rathgeber, S., Gast, A. P., Hedrick, J. L., "Structural Properties of Star-Like Dendrimers in Solution," Appl. Phys. A **74**, S396 (2002).

Rawn, C. J., Rondinone, A. J., Chakoumakos, B. C., Marshall, S. L., Stern, L. A., Circone, S., Kirby, S. H., Jones, C. Y., Toby, B. H., Ishii, M., "Neutron Powder Diffraction Studies as a Function of Temperature of Structure II Hydrate Formed a Methane + Ethane Gas Mixture," in *Proceedings of the 4th International Conference on Gas Hydrates*, (Yokohama, Japan, 2002), in press.

Reynolds, A. P., Tang, W., Gnäupel-Herold, T., Prask, H., "Structure, Properties, and Residual Stress of 304L Stainless Steel Friction Stir Welds," Scripta Mater. **48** (9), 1289 (2003).

Riseman, T. M., Forgan, E. M., "Maximum Entropy μSR Analysis I: Planting the Kernel," in *Conference Proceedings, 9th International Conference on Muon Spin Rotation/Relaxation/Resonance*, Physica B **326**, 226 (2003).

Riseman, T. M., Forgan, E. M., "Maximum Entropy μSR Analysis II: The Search For Truthful Errors," in *Conference Proceedings, 9th International Conference on Muon Spin Rotation/Relaxation/Resonance,* Physica B **326**, 230 (2003).

Riseman, T. M., Forgan, E. M., "Maximum Entropy μSR Analysis III: Automatic Selection of the Default Level and Looseness Factor," in *Conference Proceedings, 9th International Conference on Muon Spin Rotation/Relaxation/Resonance,* Physica B **326**, 234 (2003).

Rondinone, A. J.; Jones ,C. Y.; Marshall, S. L.; Chakoumakos, B. C.; Rawn, C. J.; Lara-Curzio, E. "A Sapphire Cell for High-Pressure, Low-Temperature Neutron Scattering Experiments on Gas Hydrates," Can. J. Chem., **81** (1-2), 381 (2003).

Rothman, M. S., Blackman, M. J., "Late Fifth Millennium and Earliest Fourth Millennium B. C. Exchange Systems in Northern Mesopotamia: Chemical Characterization of Sprig and Impressed Ware," Al-Rafidan XXIV, 1 (2003).

Rush, J. J., Udovic, T. J., "Modern Neutron Methods for the Study of Hydrogen in Materials," in EPD Congress 2002 and Fundamentals of Advanced Materials for Energy Conversion, edited by P. R. Taylor, D. Chandra, and R. G. Bautista, (The Minerals, Metals & Materials Society, Warrendale, PA, 2002) p. 161.

Ruzette, A.-V. G., Mayes, A. M., Pollard, M., Russell, T. P., Hammouda, B., "Pressure Effects on the Phase Behavior of Styrene/n-Alkyl Methacrylate Block Copolymers," Macromol. **36** (9), 3351 (2003).

Sackett, D. L., Chernomordik, V., Krueger, S., Nossal, R., "Use of Small-Angle Neutron Scattering To Study Tubulin Polymers," Biomacro. **4** (2), 461 (2003).

Saiz, L., Bandyopadhyay, S., Klein, M. L., "Effect of the Pore Region of a Transmembrane Ion-Channel on the Physical Properties of a Simple Membrane," in *Proceedings of the National Academy of Science USA*, in press.

Saiz, L., Bandyopadhyay, S., Klein, M. L., "Towards an Understanding of Complex Biological Membranes from Atomistic Molecular Dynamics Simulations," Bioscience Reports **22**, 151 (2002).

Saiz, L., Klein, M. L., "Computer Simulation Studies of Model Biological Membranes," Acc. Chem. Res. **35**, 482 (2002).

Saiz, L., Klein, M. L., "Electrostatic Interaction in a Neutral Model Phospholipid Bi-Layer by Molecular Dynamics Simulations," J. Chem Phys. **116**, 3052 (2002).

Saiz, L., Koubi, L., Tarek, M., Scharf, D., Klein, M. L., "Influence of Anesthetic and Non-Immobilizer Molecules on the Physical Properties of a Polyunsaturated Lipid Bilayer," J. Phys. Chem., in press.

Sato, T. J., Lee, S.-H., Katsufuji, T., Masaki, M., Park, S., Copley, J. R. D., Takagi, H., "Unconventional Spin Fluctuations in the Hexagonal Antiferromagnet $YMnO_3$," Phys. Rev. B **68**, 014432 (2003).

Sayer, E. V., Yener, A. K., Joel, E. C., Blackman, M. J., Özbal, H., "Stable Lead Isotope Studies of Black Sea Anatolian Ore Sources and Related Bronze Age and Phrygian Artifacts From Nearby Archaeological Sites Appendix: New Central Taurus Ore Data," Archaeometry, in press.

Schneider, J. P., Pochan, D. J., Ozbas, B., Rajagopal, K., Pakstis, L. M., Gill, J. "Responsive Hydrogels From the Intramolecular Folding and Self-Assembly of a Designed Peptide," J. Am. Chem. Soc. **124**, 15030 (2002).

Schoen, K., Kaiser, H., Werner, S. A., Arif, M., Huffman, P. R., Jacobson, D. L., Black, T. C., Snow, W. M., Lamoreaux, S. K., "Precision Neutron Interferometric Measurements of the n-H and n-D Coherent Neutron Scattering Lengths," Phys. Rev. C **67**, 044005 (2003).

Schubert, B. A., Kaler, E. W., Wagner, N. J., "The Microstructure and Rheology of Mixed Cationic/anionic Wormlike Micelles," Langmuir **19** (10), 4079 (2003).

Sen, P., Gulseren, O., Yildirim, T., Batra, I. P., Ciraci, S., "Pentagonal Nanowires: A First-Principles Study of Atomic and Electronic Structure," Phys. Rev. B **65**, 235433 (2002).

Shah, S. A., Ramakrishnan, S., Chen, Y. L., Schweizer, K. S., Zukoski, C. F., "Scattering Structures of Colloid-Polymer Suspensions and Gels," Langmuir **19** (12), 5128 (2003).

Shapiro, S. M., Bao, W., Raymond, S., Lee, S. H., Motoya, K., "Observation of Linear Spin Wave Dispersion in Re-Entrant Spin Glass $Fe_{0.7}Al_{0.3}$," Appl. Phys. A **74**, S859 (2002).

Shin, K., Koga, T., Zhang, Y., Seo, Y., Occhiogrosso, R., Rafailovich, M. H., Sokolov, J. C., Chu, B., Satija, S. K., "Anomalous Carbon Dioxide-Induced Swelling of Polymer Thin Films at Gas-Supercritical Transition," J. Am. Chem. Soc., in press.

Shirane, G., Gehring, P. M., "Structure and Dynamics of the Ferroelectric Relaxors $Pb(Mg_{1/3}Nb_{2/3})O_3$ and $Pb(Zn_{1/3}Nb_{2/3})O_3$," in *Proceedings of the 104th Annual Meeting of the American Ceramics Society*," Ceramic Transactions **136**, 17 (2003).

Silas, J. A., Kaler, E. W., "Effect of Multiple Scattering on SANS Spectra from Bicontinuous Microemulsions", J. Coll. Interface Sci., **257** (2), 291 (2003).

Simmons, B., Agarwal, V., McPherson, G., Arijit Bose, J., "A Small Angle Neutron Scattering Study of Mixed AOT + Lecithin Reverse Micelles," Langmuir **18**, 8345 (2002).

Sitepu, H., Schmahl, W. W., Stalick, J. K., "Correction of Intensities for Preferred Orientation in Neutron-Diffraction Data of NiTi Shape-Memory Alloy Using the Generalized Spherical-Harmonic Description," Appl. Phys. A **74**, S1719 (2002).

Skripov, A. V., Buzlukov, A. L., Kozhanov, V. N., Udovic, T. J., Huang, Q., "Hydrogen in $Nb(V_{1-y}Cr_y)_2$ Laves-phase Compounds: Neutron Diffraction and Nuclear Diffraction and Nuclear Magnetic Resonance Studies," J. Alloys. Compnds., **359**, 27 (2003).

Skripov, A. V., Cook, J. C., Udovic, T. J., Gonzalez, M., Hempelmann, R., Kozhanov, V. N., "Quasielastic Neutron Scattering Study of Hydrogen Motion in C15-type YMn_2H_x," J. Phys.: Condens. Matter **15**, 3555 (2003).

Smee, S. A., Orndorff, J. D., Scharfstein, G. A., Qiu, Y., Brand, P. C., Broholm, C. L., Anand, D. K., "MACS Low-Background Doubly Focusing Neutron Monochromator," Appl. Phys. A **74**, S255 (2002).

Soles, C. L., Douglas, J. F., Lin, E. K., Lenhart, J. L., Jones, R. L., Wu, W.-L., "Incoherent Neutron Scattering and the Dynamics of Thin Film Photoresist Polymers," J. Appl. Phys. **93** (4), 1978 (2003).

Soles, C. L., Douglas, J. F., Wu, W.-L., Dimeo, R. M., "Incoherent Neutron Scattering as a Probe of the Dynamics in Molecularly Thin Polymer Films," Macromol. **36** (2), 373 (2003).

Soles, C. L., Douglas, J. F., Wu, W.-L., Peng, H., Gidley, D. W., "A Broad Perspective on the Dynamics of Highly Confined Polymer Films," in *Proceedings of the MRS Conference* **710**, DD3.7.1 (2002).

Spiecker, P. M., Gawrys, K. L., Kilpatrick, P. K., "Aggregation and Solubility Behavior of Asphaltenes and Their Subfractions," J. Colloid Interf. Sci., in press.

Spiecker, P. M., Gawrys, K. L., Trail, C. B., Kilpatrick, P. K., "Effects of Petroleum Resins on Asphaltene Aggregation and Water-in-Oil Emulsion Formation," Colloids and Surfaces A **220**, 9 (2003).

Starr, F. W., Sastry, S., Douglas, J. F., Glotzer, S. C., "What Do We Learn from the Local Geometry of Glass-Forming Liquids?," Physical Review Letters **89**, 5501 (2002).

Stellbrink, J., Allgaier, J., Wilner, L., Richter, D., Slawecki, T., Fetters, "Real Time SANS Study on Head Group Self-Assembly for Lithium Based Anionic Polymerizations," Polymer **43** (25), 7101 (2002).

Stock, C., Birgeneau, R. J., Wakimoto, J. S., Gardner, J. S., Chen, W., Ye, Z.-G., Shirane, G., "Universal Static and Dynamic Properties of the Structural Transitions in $Pb(Zn_{1/3}Nb_{2/3})O_3$," Phys. Rev. B, in press.

Stone, M. B., Reich, D. H., Broholm, C., Lefmann, K., Rischel, C., Landee, C. P., Turnbull, M. M., "Extended Quantum Critical Phase in a Magnetized Spin-1/2 Antiferromagnetic Chain," Phys. Rev. Lett. **91**, 037205 (2003).

Stone, M. B., Rittner, J., Chen, Y., Yardimci, H., Reich, D. H., Broholm, C., Ferraris, D. V., Lectka, T., "Frustrated Three-Dimensional Quantum Spin Liquid in CuHpCl," Phys. Rev. B **65**, 064423 (2002).

Suarez, A. E., Ondov, J. M., "Atmospheric Deposition of Trace Elements to the Chesapeake Bay: Influence of Urban and Industrial Sources in Baltimore," Environ. Sci. Tech., in press.

Suarez, A. E., Ondov, J. M., "Contributions of Some Cytokine-Active Metals from Coal and Oil Fired Power Plants," Energy and Fuels **16**, 562 (2002).

Sung, L., Karim, A., Douglas, J. F., Han, C. C., "Modification of Thin Film Phase Separation by a Surfactant," Macromol., in press.

Tang, F., Gnäupel-Herold, T., Prask, H. J., Anderson, I. E., "Neutron Diffraction Study of Residual Stresses in Al/AlCuFe Composites," in Advance in Powder Metallurgy & Particulate Materials 2003, (International Conference on Powder Metallurgy & Particulate Materials, June 8-12, 2003, Las Vegas, Nevada, sponsored by the MPIF/APMI), in press.

Tang, F., Gnäupel-Herold, T., Prask, H. J., Anderson, I. E., "Neutron Diffraction Measurement on Residual Stresses and Stress Partitioning in Al/AlCuFe Composites," Matl. Sci. Eng., in press.

Tang, F., Gnäupel-Herold, T., Prask, H. J., Anderson, I. E., "Pure Al Matrix Composites Produced by Vacuum Hot Pressing: Tensile Properties and Strengthening Mechanisms," Metall. Trans. A., in press.

Tarek, M., Neumann, D. A., Tobias, D. J., "Characterization of Sub-nanosecond Dynamics of the Molten Globule State of α-Lactalbumin using Quasielastic Neutron Scattering and Molecular Dynamics Simulations," Chem. Phys. **292**, 435 (2003).

Tarek, M., Tobias, D. J., "Single Particle and Collective Dynamics of Protein Hydration Water: A Molecular Dynamics Study," Phys. Rev. Lett. **89** (27), 275501 (2002).

Tennant, D. A., Broholm, C., Reich, D. H., Nagler, E., Granroth, G. E., Barnes, T., Damle, K., Xu, G., Chen, Y., Sales, B. C., "Neutron Scattering Study of Two-Magnon States in the Quantum Magnet Copper Nitrate," Phys. Rev. B **67** (5), 054414 (2003).

Terry, J. S., Heller-Zeisler, S., Ondov, J. M., "Behavior of Three Atmospheric Tracer Materials in a Pilot-Scale Coal Combuster," J. Radio. Analyt. Nuc. Chem. **251**, 205 (2002).

Thornton, J., McMahon, P. J., Allman, B. E., Murphy, J. E., Nugent, K. A., Jacobson, D. L., Arif, M., Werner, S. A., "The Detection and Sizing of Flaws in Components from the Hot-end of Gas Turbines Using Phase-Contrast Radiography With Neutrons: a Feasibility Study," NDT & E International **36** (5), 289 (2003).

Toby, B. H., "A Program for Viewing and Editing CIF's," J. Appl. Crystall., in press.

Toby, B. H., "Inspecting Rietveld Fits from pdCIF: pdCIFplot," J. Appl. Crystall., in press.

Toby, B. H., "The Classification of Powder Diffraction Data," International Tables for Crystallography, in press.

Toby, B. H., Von, Dreele, R. B., Larson, A. C., "Reporting of Rietveld Results Using pdCIF: GSAS2CIF," J. Appl. Crystall., in press.

Toney, M. F., Rubin, K. A., Choi, S.–M., Glinka, C. J., "Small Angle Neutron Scattering Measurements of Magnetic Cluster Sizes in Magnetic Recording Disks," Appl. Phys. Lett., in press.

Trouw, F., Borodin, O., Cook, J. C., Copley, J. R. D., Smith, G. D., "A Quasielastic Neutron Scattering Study of the Local Dynamics of Poly(Ethylene Glycol) in Aqueous Solution," J. Phys. Chem., in press.

Tucker, R. T., Han, C. C., Dobrynin, A. V., Weiss, R. A., "Small-Angle Neutron Scattering Analysis of Blends with Very Strong Intermolecular Interactions: Polyamide/ionomer Blends," Macromol. **36**, 4404 (2003).

Udovic, T. J., Huang, Q., Rush, J. J., "A Neutron-Powder-Diffraction Study of the Rare-Earth Deuteride Two-Phase Region," J. Alloys. Compnds. **356-357**, 41 (2003).

Vajk, O. P., Greven, M., Mang, P. K., Lynn, J. W., "Neutron Scattering, Magnetometry, and Quantum Monte Carlo Study of the Randomly-Diluted Spin-1/2 Square-Lattice Heisenberg Antiferromagnet," Solid State Commun. **126** (1-2), 93 (2003).

Vaknin, D., Krüger, P., Lösche, M., "Anomalous X-Ray Reflectivity Characterization of Ion Distribution at Biomimetic Membranes," Phys. Rev. Lett. **90**, 178102 (2003).

Vogt, B. D., RamachandraRao, V. S., Gupta, R. R., Lavery, K. A., Francis, T. J., Russell, T. P., Watkins, J. J., "Phase Behavior of Polystyrene-Block-Poly(n-alkyl Methacrylate)s Dilated with Carbon Dioxide," Macromol. **36** (11), 4029 (2003).

Wagner, N. J., Butera, R., "Shear Distortion and Relaxation Dynamics of Colloidal Crystals Investigated by SANS Time Slicing" Phys. Rev. E, in press.

Wakimoto, S., Birgeneau, R. J., Ichikawa, N., Kim, Y. J., Kojima, K. M., Lee, S.-H., Tranquada, J. M., Uchida, S., Zimmermann, M. V., "Effect of a Magnetic Field on the Spin-and Charge-Density Wave Order on $La_{1.45}Nd_{0.4}Sr_{0.15}CuO_4$," Phys. Rev. B **67**, 184419 (2003).

Wakimoto, S., Stock, C., Ye, Z.-G., Chen, W., Gehring, P. M., Shirane, G., "Mode-Coupling and Polar Nanoregions in the Relaxor Ferroelectric $Pb(Mg_{1/3}Nb_{2/3})O_3$," Phys. Rev. B **66** (22), 224102-1 (2002).

Wang, C. Y., Prabhu, V. M., Soles, C. L., Vogt, B. D., Wu, W. L., Lin, E. K., Satija, S. K., "Interdiffusion in Polystyrene and End-Functional Polystyrene Thin Films near a Solid Surface," in *ACS Polymeric Materials: Science and Engineering*, (New York, NY, September 2003), in press.

Wang, H. Douglas, J. F., Satija, S. K., Composto, R. J., Han, C. C., "Early-Stage Compositional Segregation in Poymer Blend Films," Phys. Rev. E, **67** (6), 061801 (2003).

Wang, H., Nieh, M.-P., Hobbie, E. H., Glinka, C. J., Katsaras, J., "Kinetic Pathway of the Bilayered-Micelle to Perforated-Lamellae Transition," Phys. Rev. E **67**, 060902 (2003).

Wang, H., Zhao, B., Wyslouzil, B., Streletzky K., "Small-Angle Neutron Scattering of Soot Formed in Laminar Premixed Ethylene Flames," Proc. Combust. Inst. **29** 2749, Part 2 (2003).

Wang, X. H., Dormidontova, E. E., Lodge, T. P., "The Order-Disorder Transition and the Disordered Micelle Regime for Poly(ethylenepropylene-b-dimethylsiloxane) Spheres," Macromol. **35** (26), 9687 (2002).

Welp, K. A., Co, C., Wool, R. P., "Improved Reflectivity Fitting Using SERF: Spreadsheet Environment Reflectivity Fitting," J. Neutron Res., in press.

Wesley, R., Armes, S. P., Thompson, L. J., "Block Copolymer Interactions With Surfactants," Langmuir, in press.

White, C. C., Wu, W. L., Pu, Y., Rafailovich, M., Sokolov, J., "Probe Segregation and T Determination of a Supported Ultra-Thin Polystyrene Film Studied by X-ray and Neutron Reflectivity, and SIMS," Poly. Eng. Sci. **43**, 1241 (2003).

Winn, B. L., Shapiro, S. M., Erwin, R., Schlagel, D. L., Lograsso, T., "Anomalous Phonon Damping in the High Temperature Shape Memory Alloy $Ti_{50}Pd_{42}Cr_8$," Appl. Phys. A **74**, S1182 (2002).

Wiyatno, W., Fuller, G. G., Pople, J. A., Gast, A. P., Chen, Z. R., Waymouth, R. M., Myers, C. L., "Component Stress-strain Behavior and Small-Angle Neutron Scattering Investigation of Stereoblock Elastomeric Polypropylene", Macromol. **36** (4), 1178 (2003).

Wiyatno, W., Pople, J. A., Gast, A. P., Waymouth, R., Fuller, G. G., "A Scattering Study of Elastomeric Polypropylene," in press.

Woodward, P. M., Karen, P., "Mixed Valency in $YBaFe_2O_5$," Inorg. Chem. **42**, 1121-1129 (2003).

Wu, S. Y., Yang, C. C., Tsao, F. C., Li, W.-H., Lee, K. C., Lynn, J. W., Yang, H. D., "Crystal Structure and Magnetic Ordering of Mn and Ce in $La_{0.7}Ce_{0.15}Ca_{0.15}MnO_3$," J. Phys. Condens. Mat. **14** (47), 12585 (2002).

Xu, G., Aeppli, G., Broholm, C., DiTusa, J. F., Ito, T., Oka, K., Takagi, H., "Mesoscopic Phase Coherence in a Quantum Spin Fluid," Nature, in press.

Yamada, K., Kurahashi, K., Uefuji, Fujita, M., Park, S. I., Lee, S.-H., Endoh, Y., "Commensurate Spin Dynamics in the Superconducting State of an Electron-Doped Cuprate Superconductor," Phys. Rev. Lett. **90** (13), 137004-1 (2003).

Yamaura, K., Huang, Q., Young, D. P., Arai, M., Takayama-Muromachi, E., "Electronic Properties of the Novel 4d Metallic Oxide $SrRhO_3$," Physica B **329**, 820 (2003).

Yamaura, K., Huang, Q., Young, D. P., Noguchi, Y., Takayama-Muromachi, E., "Crystal Structure and Electronic and Magnetic Properties of the Bilayered Rhodium Oxide $Sr_3Rh_2O_7$," Phys. Rev. B **66**, 134431 (2002).

Yang, C. C., Wu, S. Y., Li, W.-H., Lee, K. C., Lynn, J. W., Liu, R. S., Shen, C. H., "Short-Range Magnetic Correlations in Spinel $LiMn_2O_4$," Mater. Sci. Eng. B **95** (2), 162 (2002).

Yang, C. C., Wu, S. Y., Li, W.-H., Lee, K. C., Lynn, J. W., Wu, C.-G., "Magnetic Ordering of Fe in NCH_5-Intercalated Iron Phosphate $Fe(OH)PO_4$," Physica B, **325** (1-4), 240 (2003).

Yang, G. Y., Briber, R. M., Huang, E., Rice, P. M., Volksen, W., Miller, R. D., "Morphological Development in Nanoporous PMSSQ Films," Chem. Mater., in press.

Yang, G. Y., Briber, R. M., Huang, E., Rice, P. M., Volksen, W., Miller, R. D., "Morphology of Nanoporous PMSSQ Films," Appl. Phys. Lett., in press.

Yang, L., Dzhosyuk, S. N., Gabrielse, J., Huffman, P. R., Mattoni, C. E. H., Maxwell, S. E., McKinsey, D. N., Doyle, J. M., "Performance of a Large-Area Avalanche Photodiode at Low Temperature for Scintillation Detection," Nucl. Instrum. Meth. A, in press.

Yildirim, T., "Lattice Dynamics of Solid Cubane within the Quasi-Harmonic Approximation," Solid State Comm. **124** (12), 449 (2002).

Yildirim, T., "The Surprising Superconductor of 2001," Materials Today **5** (4), 40 (2002).

Yildirim, T., Gulseren, O., "A Simple Theory of 40K Superconductivity in MgB_2; First-Principles Calculations of T_c, its Dependence on Boron Mass and Pressure," J. Phys. Chem. Solids **63**, 2201 (2002).

Yildirim, T., Gulseren, O., "First-Principles Zone-Center Theory of Superconductivity in MgB_2," Appl. Phys. A **74**, S945 (2002).

Yildirim, T., Harris, A. B., "Rotational and Vibrational Dynamics of Interstitial Molecular Hydrogen," Phys. Rev. B **66** (21), 214301 (2002).

Yildirm, T., Harris, A. B., "Quantum Dynamics of a Hydrogen Molecule Confined in a Cylindrical Potential," Phys. Rev. B **67**, 245413 (2003).

Yim, H., Kent, M. S., Huber, D. L., Satija, S., Majewski, J., Smith, G. S., "Conformation of End-Tethered PNIPAM Chains in Water and in Acetone by Neutron Reflectivity," Macromol. **36**, 5244 (2003).

Yim, H., Kent, M. S., Matheson, A., Stevens, M. J., Ivkov, R., Satija, S. K., Majewski, J., Smith, G. S., "Adsorption of Sodium Poly(styrenesulfonate) to the Air Surface of Water by Neutron and X-ray Reflectivity and Surface Tension Measurements: Polymer Concentration Dependence," Macromol. **35**, 9737 (2002).

Young, S. K., Trevino, S. F., Beck Tan, N. C., "Small-Angle Neutron Scattering Investigation of Structural Changes in Nafion Membranes Induced by Swelling with Various Solvents," J. Poly. Sci. B: Poly. Phys. **40** (4), 387 (2002).

Young, S. K., Trevino, S. F., Beck Tan, N. C., Paul, R. L., "Utilization of Prompt-Neutron Activation Analysis in the Evaluation of Nafion Membranes," J. Poly. Sci. B: Poly. Phys. **41** (3), 1485 (2003).

Zaliznyak, I. A., "Continuum Spin Excitations in S=1 One-Dimensional Antiferromagnet," J. Appl. Phys. 91, 81221 (2002).

Zeder, M. A., Blackman, M. J., "Economy and Administration at Banesh Malyan Exploring the Potential of Faunal and Chemical Data for Understanding State Process," in Yeki Bud, Yeki Nabud: Essays on the Archaeology in Honor of William M. Summer, edited by N. F. Miller, and K. Adbi (Cotsen Institute of Archaeology, University of California at Los Angeles) **48** (2003), p. 121.

Zeisler, R., "New NIST Sediment SRMs for Inorganic Analysis," J. of Radioanal. Nucl. Chem., in press.

Zeisler, R., Demiralp, R., "The Use of INAA in the Development of Urban Air Particulate Matter SRMs," J. Radioanal. Nucl. Chem., in press.

Zeisler, R., Lindstrom, R. M., Greenberg, R. R. "Instrumental Neutron Activation Analysis, a Valuable Link in Chemical Metrology," J. of Radioanal. Nucl. Chem., in press.

Zhang, Y., Ge, S., Tang, B., Rafailovich, M. H., Sokolov, J., Peiffer, D., Li, Z., Lin, M., Dias, J. A., McElrath, K. O., Nguyen, D., Satija, S., Schwarz, S. A., "Interfacial Properties of Brominated Isobutylene-co-p-Methylstyrene and Butadiene Polymers" in *Proceedings of the American Chemical Society 154th Rubber Conference*, in press.

Zhao, L., Robinson, L., Paul R. L., Greenberg, R. R., Miao, S., "Determination of Carbon, Nitrogen, and Phosphorus in Cattail (Typha latifolia) by Cold Neutron Prompt Gamma Activation Analysis," J. of Radioanal. Nucl. Chem., in press.

Zheludev, A., Honda, Z., Broholm, C. L., Katsumata, K., Shapiro, S. M., Kolezhuk, A., Park, S., Qiu, Y., "Massive Triplet Excitations in a Magnetized Anisotropic Haldane Spin Chain," Phys. Rev. Lett., in press.

Zheludev, A., Maslov, S., Zaliznyak, I., Regnault, L. P., Masuda, T., Uchinokura, K., Erwin, R., Shirane, G., "Experimental Evidence for Shekhtman-Entin-Wohlman-Aharony (SEA) Interactions in $Ba_2CuGe_2O_7$," Phys. Rev. B, in press.

Zhou, J., Deyhim, A., Krueger, S., Gregurick, S. K., "Small Angle Neutron Scattering Studies of PNA and DNA Systems,"Abstr. Pap. Am. Chem. Soc. **224**, 262 (2002).

Zhou, C., Hobbie, E. K., Bauer, B. J., Han, C. C., "Equilibrium Structure of Hydrogen-Bonded Polymer Blends," J. Polym. Sci. Part B: Poly. Phys., in press.

Zimmerman, M. V., "X-Ray Scattering Studies of Orbital and Charge Ordering in $Pr_{1-x}Ca_xMnO_3$," Phys. Rev. B, in press.

Instruments and Contacts

High resolution powder diffractometer (BT-1)
J. K. Stalick, (301) 975-6223, judith.stalick@nist.gov
B. H. Toby, (301) 975-4297, brian.toby@nist.gov

DARTS, Residual stress and texture diffractometer (BT-8)
H. J. Prask, (301) 975-6226, hank@nist.gov
T. Gnäupel-Herold, (301) 975-5380, thomas.gnaeupel-herold@nist.gov

30-m SANS instrument (NG-7)
C. J. Glinka, (301) 975-6242, cglinka@nist.gov
J. G. Barker, (301) 975-6732, john.barker@nist.gov
L. Porcar, (301) 975-5049, lionel.porcar@nist.gov

30-m SANS instrument (NG-3) (CHRNS)
B. Hammouda, (301) 975-3961, hammouda@nist.gov
S. R. Kline, (301) 975-6243, steven.kline@nist.gov
D. Ho, (301) 975-6422, derek.ho@nist.gov

8-m SANS instrument (NG-1)
D. Ho, (301) 975-6422, derek.ho@nist.gov
C. J. Glinka, (301) 975-6242, cglinka@nist.gov
J. G. Barker, (301) 975-6732, john.barker@nist.gov

USANS, Perfect SANS (BT-5) (CHRNS)
J. G. Barker, (301) 975-6732, john.barker@nist.gov
M.-H. Kim, (301) 975-6469, man-ho.kim@nist.gov
C. J. Glinka, (301) 975-6242, cglinka@nist.gov

Cold neutron reflectometer-vertical sample-polarized beam option (NG-1)
C. F. Majkrzak, (301) 975-5251, cmajkrzak@nist.gov
J. A. Dura, (301) 975-6251, jdura@nist.gov

Advanced neutron diffractometer/reflectometer (NG-1):
M. Lösche, (301) 975-8128, loesche@nist.gov
TBA

Cold neutron reflectometer-horizontal sample (NG-7)
S. K. Satija, (301) 975-5250, satija@nist.gov
Young-Soo Seo, (301) 975-5660, ysseo@nist.gov

Triple-axis polarized-beam spectrometer (BT-2)
J. W. Lynn, (301) 975-6246, jeff.lynn@nist.gov
R. W. Erwin, (301) 975-6245, rerwin@nist.gov

Triple-axis fixed incident energy spectrometer (BT-7)
J. W. Lynn, (301) 975-6246, jeff.lynn@nist.gov
R. W. Erwin, (301) 975-6245, rerwin@nist.gov

Triple-axis spectrometer (BT-9)
R. W. Erwin, (301) 975-6245, rerwin@nist.gov
P. M. Gehring, (301) 975-3946, pgehring@nist.gov

SPINS, Spin-polarized triple-axis spectrometer (NG-5) (CHRNS)
S-H. Lee, (301) 975-4257, seung-hun.lee@nist.gov
S. Park, (301) 975-8369, sungil.park@nist.gov

FANS, Filter-analyzer neutron spectrometer (BT-4)
T. J. Udovic, (301) 975-6241, udovic@nist.gov
C. M. Brown, (301) 975-5134, craig.brown@nist.gov

FCS, Fermi-chopper time-of-flight spectrometer (NG-6)
C. M. Brown, (301) 975-5134, craig.brown@nist.gov
T. J. Udovic, (301) 975-6241, udovic@nist.gov

DCS, Disk-chopper time-of-flight spectrometer (NG-4) (CHRNS)
J. R. D. Copley, (301) 975-5133, jcopley@nist.gov
I. Peral, (301) 975-6235, inma@nist.gov
Y. Qiu., (301) 975-3274, yiming.qiu@nist.gov

HFBS, High-flux backscattering spectrometer (NG-2) (CHRNS)
Z. Chowdhuri, (301) 975-4404, zema.chowdhuri@nist.gov
E. Mamontov, (301) 975-6232, mamontov@nist.gov

NSE, Neutron spin echo spectrometer (NG-5) (CHRNS)
N. S. Rosov, (301) 975-5254, nrosov@nist.gov
D. Bossev, (301) 975-4662, dobrin.bossev@nist.gov

Prompt-gamma neutron activation analysis (NG-7)
R. M. Lindstrom, (301) 975-6281, dick.lindstrom@nist.gov
R. L. Paul, (301) 975-6287, rpaul@nist.gov

Other activation analysis facilities
R. R. Greenberg, (301) 975-6285, rgreenberg@nist.gov

Cold neutron depth profiling (NG-0)
G. Lamaze, (301) 975-6202, lamaze@nist.gov

Instrument development station (NG-0)
D. F. R. Mildner, (301) 975-6366, mildner@nist.gov

Neutron interferometer (NG-7)
M. Arif, (301) 975-6303, muhammad.arif@nist.gov

Fundamental neutron physics station (NG-6)
M. S. Dewey, (301) 975-4843, mdewey@nist.gov

Theory and modeling
N. F. Berk, (301) 975-6224, nfb@nist.gov
T. Yildirim, (301) 975-6228, taner@nist.gov

Sample environment
D. C. Dender, (301) 975-6225, dender@nist.gov

NIST